THE DEVELOPMENT AND VERIFICATION OF THEORETICAL MODELS FOR THE PERFORMANCE OF WIRE CLOTH FILTER MEDIA

By

ROGER HARRELL TUCKER

Bachelor of Science
Oklahoma State University
Stillwater, Oklahoma
1961

Master of Science
Oklahoma State University
Stillwater, Oklahoma
1963

Submitted to the Faculty of the Graduate College
of the Oklahoma State University
in partial fulfillment of the requirements
for the degree of
DOCTOR OF PHILOSOPHY
July, 1966

THE DEVELOPMENT AND VERIFICATION OF THEORETICAL

MODELS FOR THE PERFORMANCE OF

WIRE CLOTH FILTER MEDIA

Thesis Approved:

E. L. Feltch
Thesis Adviser

J. Leroy Folks

A. M. Rowe, Jr.

A. G. Comer

J. H. Boggs
Dean of the Graduate College

ACKNOWLEDGEMENTS

I wish to express my gratitude to Professor E. C. Fitch, Chairman of my advisory committee for his assistance and guidance during my doctoral studies. As a result of his efforts I have had the opportunity to participate in the NASA Filtration Mechanics Research Project from which much of the present work has resulted.

I also wish to thank the other members of my advisory committee, Professors A. G. Comer, A. M. Rowe, and J. L. Folks, for their advice during the preparation of this dissertation.

Mr. R. F. Church served as the Contract Monitor for the NASA Filtration Mechanics Project. In this capacity he provided me with the freedom to pursue my studies in this research endeavor.

Mr. John Winzen, President of the Wintec Filter Corporation, supplied me with the wire cloth filter samples and because of his interest my efforts were encouraged.

Appreciation is expressed to Mrs. V. F. Snider for her assistance in performing the particle count analyses required for this research. Appreciation is also expressed to Professor Peter Dransfield who offered many helpful criticisms regarding the content of this dissertation.

I have had the unique opportunity to work with an outstanding group of colleagues in the Fluid Power Controls Group. I wish to thank them for their willing cooperation and assistance in this study.

Finally, I want to thank my wife, Pat, for the understanding and encouragement which she has provided throughout my graduate study. I am especially grateful to her for typing this manuscript.

TABLE OF CONTENTS

LIST OF TABLES

LIST OF FIGURES

CHAPTER I

INTRODUCTION

The development and application of high performance hydraulic components with low contaminant tolerances has necessitated the use of filter media which are more effective in the removal of hydraulic system contaminants. The search for filter media has led to the consideration of media such as paper, sintered metal powder, sintered metal fiber, and woven wire cloth. The latter medium has found wide acceptance in the aerospace industries because of its low flow resistance and closely controlled pore size. The criterion for selecting one medium over another is often based on the experience of the designer rather than the knowledge of what contribution the filter medium is actually making to the system. Often, this approach has been forced on the designer because applicable filter design information has either been of a vague, empirical nature, or totally lacking.

The evolution of sophisticated hydraulic control systems into industrial applications such as the mobile equipment industry, requires a different approach to filter design than has been followed for aerospace applications. In the aerospace industry, where relatively few units containing a given control system are built, the economic penalties resulting from an overdesigned filtration system are often insignificant. However, in industrial applications where the system design has the potential of being used on thousands of units, the need for selecting the

most economical filtration compatible with proper system operation is paramount.

The following three items of information are required before an effective filtration system can be designed economically for a given fluid control system application:

(1) The contaminant levels which can be expected in the system fluid under operating conditions must be known.

(2) The contaminant environment in which the system can operate with no loss in performance must be defined.

(3) The capabilities of the available filter materials to reduce existing system contaminant levels to acceptable levels must be known.

Information regarding the first two items above is beginning to appear in the literature as users and manufacturers of hydraulic components are attempting to define the contaminant generation characteristics of their systems and determine the contaminant tolerance levels of critical components. To provide fluid which does not exceed specified contaminant tolerance levels, the filter designer must either resort to a trial-and-error filter selection procedure or have available more comprehensive information about filter performance.

The present research has been conducted in order to provide the hydraulic system designer with applicable information regarding the characteristics of wire cloth media. Mathematical models for the flow and filtration performance have been developed and experimentally verified. These models are applicable for media used both singly and in series and parallel configurations.

CHAPTER II

PREVIOUS INVESTIGATIONS

The two important functions of a filter medium are diametrically opposed to one another. A filter is required to provide maximum restriction to the passage of particulate contaminants, while offering minimum resistance to flow of the system fluid. Therefore, a study of the performance of filter media should consider both the flow and filtration characteristics of the material. In addition to defining the characteristics of the material, a knowledge of the contaminant environment in which the material is to be used is required. Also, the contaminant sensitivity of the components to be protected is basic to the proper selection of a filter medium. The following discussion gives a cross section of the available information regarding these four pertinent areas.

2.1 Flow Through Porous Media. In order to discuss the flow through porous media, a definition of the characteristics of a porous medium must be given. A porous medium can be defined as a medium containing pores and capillaries. Figure 2.1.1 shows a simplified representation of a porous medium. Capillaries are passages from one side of the medium to the other and pores are individual restrictions within capillaries. Figure 2.1.2 is a typical graph of diameter as a function of position within a capillary. A pore exists when the diameter reaches a relative minimum. These definitions apply throughout the remainder of this thesis.

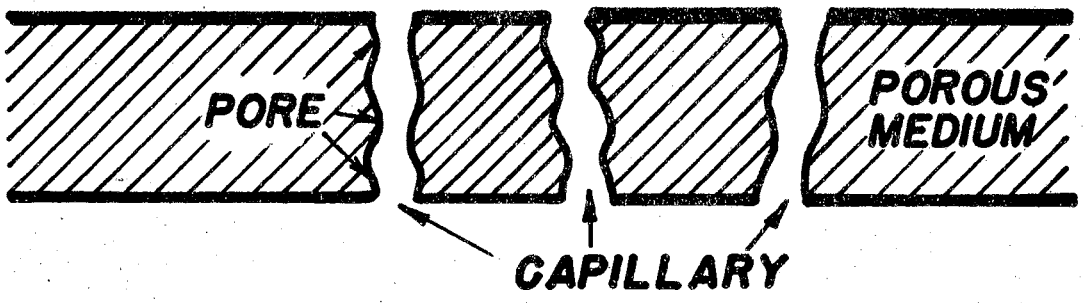

Figure 2.1.1. Simplified Representation of a Porous Medium

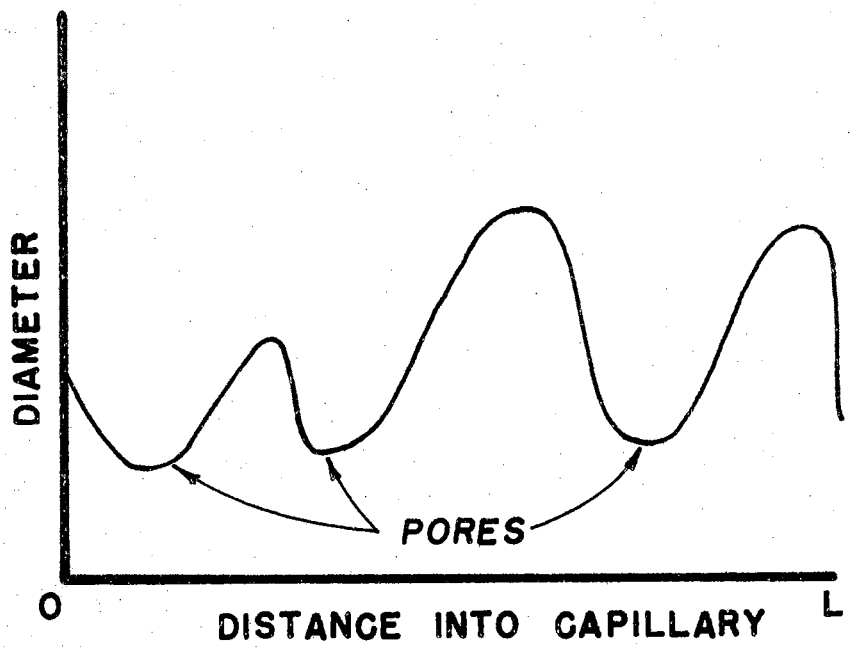

Figure 2.1.2. Graph of Diameter as a Function of Position Within a Capillary

The mechanism of flow through porous media has been studied by many investigators. Their investigations usually begin with the selection of one of the two primary equations covering laminar flow through porous media. The first of these basic equations was formulated by the French engineer, Henri Darcy, in 1856. He observed that the fluid velocity within a porous medium was proportional to the pressure loss per unit length. Later investigators extended Darcy's findings to include the viscosity of the flowing fluid. Darcy's equation for horizontal flow can be stated mathematically by the differential equation,

$$v = -\frac{K}{\mu}\frac{dP}{dL}. \qquad (2.1.1)$$

where:

v is the fluid velocity in the capillary.

μ is the dynamic viscosity of the fluid.

$\frac{dP}{dL}$ is the pressure gradient in the medium.

K is a proportionality constant, defined as permeability.

The negative sign in the equation above results from the fact that the pressure gradient is a negative quantity. The permeability of a porous medium, as defined by Equation 2.1.1, has the dimensions of length squared and is generally considered to be a complex function of the porous media.

The second basic equation describing laminar flow of fluids in a porous medium is the well known law of Hagen-Poiseuille. In this case the porous medium is modeled by a bundle of straight parallel capillaries of uniform diameter D. A common form of the Hagen-Poiseuille equation is

$$v = -\frac{D^2}{32\mu}\frac{dP}{dL}. \qquad (2.1.2)$$

A comparison of Equation 2.1.1 and 2.1.2 shows that the permeability of

the straight capillaric model is given by

$$K = \frac{D^2}{32} . \qquad (2.1.3)$$

Several investigators have attempted to define the permeability of a porous medium in terms of the properties of the medium. Scheidigger (1)[1] in a comprehensive study of the physics of flow through porous media describes the efforts of these investigators. One of the most notable contributions in this area has been that of Kozeny (2). He characterized permeability as a function of the porosity and internal surface area of the medium. The relationship which he proposed is

$$K = \frac{C \phi^3}{S^2} . \qquad (2.1.4)$$

where:

ϕ is the porosity, ratio of void volume to total volume.

S is the internal surface area per unit total volume.

C is the Kozeny constant.

The value of C depends on the shape of the flow passage and is equal to 0.50 for a circle, 0.56 for a square, and 0.60 for an equilateral triangle.

Carman (3) proposed a much used modification to the Kozeny equation. His modification, referred to as the Kozeny-Carman equation, is given in Equation 2.1.5.

$$K = \frac{\phi^3}{5 S_o^2 (1-\phi)^2} . \qquad (2.1.5)$$

---

[1]Numbers in parentheses refer to Bibliography.

where:

S_o is the ratio of the internal surface area to the solid volume.

Schiedigger (1) states that the Kozeny theory contains some vague factors and that little more than a qualitative description of the phenomenon can be expected from it. Sullivan (4) showed that Kozeny's law breaks down in the case of porous fiberous materials.

Despite the apparent anomalies, Kozeny's equation has been utilized in many instances to describe the permeability term. Green and Duwez (5) depicted the pressure gradient through a porous metal medium as the sum of two terms,

$$-\frac{dP}{dL} = \alpha \mu V + \beta \rho V^2. \qquad (2.1.6)$$

where:

α is the viscous resistance coefficient, length $^{-2}$.

β is the inertial resistance coefficient, length $^{-1}$.

For laminar flow only the first term is significant; however, at high flow rates the second term must also be considered. The values for α and β were represented by the equations,

$$\alpha = C_1 S^2 \frac{(1-\phi)^2}{\phi^3} \quad . \qquad (2.1.7)$$

and,

$$\beta = C_2 S \frac{(1-\phi)}{\phi^3} \quad . \qquad (2.1.8)$$

where:

C_1 and C_2 are dimensionless constants.

The presence of the Kozeny equation in the expression for α is readily apparent.

Rainard (6), although using a Poiseuille flow model, suggested an equation similar to 2.1.6 in describing the flow of air through textile materials. His flow equation is similar in that the pressure loss term is the sum of an inertial term and a viscous term.

$$\Delta P = \frac{16 m \rho}{\pi D^4} Q^2 + \frac{128 \mu L}{\pi D^4} Q \cdot \qquad (2.1.9)$$

where:

m is a constant to account for changes in velocity gradient.

ρ is the fluid density.

If the expression is divided by Q, it can be changed to the form

$$\frac{\Delta P}{Q} = \frac{16 m \rho}{\pi D^4} Q + \frac{128 \mu L}{\pi D^4} = K_1 Q + K_2 \cdot \qquad (2.1.10)$$

Rainard theorized that since K_2 is a function of L then K_2 should double for two layers of fabric, triple for three layers and so on. Further, since K_1 does not include the length term, L, it should remain constant for multiple layers. His experimental work verified the proportionality of K_2 to the number of layers of media. However, the experimental value of K_1 did not remain constant as the flow model had predicted. K_1 also increased with increasing layers. Rainard hypothesized that as the media were placed in series, the holes in the respective media did not coincide. Therefore, the effective diameter, D, was decreased and K_1 increased. This explanation does not seem plausible since such a decrease in the value of D would have affected K_2 also, and this was not demonstrated in his experimental results.

A considerable number of empirical studies have been carried out to

describe the flow of gases through screens. The use of screens in most of the following cases have not been for filtration, but rather for the reduction of or inducement of turbulance in ducts. The approach by Baines and Peterson (7) is typical of that taken by most investigators in this area. A pressure loss coefficient, defined by Equation 2.1.11, is used to describe gas flow through a screen.

$$R = \frac{\Delta P}{\frac{\rho V^2}{2}} . \qquad (2.1.11)$$

where:

R is the pressure loss coefficient.

The loss coefficient, R, is then empirically determined as a function of the Reynolds number based on the wire diameter, the porosity of the screen, and the type of weave. For the plain weave shown in Figure 2.1.3 the porosity is given by

$$\phi = \frac{\text{Open Area}}{\text{Total Area}} = \left(1 - \frac{D_w}{W}\right)^2 . \qquad (2.1.12)$$

where:

W is the weave spacing.

D_w is the wire diameter.

MacDougall (8) correlated the loss coefficient for a plain weave in the Reynolds number (N_R) range between 0.006 and 20. His empirical findings are given by

$$R = \frac{33.9}{N_R} \frac{(1-\phi)\phi^{-1.27}}{1+\phi^{0.5}} . \qquad (2.1.13)$$

Weighardt (9) covered the range of Reynolds numbers from 60 to 1000 and proposed the equation,

Figure 2.1.3. Pattern for a Plain Weave

$$R = \frac{6}{N_R^{1/3}} \frac{1-\phi}{\phi^{5/3}} . \qquad (2.1.14)$$

Cornell (10), although not expressing his findings in equation form, presents experimental curves which cover values of N_R between 40 and 17,000.

Some investigators, including Wuest (11), have reported a flow-pressure relationship for screens which differs from Equation 2.1.11. Wuest observed a relationship of the form,

$$\Delta P = R \frac{\rho V^n}{2} . \qquad (2.1.15)$$

The exponent n approached 1 for lower velocities and approached 2 for higher velocities. Lovett (12) reported values of n which ranged from 1.7 to 1.9 for water flowing through coarse wire cloth screens. Seed and Fowle (13) in measuring the flow-pressure characteristics of paper filter media observed that the pressure differential was proportional to the flow-rate raised to a power ranging from 1.1 to 1.6.

Lewis (14) measured the flow rate-pressure differential characteristics for eight types of stainless steel filter cloths, four of a Dutch twill weave, and four of a plain weave which had been calendered to the thickness of the wires. He was attempting to determine whether the flow pressure relationship was similar to that which could be expected through parallel orifices, namely, pressure proportional to the square of the flow rate. The relationship was established as being non-linear for the media with the plain weave. However, the exponent of the flow rate was measured at approximately 1.5 rather than the expected value of 2.0. For the four media with the Dutch twill weave, the differential pressure was found to be a linear function of flow rate.

Several authors have applied Poiseuille's law to flow through filter media. Grace (15) and Seed and Fowle (13) both suggest the following form of Equation 2.1.2,

$$Q = \frac{\pi N A D^4}{128 \mu L} \Delta P \, . \qquad (2.1.16)$$

where:

N is the number of pores per unit area.

A is the total area of medium.

Q is the flow rate through the medium.

Fitch (16) also suggests a form of the equation above which includes tortuosity of the filter medium as a parameter. His result can be stated mathematically as

$$Q = \frac{\phi^2 A^2}{8 \pi N \tau \mu L} \Delta P \, . \qquad (2.1.17)$$

where:

τ is the tortuosity, which is equal to the ratio of actual capillary length to the thickness of the medium.

Cranston (17) also included the effects of the tortuosity of the filter medium in his application of Poiseuille's law. In addition to this modification he represented the effective flow diameter of the capillaries as the product of a constant, α , and a diameter characteristic of the filtration properties of the medium. The flow through a single capillary is then given by

$$q = \frac{\pi \alpha^4 D_c^4}{128 \mu \tau L} \Delta P \, . \qquad (2.1.18)$$

where:

D_c is a diameter characteristic of the filtration properties of the material.

q is the rate of flow through a single capillary.

If the medium is considered to consist of a number of capillaries having a size distribution, $f(D_c)$, the total flow through the medium can be represented in the form of the integral,

$$Q = \left[\frac{\pi \alpha^4}{128 \tau L}\left(\int_0^\infty D_c^4 f(D_c)\, dD_c\right)\right]\frac{\Delta P}{\mu}. \qquad (2.1.19)$$

Cranston, although proposing the equation above, found that the accuracy of his experimental results were insufficient for carrying out a detailed analysis of the validity of the equation. Instead he grouped the bracketed quantity into a flow constant term, which he could obtain experimentally. He suggested that the flow constant and the filter area be used to describe the flow properties of various media.

Although investigators have proposed several theoretical models to describe the flow-pressure relationship through porous media, none of the models has been proven to be valid by experimental data. The failure to verify any of these models has been due primarily to the inability of the investigators to accurately measure the porperties of the porous medium. It will be shown in a later section that a form of Poiseuille's equation can be used to describe the flow-pressure relationship through wire cloth media.

2.2 Mechanisms of Filtration. Filter media can be divided into three general classifications based on the mechanism by which they accomplish contaminant removal. The three removal mechanisms are absorption,

adsorption, and mechanical filtration. An absorbent medium accomplishes contaminant removal by sponging a mixture of oil, additives, and chemical contaminants from the fluid. An adsorbent medium effects filtration by attracting contaminants to its surface by a mechanism such as capillary condensation, electrical or polar attraction, or chemical bonding. Absorption and adsorption filtration is usually applied where large volumes of fluid are to be purified and the size and weight of the filter is not a critical parameter.

The third mechanism and the one which will be considered in this research is mechanical filtration. Mechanical filtration is accomplished by the direct interception of particulate contamination in the interstices of the filter medium. Media which exhibit this characteristic are classified into surface and depth type media depending upon the manner in which the interstice blockage occurs. In surface media the capillaries are continuous with no change in direction within the capillaries. Filtration occurs on the surface of the medium in a seiving process. Perforated plates, metal edge (wire wound) media, and plain woven wire mesh media are typical surface type filter media. Depth media offer a tortuous path for the fluid to follow as they contain capillaries which are neither straight nor continuous. Dutch twill wire cloths, Figure 2.2.1, although usually referred to as surface media, do exhibit some of the properties of depth media as the fluid must follow a somewhat tortuous path through a series of four pores.

The mechanisms of mechanical filtration have received the attention of several investigators. Hermans and Bredee (18) proposed the following series of filtration mechanisms:

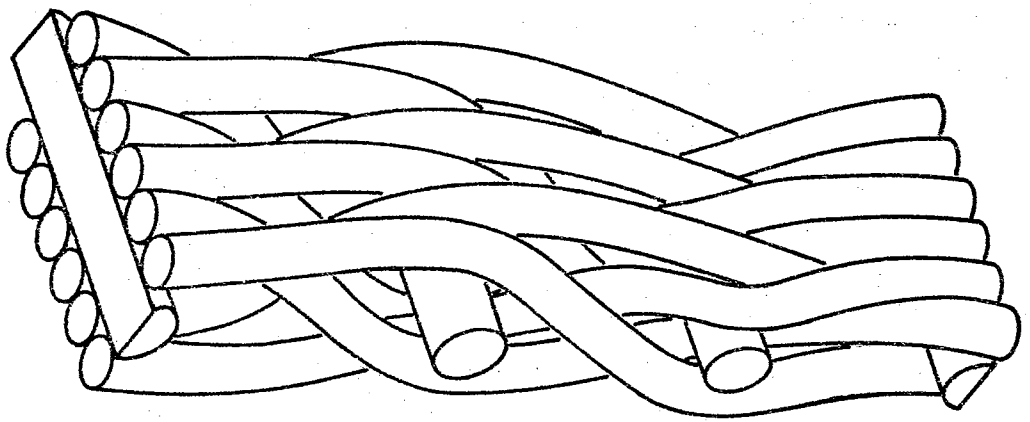

Figure 2.2.1. Pattern for a Dutch Twill Weave

(1) Complete Blocking occurs when the individual particles are large enough to directly plug the filter pores.

(2) Standard Blocking occurs when particulate contaminants in streamlines adjacent to the walls of the capillaries adhere to the walls. The deposited particles can be smaller than the pores in the capillaries. A continuous deposition of particles will eventually block the capillary.

(3) Cake Filtration occurs when solid particles of contamination retained at the filter surface build up to form a porous cake as more contaminated fluid reaches the filter. Impingement and subsequent stacking of the particles gradually thickens the cake, which then acts as the primary barrier to flow through the filter element.

(4) Intermediate Blocking is loosely defined as a filtration mode between standard blocking and cake filtration.

Hermans and Bredee suggested that these mechanisms occur at various points in the filtration cycle of a filter from its clean condition throughout its useful life. Each mechanism can be described by the filtration rate equation,

$$\frac{d^2t}{dV^2} = C_p\left(\frac{dt}{dV}\right)^n \qquad (2.2.1)$$

for constant pressure drop filtration; and

$$\frac{d(\Delta P)}{dV} = C_q(\Delta P)^n \qquad (2.2.2)$$

for constant flow rate filtration.

where:

t is time.

V is the volume of filtrate which has passed.

C_p and C_q are constants depending on the type and size of the contaminant present, the properties of the filter medium, and on the flow parameters such as flow rate, viscosity, etc.

n is an exponent depending on the mechanism of filtration occuring.

It was suggested that n has the values:

n = 2.0 for complete blocking,

n = 1.5 for standard blocking,

n = 1.0 for intermediate blocking,

n = 0.0 for cake filtration.

Using the constant flow-rate case, which is applicable to the present work, the following relationships can be developed:

For complete blocking,

$$\frac{\Delta P_o}{\Delta P} = 1 - \frac{C_b V}{Q} . \qquad (2.2.3)$$

For standard blocking,

$$\left(\frac{\Delta P_o}{\Delta P}\right)^{1/2} = 1 - \frac{C_s}{2} V . \qquad (2.2.4)$$

For intermediate blocking,

$$Ln\left(\frac{\Delta P}{\Delta P_o}\right) = C_i V . \qquad (2.2.5)$$

For cake filtration,

$$\frac{\Delta P}{\Delta P_o} = 1 + C_c Q V . \qquad (2.2.6)$$

where:

C_b, C_s, C_i, and C_c are the appropriate plugging constants.

ΔP_o is the pressure drop required to force a flow rate Q of uncontaminated oil through the filter.

Gonsalves (19), although making different assumptions for the physical mechanisms of pore blocking, confirmed Equations 2.2.1 and 2.2.2. Gonsalves' principle objection to the work of Hermans and Bredee was their suggestion of the standard blocking filtration mechanism. However, Grace (15) experimentally observed that the standard blocking mode has been found to fit data on textile media for a significant portion of the filtration cycle. The complete blocking and intermediate blocking modes of filtration were observed to have much more limited application. Grace stated that a small number of systems containing particles larger than the pores of the medium appear to follow the complete blocking mode of filtration. He concluded that in textile media the filtration cycle generally passed through a number of modes. Standard blocking applied for a portion of the cycle, followed by a transition region which in turn was followed by a prolonged region of cake filtration. In some cases, the cake mode appeared to apply even though a true cake did not exist in a macroscopic sense.

Stone (20) investigated the filtration cycles of a 165x1400 Dutch twill wire cloth element when various size ranges of contamination were used. The curves which he obtained are shown in Figure 2.2.2. At the end of his investigation he reached the following conclusions:

(1) When a wire cloth filter is exposed to oil carrying contaminant of a narrow size band, the possible mechanisms of filtration appear to be similar to those proposed by Hermans and

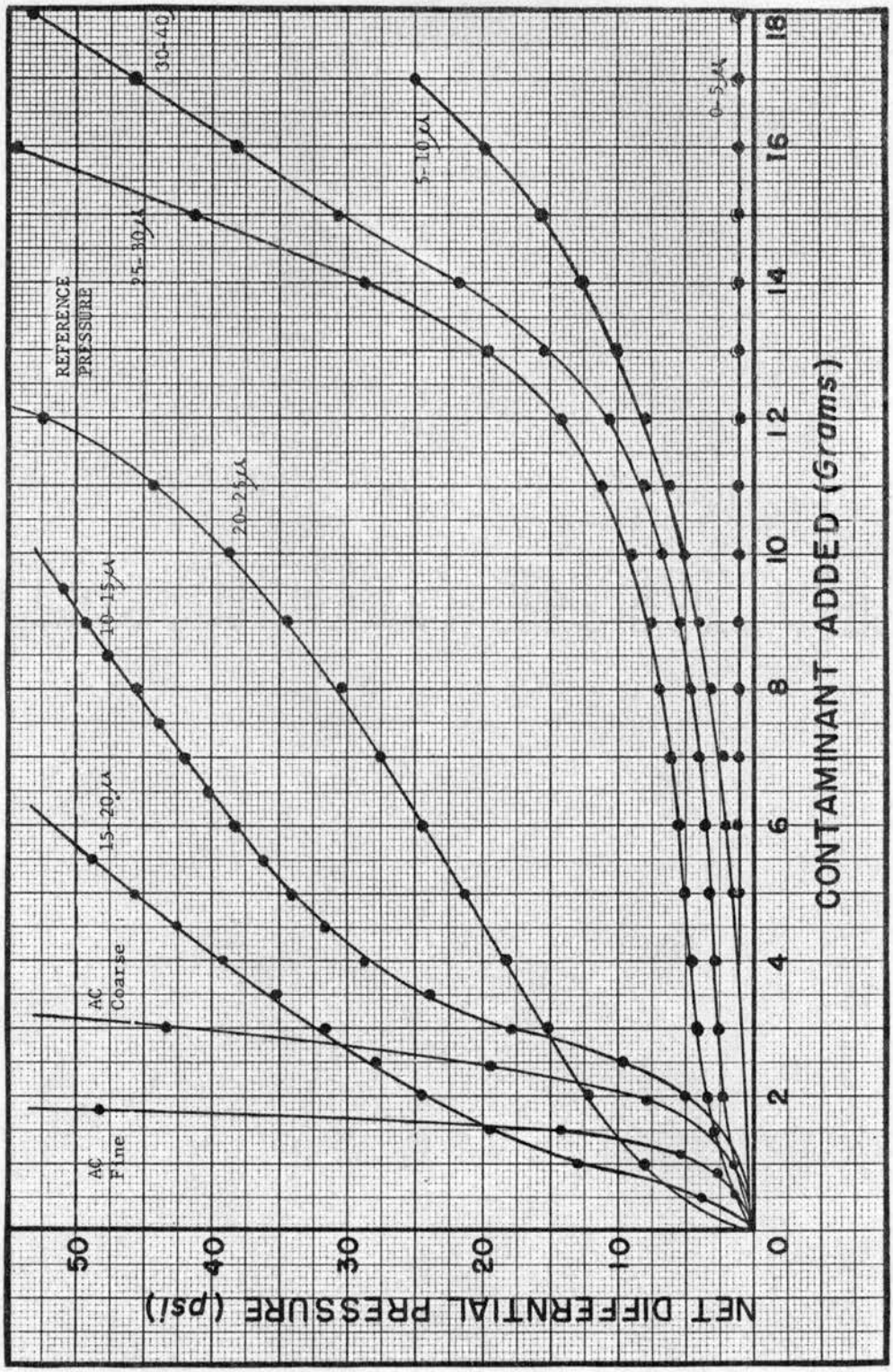

Figure 2.2.2. Filtration Cycles of a Wire Cloth Filter for Various Contaminants

Bredee from data associated with textile depth filter media.

(2) A wire cloth filter is most susceptible to particles in a size range just below the mean pore size indicated by efficiency or porosimeter tests on the wire cloth.

(3) When subjected to narrow size cuts of particles in the size ranges about its mean pore size, the wire cloth contamination cycle includes a substantial amount of cake filtration. For size cuts below the mean pore size, the filter initially experiences the intermediate blocking mechanism for a region of the cycle which decreases as the particle size range increases. Following this, the cycle enters the incompressible cake filtration region. For particle size cuts around and greater than the mean pore size of the wire cloth, the initial mechanism of filtration is indeterminate and of short duration prior to development of the incompressible cake mechanism. If sufficient contaminant is added, the increasing pressure drop can cause compression of the cake, increasing its resistance to flow.

(4) Mixed size contamination causes much more rapid blocking of the filter. For the mixed contaminants used, the filter contamination cycle followed the intermediate blocking mechanism, inferring that this was the mechanism most likely to occur in actual filter performance.

A filtration theory proposed by Cranston (17) in 1952 assumed the complete blocking mode to be the filtration mechanism. His work represents a significant contribution to the study of the mechanisms of filtration and will be referenced in detail. Cranston, considering the filter medium in the same manner as shown in Figure 2.1.1, represented the

pore sizes in the medium by a distribution function $f_c(D)$. The capillary size is determined by the smallest pore within the capillary, and therefore in a medium with only one pore per capillary the pore and capillary size distributions would be equal;

$$f_c(D) = f_p(D) \ . \qquad (2.2.7)$$

For each additional pore in the capillary the capillary size distribution is reduced in proportion to the probability that there is a pore with a diameter greater than D. For capillaries with n pores, the capillary size distribution is the distribution of the smallest of n observations;

$$f_c(D) = n f_p(D) \left[\int_D^\infty f_P(D)\, dD \right]^{n-1} . \qquad (2.2.8)$$

Figure 2.2.3 shows typical curves of $f_p(D)$ and $f_c(D)$ for a medium having a broad pore size distribution and several pores per capillary.

Cranston made the following assumptions in describing a test to measure filtration efficiency:

(1) Particles of size x have free passage through any capillary larger than x.

(2) The concentration of contaminants in the feed is insufficient to cause blockage of the medium during a test.

(3) $f_d(x)$ is the distribution of particles of size x in the filtrate.

$f_u(x)$ is the distribution of particles of size x in the feed.

(4) The number of particles larger than x reaching the filtrate will be proportional to the amount of fluid flowing through the capillaries larger than x.

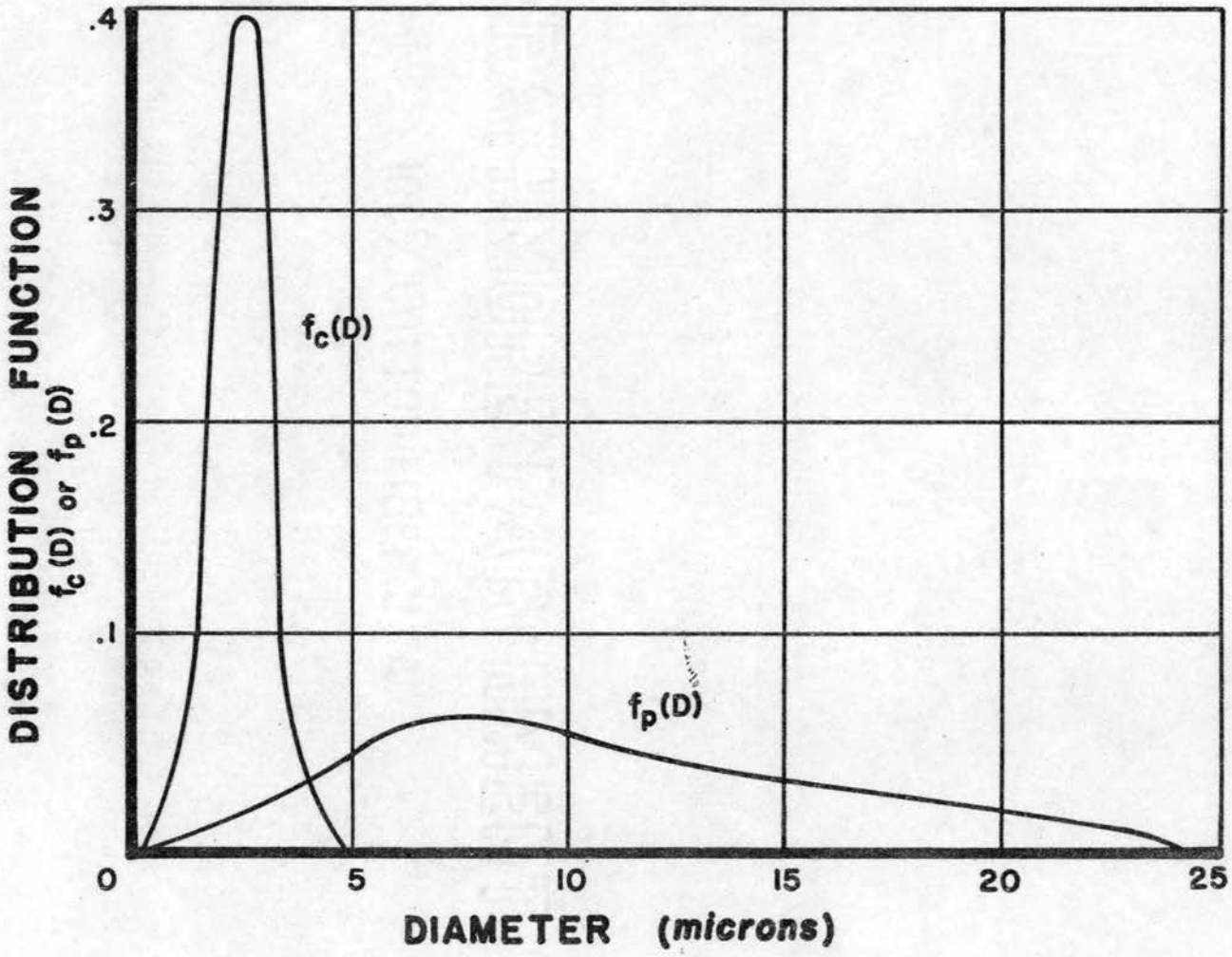

Figure 2.2.3. Pore and Capillary Size Distribution Curves

Therefore, applying Equation 2.1.19,

$$T(x) = \frac{f_d(x)}{f_u(x)} = a \frac{\int_x^\infty D^4 f_c(D)\, dD}{\int_0^\infty D^4 f_c(D)\, dD} . \qquad (2.2.9)$$

where:

T(x) is the transmission factor at size x.

a is the specific filtration area, a constant which corrects for the fact that some contaminant is deposited on the surface of the filter and never reaches the capillaries.

In performing the efficiency test, the particle size distributions in the feed and filtrate are measured, as shown in Figure 2.2.4. The transmission curve, a plot of T(x) versus x, is then prepared, Figure 2.2.5. The characteristic shape of the capillary size distribution curve can then be obtained by measuring the slope of the transmission curve at various sizes and dividing by the size raised to the fourth power, since from Equation 2.2.9,

$$f_c(D) \sim \frac{1}{D^4} \frac{d[T(D)]}{dD} . \qquad (2.2.10)$$

Ludvig (21) reports the use of Cranston's technique to measure the capillary size distributions of several types of woven wire cloth filter media. The transmission curves obtained in this manner exhibited a tendency to flatten out at a value of T(x) which was less than 50 percent as the particle size approached zero. Ludvig attributed this to the specific filtration area of the screens. Following Cranston's theory, he suggested that some of the particles in the feed smaller than the pore openings in the media were settling on the surface of the wire cloth and therefore did not appear in the filtrate. It is interesting to note that

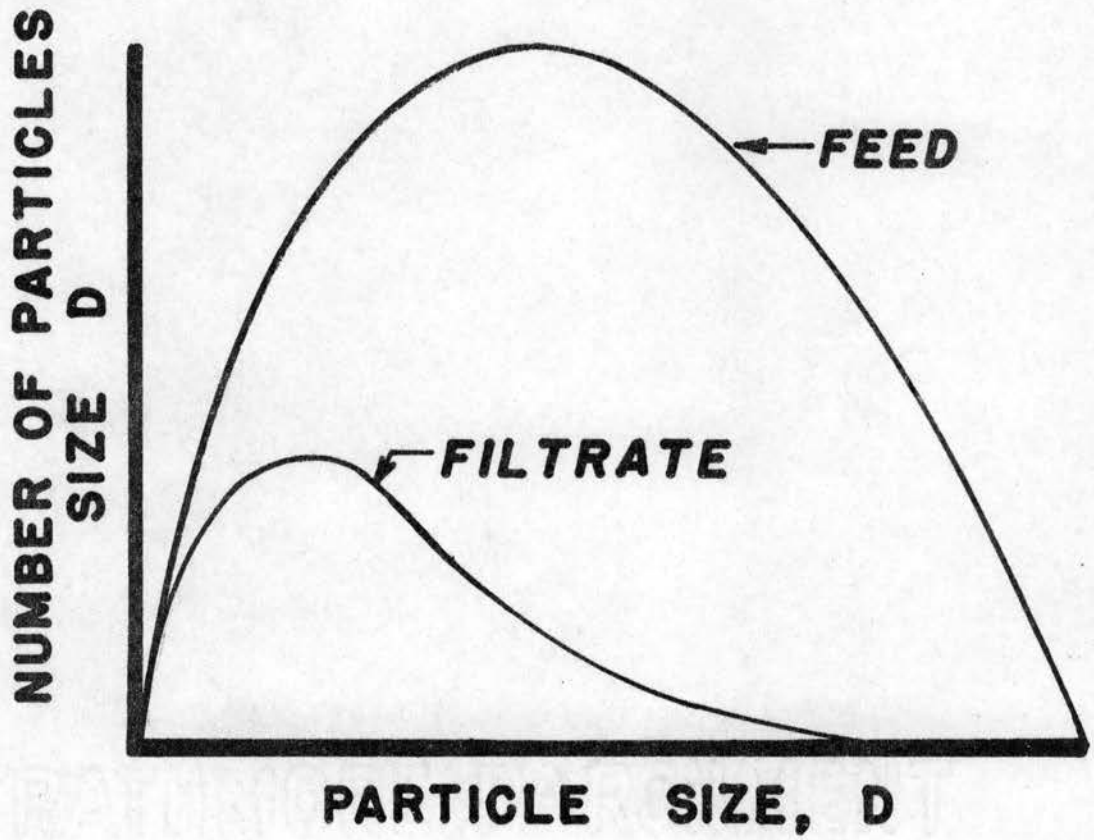

Figure 2.2.4. Partical Size Distribution Curves from an Efficiency Test

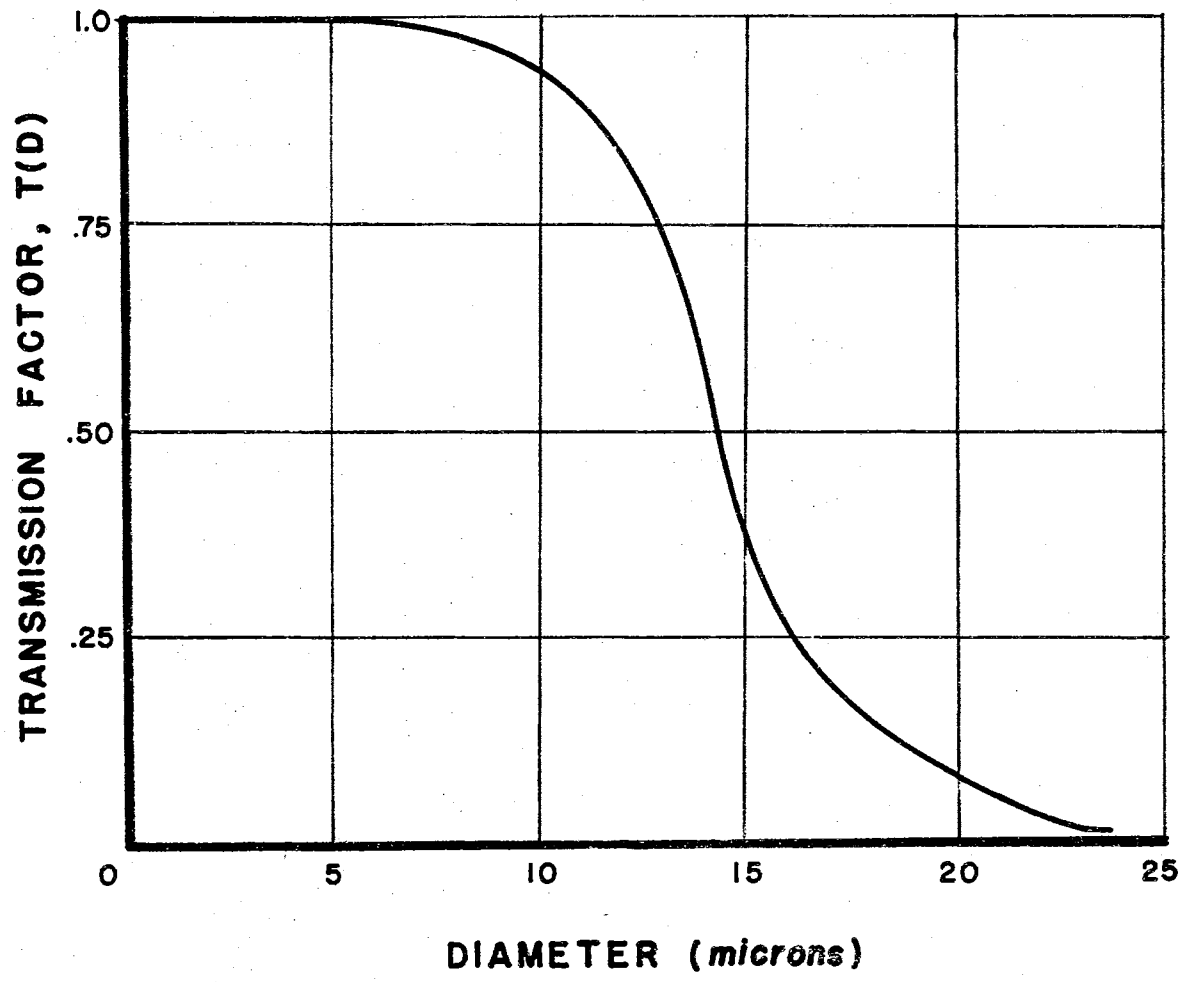

Figure 2.2.5. Typical Transmission Curve

the leveling off of the transmission curves occurred at diameters less than 10 microns in size. This coincides with the range where particle counting techniques are subject to considerable error unless special opticle equipment is used.

Casaleggi, et. al. (22) used a procedure similar to Cranston's to measure the filtration characteristics of two paper media and two wire cloth media. The tests were performed by passing glass beads, which were separated into narrow size ranges, through the medium. For each size range of beads a weight removal efficiency was determined by measuring the weight of contaminant in the feed and filtrate. This efficiency value was then assigned to a diameter equal to the average diameter by weight of the glass bead sample being used. The efficiency curves which were obtained are shown in Figure 2.2.6. Contrary to the findings of Ludvig (21), the curves exhibit a definite characteristic of 100 percent transmission at the smaller sizes. The curves undoubtedly indicate a broader distribution of pore sizes than actually exist in the media. This is because the particle size ranges for the individual test contaminants covered a 30 micron interval. This type of test could be very effective if the contaminants were accurately sized in 5 micron intervals.

The evaluation of the properties of a filter medium by measuring its efficiency or transmission characteristics is the most informative method of analysis when done properly. There are certain factors which must be taken into consideration when performing efficiency tests. Wheeler (23) states that filter efficiency is a dynamic factor which depends on the fluid velocity, the filter medium, the type of contamination, and whether there are surges or vibration in the system. High fluid velocities as well as surging or vibration can drive contaminants

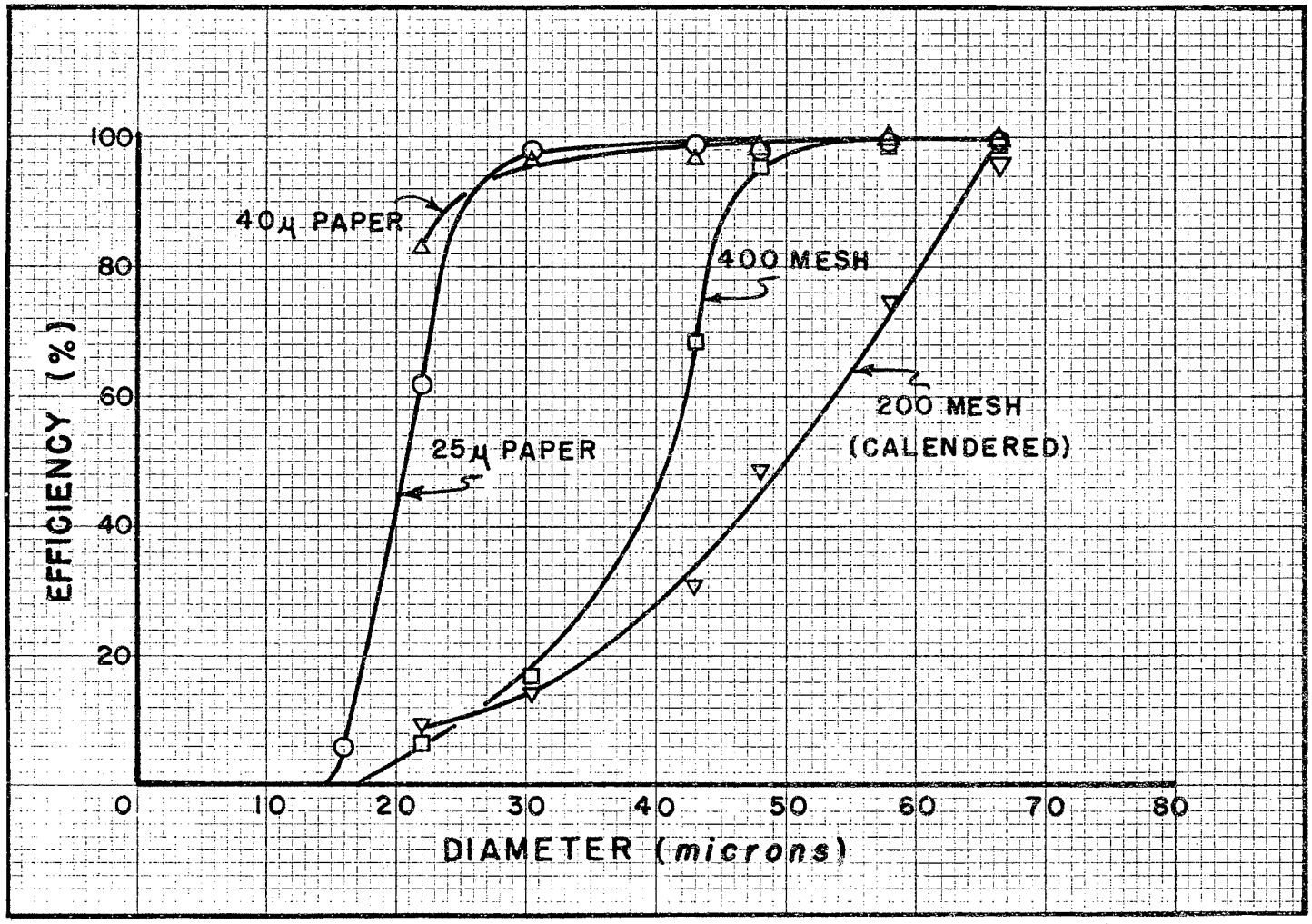

Figure 2.2.6. Efficiency Curves for Several Filter Media

through the filter therby lowering its efficiency. The attainment of valid efficiency test data is also dependent upon the withdrawal of representative samples of the contamination in the feed and filtrate and the proper assessment of the contamination in the respective samples.

Because of the difficulties involved in measuring the filter efficiency characteristics of media, other methods of rating filters have been used. The most common expressions for describing a filter medium are by either its nominal rating or its absolute rating. The definitions of these terms are as follows:

(1) Nominal rating refers to the ability of a medium to remove a certain percentage of a specified contaminant. For example, a medium which retains 95 percent by weight of glass beads 10 to 30 microns in size is usually classed as having a 10 micron nominal rating. The nominal rating is based on a particular test procedure; a medium might have different nominal ratings when tested under two different procedures. The nominal rating indicates no more about a medium than how it performed under the given test conditions.

(2) Absolute rating is defined as the maximum pore opening in the filter medium. This rating is determined by observing the largest glass bead which passes through the medium. Like the nominal rating, the absolute rating is dependent on the particular test procedure used. In service, a 25 micron absolute filter will pass irregularly shaped particles whose longest dimensions are greater than 25 microns.

There are three principle specifications to which hydraulic filters for aerospace applications are rated. Each of these specifications in-

cludes a Degree of Filtration Test in which the nominal rating of the filter is measured. In two of the specifications an absolute rating requirement is imposed on the filter. The filtration requirements for these three specifications are given below:

(1) Mil-F-5504B (24). 2000 ml. of Mil-H-5606 hydraulic fluid containing 0.5 grams of 10 to 20 microns glass beads are passed through the test element. The weight of glass beads in the filtrate, x, is measured; and the efficiency is calculated from the equation,

$$E = 100\,\frac{0.5 - x}{0.5}\,. \qquad (2.2.11)$$

A 95 percent removal is required to meet the specification.

(2) Mil-F-8815A (25). The filter must remove 94 percent by weight of APM F-9 glass beads. No spherical particle whose diameter is greater than 15 microns is permitted in the filtrate.

(3) Mil-F-27656A (26). The filter must remove 99.3 percent of an equal mixture by weight of AC Fine Test Dust and APM F-9 glass beads. This removal percentage is equivalent on a weight basis to 100 percent removal of particles larger than 5 microns and 96.6 percent removal of particles 5 microns and smaller. In addition, no spherical particle whose diameter is greater than 5 microns is permitted in the filtrate.

Each of the specifications above have one characteristic in common; the performance of the medium is a function of the test procedure which is used. Therefore, it is difficult to extend the results of such a test to predict how the medium will perform under different operating condi-

tions. In order to properly evaluate the filtration performance of a medium its capillary size distribution must be determined. Although the measurement of this distribution is dependent on test techniques, the results obtained are primarily a function of the medium itself. If the capillary size distribution curve can be described by a statistical model, then the filtration properties of the medium itself can be described in a mathematical sense. With this mathematical description, the performance of a medium in a given contaminant environment can be calculated.

2.3 Sources of Contamination. The selection of a filter medium for a specific application would be incomplete without a knowledge of the environment in which the medium is to be used. The contaminant level presented to a filter as well as the contaminant tolerances of the components to be protected dictate the characteristics of the medium.

Contamination within hydraulic systems occurs from either internal or external sources. Internal sources of contamination can result either from the generation of particles from wearing surfaces in the components or from the release of contaminants built into the system at assembly. Generation of particles within a system can occur when two moving parts abrade one another or by some other mechanism such as cavitation within some system component. Built in contaminants usually occur as undesirable by-products of manufacturing processes. These contaminants may be fine cuttings from machining operations or even the residue from a welding process. Although component cleaning techniques are constantly being improved, built in contaminants represent a significant contribution to the overall system contamination level.

External sources of contamination are also quite common. Con-

tamination of this type can enter in the hydraulic fluid itself, through breather caps on reservoirs, or from the atmosphere when a system is opened for repair. The primary constituent of this type of contamination is silica.

Until recently most of the experimental work which has been reported concerning sources of contamination in oil systems has been limited. Little active effort was expended to determine the exact source of the contaminants. LeGrand (27) suggested some particle sizes that result from various machining processes. These sizes, shown in Table I, are functions of specific machining requirements and facilities; therefore, they are only typical.

TABLE I

PARTICLE SIZES GENERATED BY MACHINING PROCESSES

Process	Particle Size Generated (microns)
Mirror Finishing	$\frac{1}{2}$
Broaching	5 to 10
Honing and Lapping	2 to 5
Thread Grinding	3 to 5

Nutt (28) reported on the sizes of abrasive particles which were removed from the fuel line of an automotive engine. These results, found in Table II, although not obtained from a hydraulic system, give an indication of the sizes of particles which can be found in operating systems.

Recent investigations at Oklahoma State University, as reported by

TABLE II

TYPICAL DISTRIBUTION OF CONTAMINANTS IN AUTOMOTIVE SYSTEMS

Particle Size (microns)	Percent by Number
0 to 5	2
5 to 12.5	15
12.5 to 37.5	37
37.5 to 76	22
76 to 114	12
114 to 153	5
Greater than 153	7

Fitch (29), have measured the contaminant generation characteristics of hydraulic system components. In particular, the generation properties of hoses, metal lines, and component housings were studied. The results showed that generation from such non-wearing surfaces was a function of the cleaning intensity of the fluid, whether due to system pulsation or chemical action. The generation characteristics of pumps were also investigated and found to be separable into three distinct periods:

(1) Break-In Period. Generation results during the initial operating life of a pump as the moving parts "wear-in".

(2) Steady-State Period. This period is characteristic of the pump during most of its effective life. Contaminant generation is very slight.

(3) Wear-Out Period. This period immediately preceeds the failure of the pump and is characterized by a rapid increase in the

generation of contaminants by the pump.

Figure 2.3.1 shows the contaminant level in 1 milliliter of the fluid from the suction and case drain of a piston pump during its break-in period. The ratio of the case drain contaminant level to the suction level is used as a measure of the generation within the pump.

Bose (30), in a Ph.D. dissertation, investigated the generation of contaminants from cavitating surfaces. He found that the maximum size of particle generated was a function of the time during which the surface had been cavitated. A typical curve for soft aluminum, Figure 2.3.2, shows a peak in the maximum size generated followed by a steady-state period during which the generated size is constant. Bose was able to correlate the maximum size generated during the steady-state period with the Brinell hardness number for a wide range of metals which are used in the manufacture of hydraulic components. His empirical curve is shown in Figure 2.3.3.

The type of research reported by the two latter authors is characteristic of a trend among individuals actively engaged in contamination control. This trend is directed toward understanding the causes of contamination in systems so that the causes can be eliminated.

Cole (31) has conducted a study which, although not dealing directly with sources of system contamination, provides a means of describing contaminants occuring in hydraulic systems, clean rooms, and other contaminant controlled areas. He observed that many contaminant distributions can be approximated by a Gaussian distribution with a logarithmic variate, commonly called a lognormal random variable. The lognormal density function is

$$\frac{n}{\sum n} = \frac{1}{\sqrt{2\pi}\,\mathrm{Ln}\sigma}\, e^{-\frac{1}{2}\left(\frac{\mathrm{Ln}X - \mathrm{Ln}M}{\mathrm{Ln}\sigma}\right)^2}. \qquad (2.3.1)$$

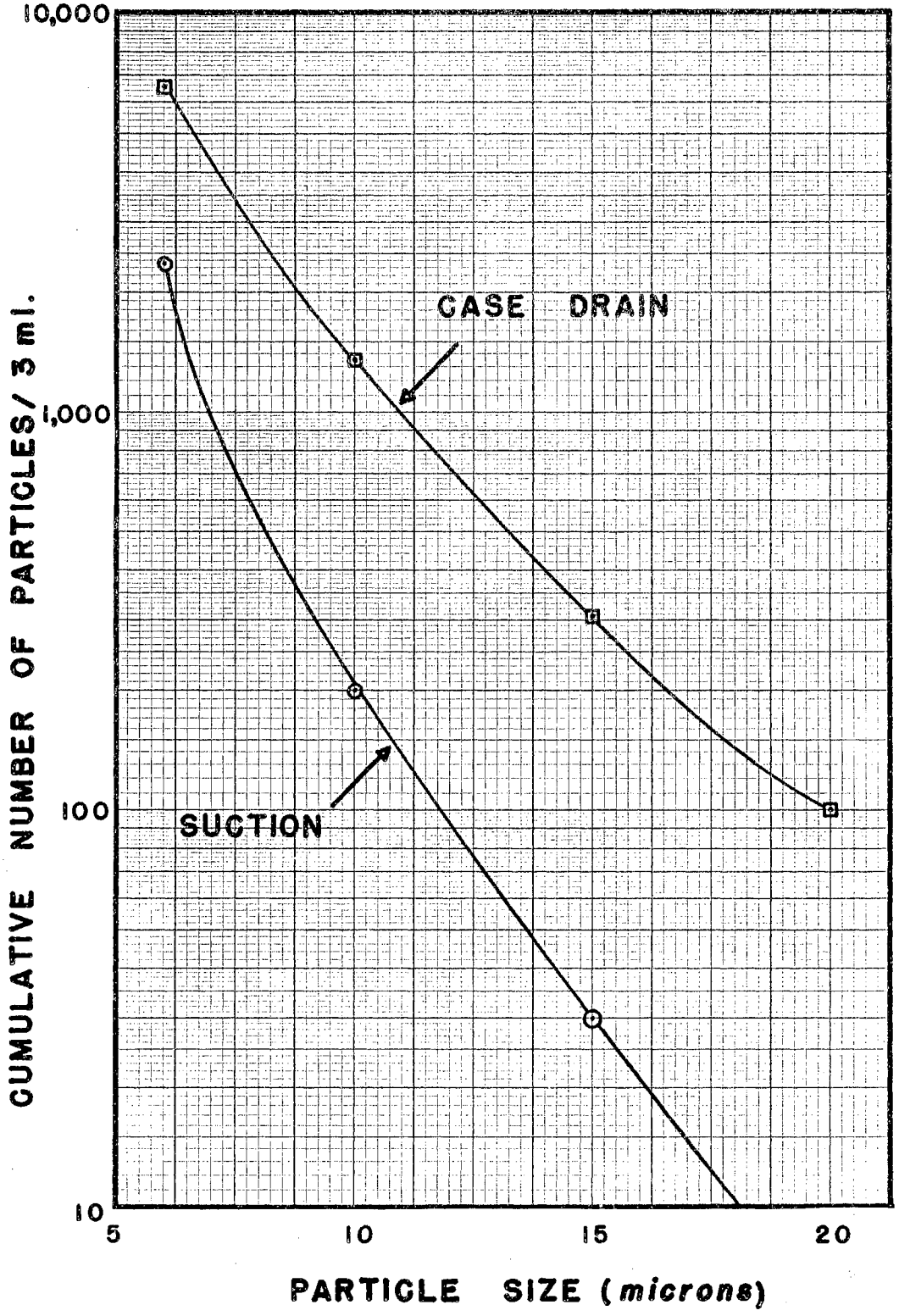

Figure 2.3.1. Contaminant Levels in a Piston Pump During Its Break-In Period

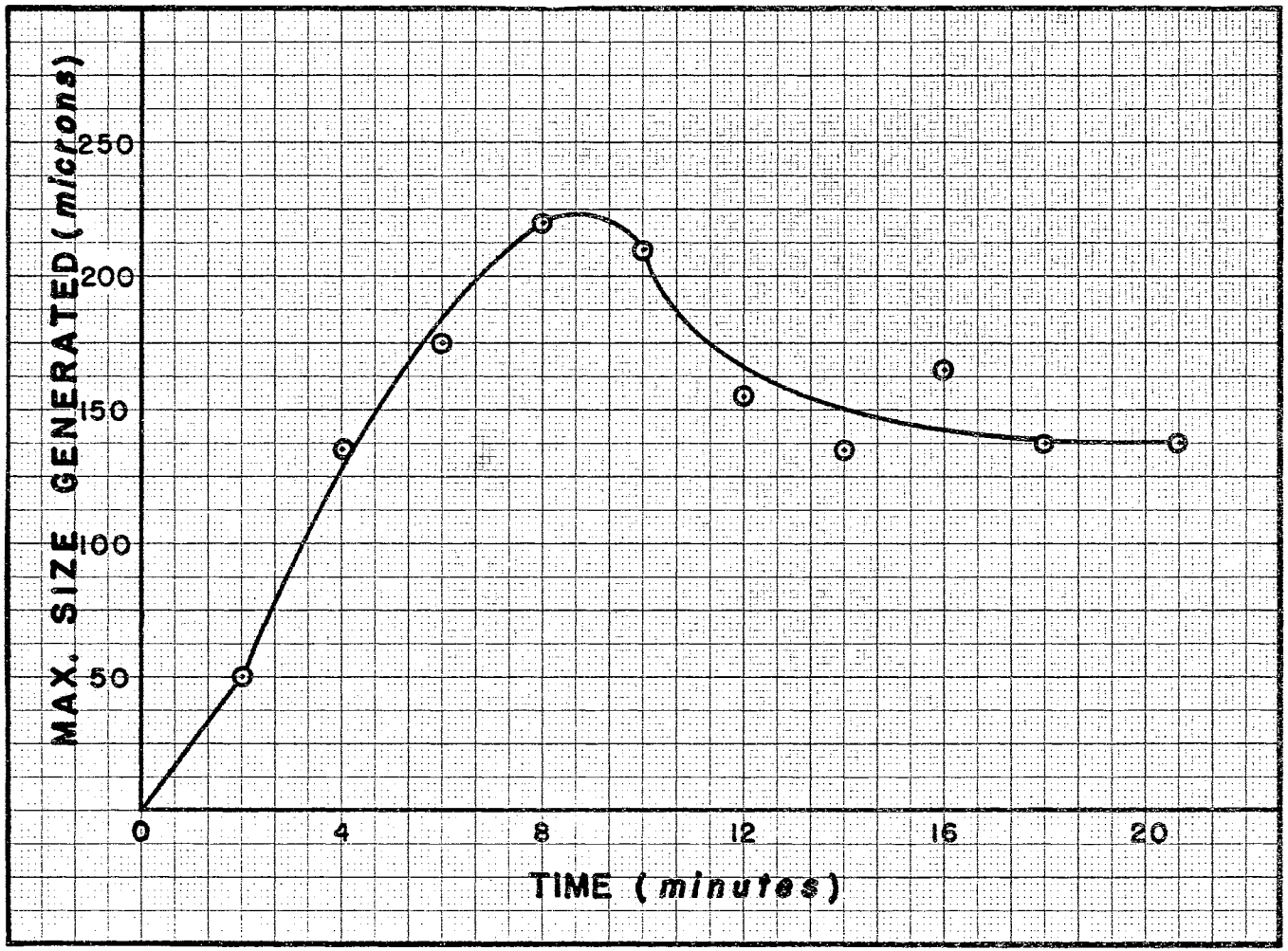

Figure 2.3.2. Contaminant Generation Cycle for Cavitation of 1100-H18 Aluminum

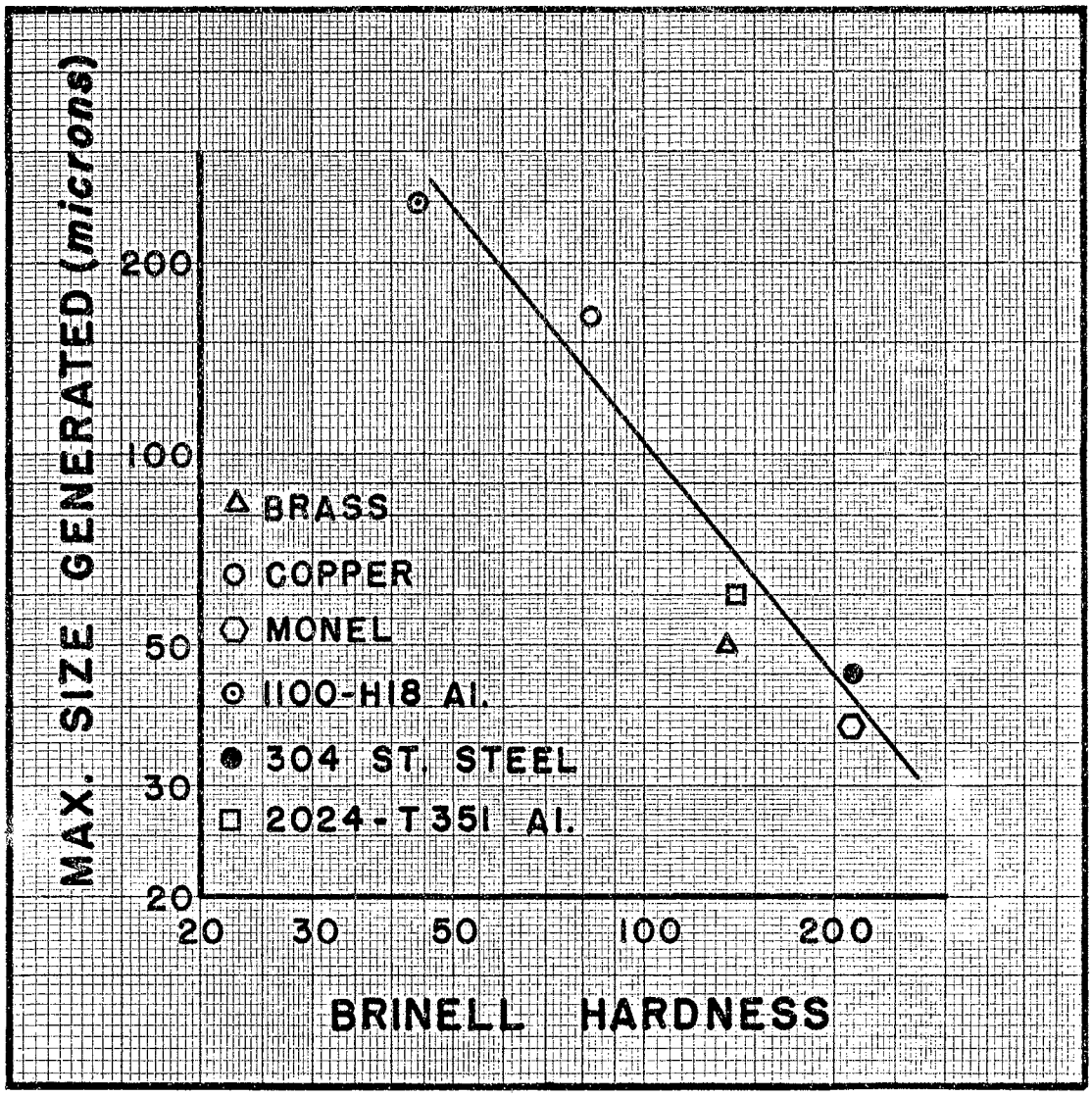

Figure 2.3.3. Correlation Curve for the Sizes of Particles Generated by Cavitation

where:

n is the number of particles, greater than x.

x is the particle size.

Lnσ is the standard deviation of the distribution function.

LnM is the mean of the distribution function.

For simplicity, Cole made the further assumption that LnM is small compared to Lnx. This suggests that Equation 2.3.1 can be reduced to a form,

$$n = A e^{-BLn^2 x} \qquad (2.3.2)$$

or,

$$Ln(n) = Ln A - BLn^2 x \qquad (2.3.3)$$

where A and B are constants. Particle size distributions can then be graphed on special paper in which n is plotted on a conventional logarithmic scale and x is plotted on a scale proportional to the square of its logarithm. Distributions which satisfy the assumptions made in the derivation will plot as a straight line on this special graph paper. Figure 2.3.4 shows the distribution curves from Figure 2.3.1 as well as the distribution curve for 10 milligrams of AC Fine Test Dust as they appear on Cole's graph paper. The straight lines obtained demonstrate the applicability of the theoretical model.

Information regarding the sources and the nature of contaminants and their distributions as they occur in hydraulic systems is necessary before a filter can be designed for a given application. Such information along with contaminant tolerance data on system components dictates the required efficiency characteristics which the filter must have. A

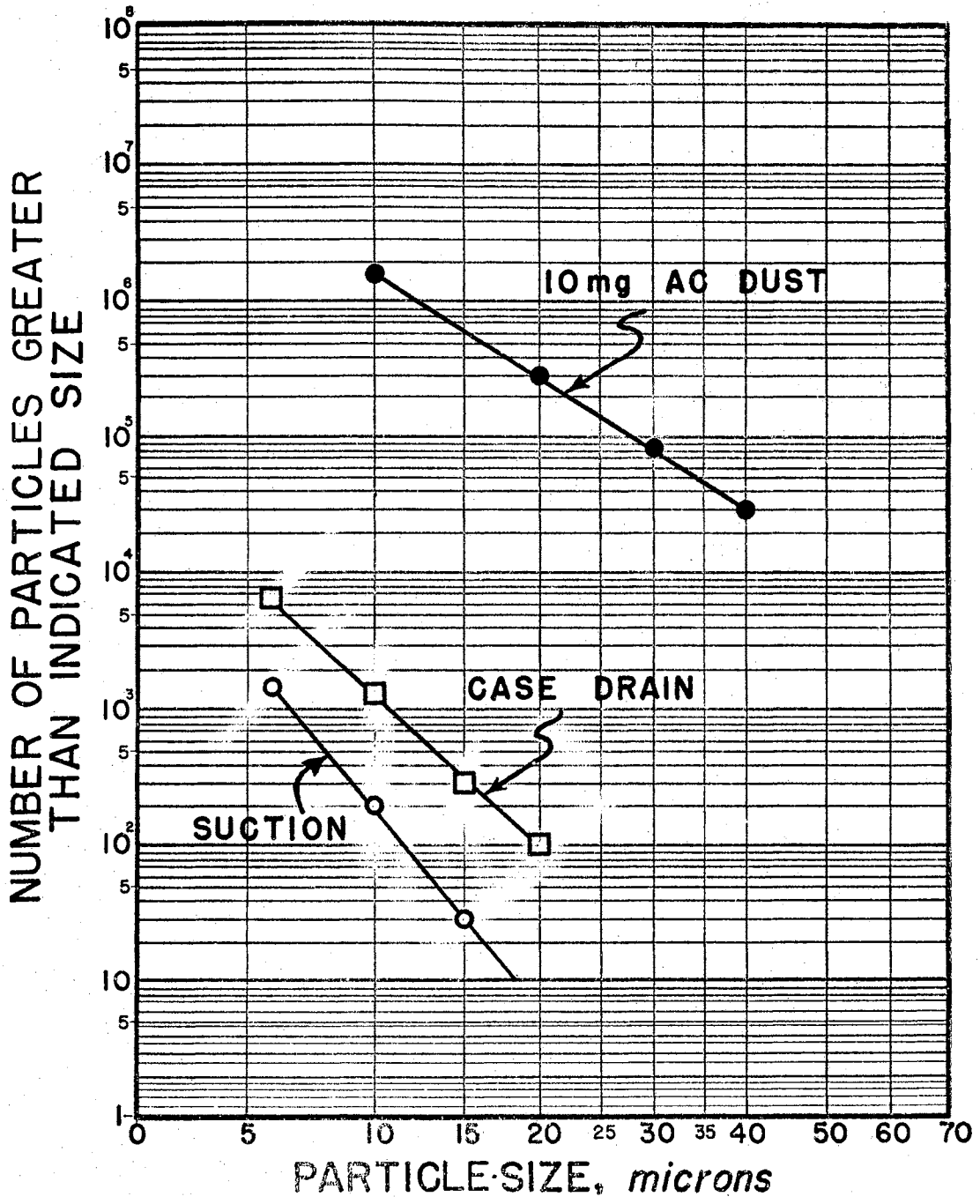

Figure 2.3.4. Contaminant Size Distributions Displayed on Log-Log Squared Graph Paper

knowledge of expected system contamination levels is also important since the physical size of a filter element is dependent upon the quantity of contaminants to be removed during its operating life.

2.4 Effects of Contamination. The most reliable test to determine whether a filter is suited for a particular application is to place the filter in the system and note if the components perform satisfactorily. This approach, although sometimes costly, is the one which has been followed almost exclusively in the selection of filters for aerospace systems. A more logical solution to the problem would be to measure the contaminant levels in which a component can perform reliably. A filter could then be selected to insure operation within this contaminant tolerance level. This approach appears to be straight forward, however only a few investigators have measured the effects of contamination on system performance.

An article written in 1944 by Thayer (32) is an exception to the norm. Thayer performed an experimental study to determine the sizes of abrasive contaminants that would be harmful to an aircraft system pump. His goal was the specification of a filter which would offer adequate protection to the pump. In his tests he operated slide valves, which had approximately the same clearances as in the pump, in a fluid contaminated with abrasives in a small size range. Thayer observed the increase in clearance over the original 10.2 microns for each size range of abrasives. The results of his testing are shown in Table III. At the conclusion of his experimental work Thayer specified that the filter required should remove all particles larger than 10 microns in size and larger and as many 5 micron particles as possible.

Stokes and Vokes (33) in studying the wear caused in automotive

TABLE III

EFFECTS OF CONTAMINANT ABRASION ON SPOOL VALVE CLEARANCES

Average size of Abrasive (microns)	Increase in Clearance (microns)	Total Clearance (microns)
3	2.5	12.7
11.5	7.5	17.7
17.5	10.2	20.4
30	17.8	28.0

engines by abrasive contaminants also made a recommendation as to the selection of a filter after first observing the effects of various sizes of contaminants. Their findings showed that although all sizes of abrasive particles influenced wear, a fairly pronounced peak of damaging capacity existed in the 10 to 15 micron range. They also observed that particles on the order of 1 micron in size had virtually no damaging effect. Consequently, a filter which was 100 percent efficient at 10 microns and totally inefficient at 1 micron would be compatible with the system requirements.

The effects of contamination on the operation of servo valves was investigated by Osgood (34). He showed that the hysterisis curve of a servo valve operating in a contaminated environment was appreciably larger than when the valve was operated in a clean system. Although Osgood encouraged the use of improved filters in servo systems, he also encouraged the redesign of hydraulic servos to make them less sensitive to contaminants. Some of his suggestions are as follows:

(1) Design larger orifices or nozzle openings.

(2) Develop a new type of hydraulic amplifier that does not

require orifices or nozzles.

(3) Reduce the spool and sleeve contact area to a minimum for low friction forces even in a contaminated system.

(4) Develop new types of metering systems having little or no sliding contact.

The need for components which are designed to be contaminant tolerant was also expressed by Klevin (35). He stated that contaminant tolerant components should be used especially in cases where system failure might endanger personnel, involve great cost, or imperil vital missions.

Fitch, et. al. (36) reported on contaminant tolerance tests performed on a sleeve type, directional control spool valve. Several valves having different clearances were operated in a system containing the 0 to 5 microns portion of AC Fine Test Dust. The contaminated fluid was circulated through the valve for a period of time and then the valve was energized. This procedure was repeated for increasing time periods until the valve failed to shift when energized. The time required to cause failure, referred to as silting time, is shown in Figure 2.4.1 for several contaminant levels. Based on these studies it was found that the valves which had increased clearances exhibited a much smaller tendency to stick.

Fitch in another report (29) presented the results of contaminant tolerance tests conducted on a hydraulic pump. The tests were performed by operating the pump in a system containing AC Fine Test Dust classified into narrow size ranges. After a break-in period the pump was operated for 30 minutes with the 5 to 10 microns contaminant. The flow delivery of the pump at the end of this period was noted. The fluid was then filtered and the test was repeated with the next larger contaminant.

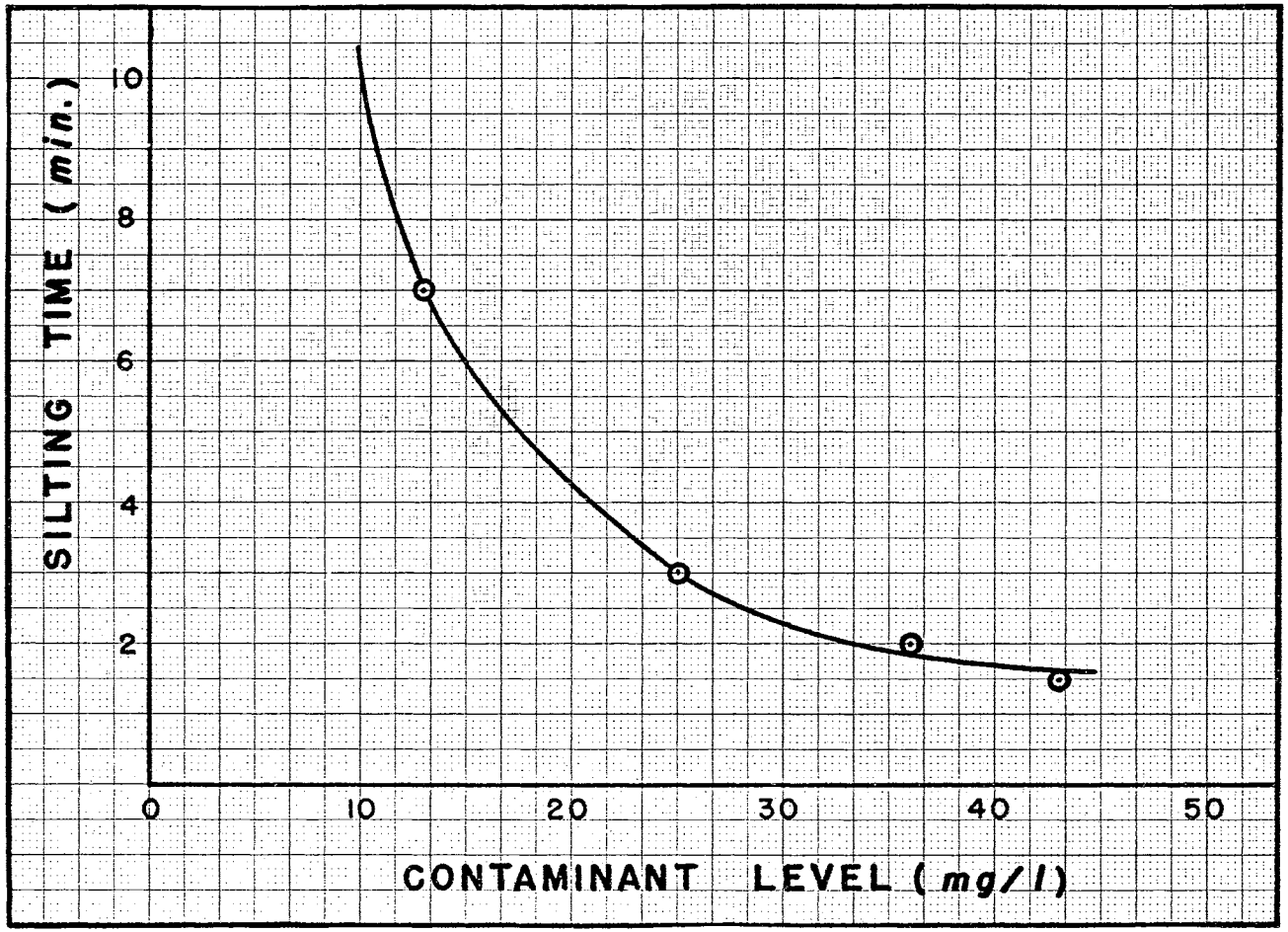

Figure 2.4.1. Time Required to Stick Valve as a Function of Contaminant Level

Figure 2.4.2 shows the flow-rate degradation curve versus time for a number of contaminant sizes. The downward break in the curve for the contaminant in the 25 to 30 micron range indicates that this is the size at which the pump begins to show sensitivity. For proper protection the suction filter for this type of pump should eliminate contaminants in this size range.

As more information about the contaminant tolerance characteristics of various types of hydraulic components becomes available, the selection of system filter can become a routine task. However, the attainment of a routine filter selection technique depends upon the availability of pertinent filtration and flow performance information on various types of filter media.

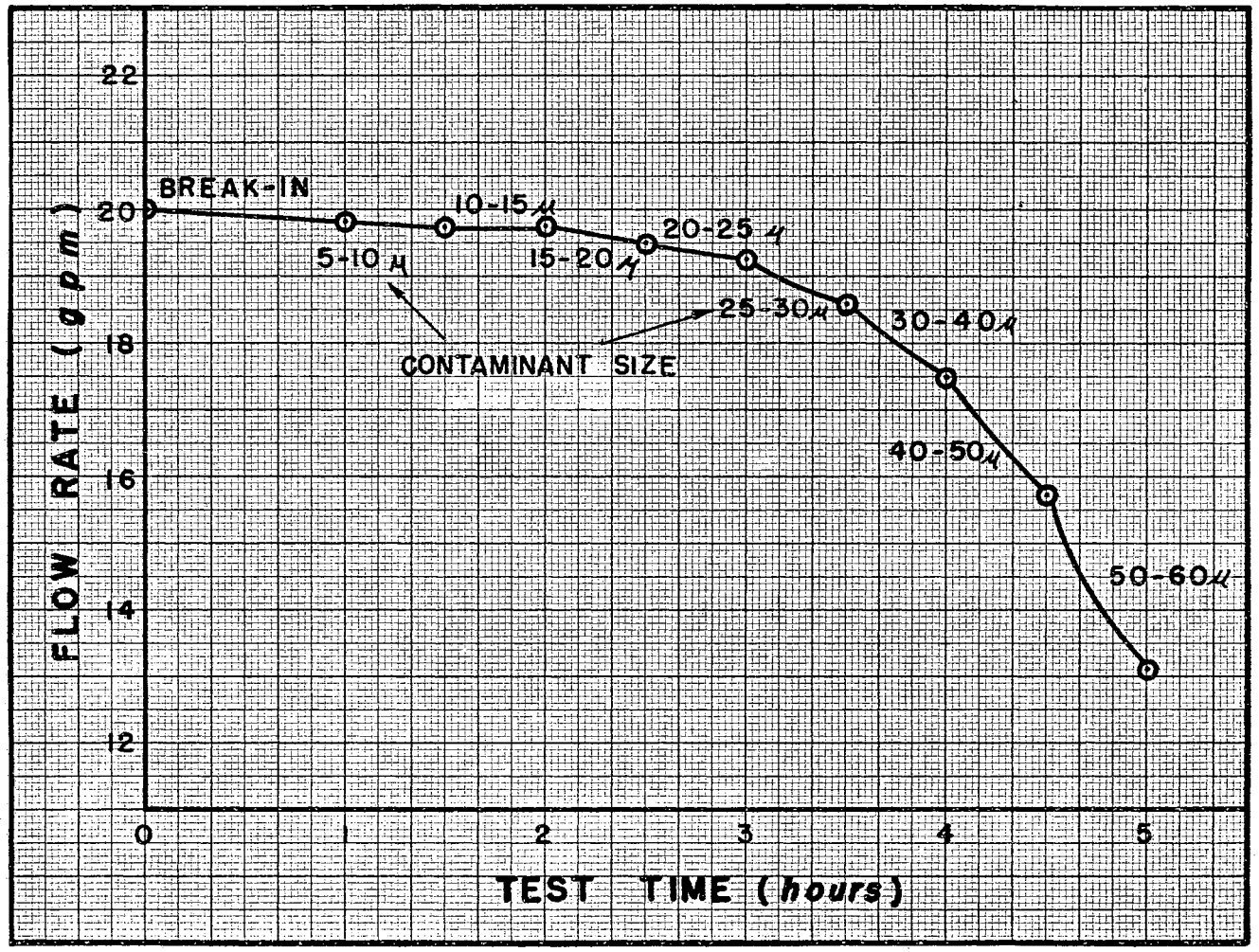

Figure 2.4.2. Pump Contaminant Tolerance Level Curve

CHAPTER III

DEVELOPMENT OF FLOW PERFORMANCE MODELS

Previous attempts to describe the flow performance of a filter medium by a theoretical model have been only partially successful. There is general agreement on which properties of the medium and the fluid are important to such a model, but the inter-relationship between these properties has eluded investigators. In this chapter, an equation is derived which accurately describes the flow-pressure relationship for single and multiple layers of wire cloth filter media. The equation represents a modification of Poiseuille's equation for laminar flow through straight cylindrical capillaries.

3.1 Single-Layered Medium. Consider a hypothetical model of a porous medium consisting of N straight cylindrical capillaries of diameter, D, and length, L. An equation for the flow through such a medium can be obtained by performing a force balance on the fluid within the medium, as shown in Figure 3.1.1. The external force on the fluid is given by the product of the differential pressure across the capillary and the cross-sectional area.

$$F_e = A_p \Delta P = \frac{\pi D^2}{4} \Delta P \,. \qquad (3.1.1)$$

where:

F_e is the external force on the interstitial fluid.

A_p is the cross sectional area of the capillary.

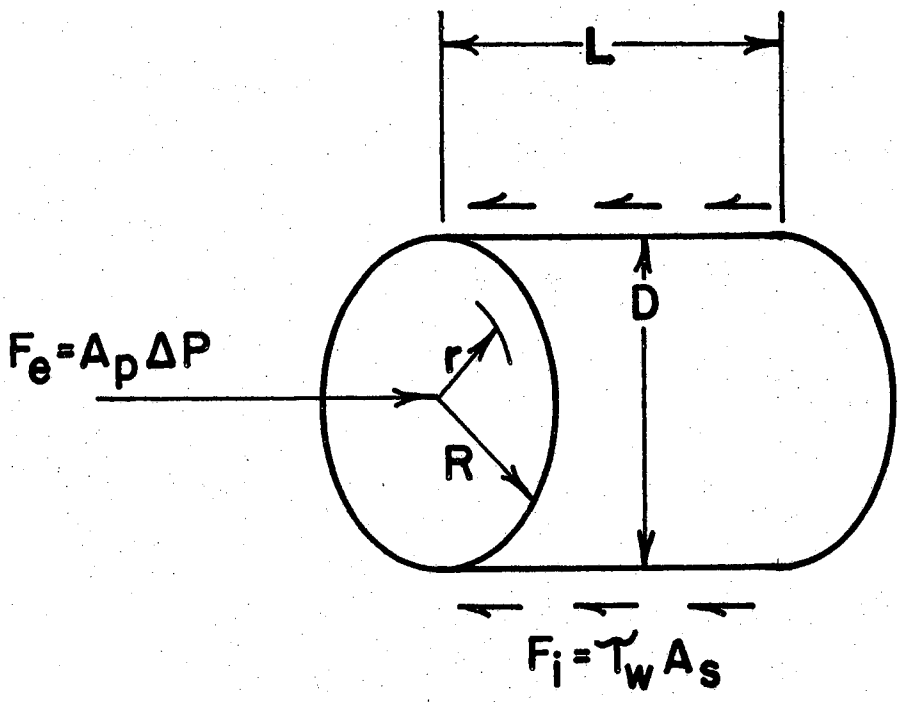

Figure 3.1.1. Force Balance on Fluid in a Cylindrical Capillary

ΔP is the pressure differential across the medium.

The internal drag force on the interstitial fluid can be equated to the product of the internal surface area of the capillary and the viscous shearing stress at the capillary wall as in the following equation;

$$F_i = \tau_w A_s = \pi D L \tau_w \quad . \tag{3.1.2}$$

where:

F_i is the internal force on the interstitial fluid.

τ_w is the viscous shearing stress at the capillary wall.

A_s is the internal surface area of the capillary.

The shearing stress is given by its defining equation as

$$\tau_w = \mu \left(-\frac{dv}{dr} \right)_{r=\frac{D}{2}} \quad . \tag{3.1.3}$$

where:

μ is the dynamic viscosity of the fluid.

$\frac{dv}{dr}$ is the velocity gradient within the capillary.

For laminar flow, the velocity distribution within the capillary is parabolic. Therefore, at any radius, r, the velocity can be expressed by

$$v = 2 V_a \left(1 - \frac{4r^2}{D^2} \right) \quad . \tag{3.1.4}$$

where:

V_a is the average velocity in the capillary.

It follows that,

$$\left(\frac{dv}{dr} \right)_{r=\frac{D}{2}} = -\frac{8 V_a}{D} \quad . \tag{3.1.5}$$

If results of Equations 3.1.5 and 3.1.3 are substituted into Equation

3.1.2, the result is

$$F_i = 8\pi\mu L V_a \cdot \tag{3.1.6}$$

Representation of V_a in terms of the flow rate through the individual capillary, q, gives

$$F_i = \frac{32\mu L q}{D^2} \cdot \tag{3.1.7}$$

If the internal drag force, F_i, is equated with the external pressure force, F_e, the flow rate through the capillary is given by

$$q = \frac{\pi D^4}{128\mu L} \Delta P. \tag{3.1.8}$$

Equation 3.1.8 gives the familiar form of the Hagen-Poiseuille law for flow through a single capillary. The total flow, Q, through the N capillaries of equal physical dimensions in the hypothetical medium may be calculated from

$$Q = \frac{N\pi D^4}{128\mu L} \Delta P \cdot \tag{3.1.9}$$

The fact that Equation 3.1.9 requires the measurement of the number of capillaries in the medium limits its application. The value of N can be determined for woven wire cloths from their geometric properties. However, for depth type media the measurement of the number of capillaries becomes a difficult task. Therefore, it is advantageous to eliminate the parameter N from Equation 3.1.9. This can be accomplished by introducing the porosity of the medium as a parameter. Recalling the definition given for porosity in Equation 2.1.4, the porosity for the model under consideration is

$$\phi = \frac{N\pi D^2}{4A} \cdot \tag{3.1.10}$$

where:

A is the total surface area of the medium.

Solving for N from this expression gives

$$N = \frac{4\phi A}{\pi D^2} , \qquad (3.1.11)$$

which can be substituted into Equation 3.1.9 to yield

$$Q = \frac{\phi A D^2}{32 \mu L} \Delta P. \qquad (3.1.12)$$

Extension of Equation 3.1.12 to modern filter media, such as wire cloth and sintered metals, requires the recognition that several of the assumptions which were valid for the ideal model may no longer be adequate. Deviations which may be expected from the ideal case are as follows:

(1) The cross-sectional areas of the capillaries are not constant through a medium. In the case of Dutch twill wire cloth the capillary varies from a rectangular shape at the surface openings to a triangular opening within the medium. Therefore, the appropriate diameter for use in the flow equation must represent the effective flow diameter of the medium.

(2) The flow path is not straight and consequently has a length greater than the thickness of the medium. This deviation is more pronounced in depth media since the fluid must follow a more tortuous path through the porous material.

Equation 3.1.12 can be revised for an actual medium to account for these two areas of concern by using the concept of an equivalent circular diameter for the capillary. Consider the representation of an irregularly shaped capillary shown in Figure 3.1.2. Let the hydraulic diameter at

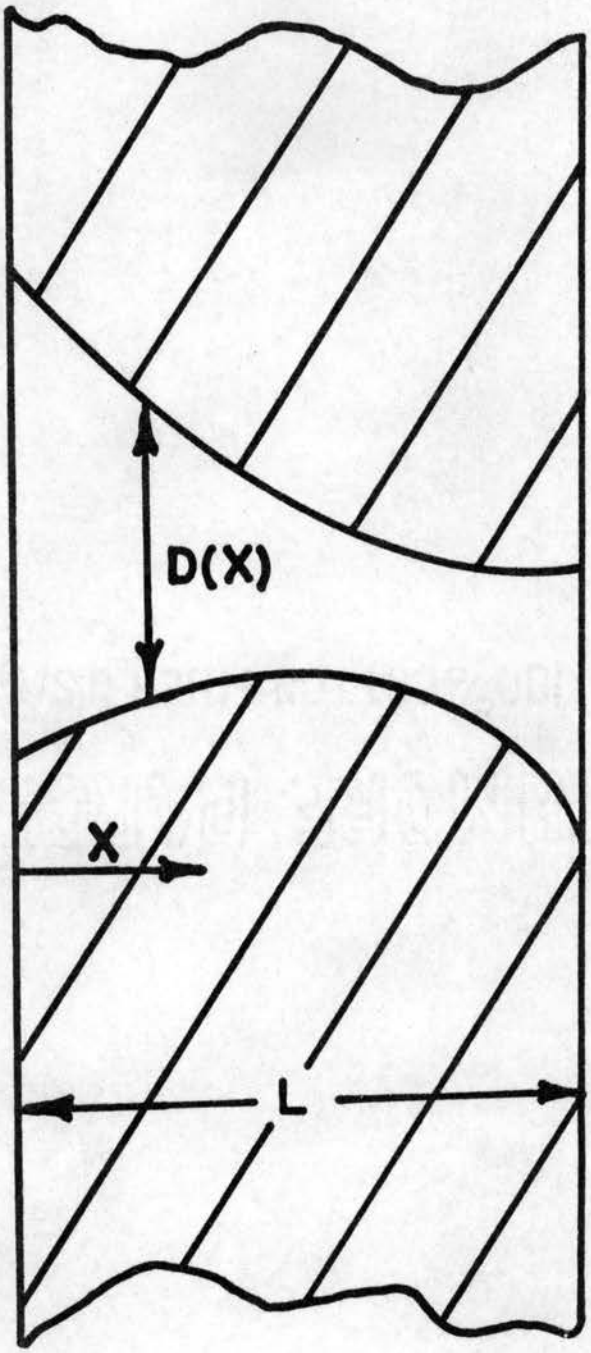

Figure 3.1.2. Irregularly Shaped Capillary

a distance x into the medium be given by D(x). The volume of the capillary, V_c, may then be calculated from the integral,

$$V_c = \int_0^L \frac{\pi [D(x)]^2}{4} \, dx . \qquad (3.1.13)$$

Taking this volume and representing it by a straight cylindrical capillary of diameter, D_a, and length, L, gives

$$D_a = \sqrt{\frac{4V_c}{\pi L}} = \left[\frac{1}{L}\int_0^L [D(x)]^2 \, dx\right]^{1/2} . \qquad (3.1.14)$$

In this manner an actual medium can fit the theoretical model if D_a can be measured. Accepting this fact, Equation 3.1.12 is correct providing that the equivalent cylindrical diameter is substituted for D to give

$$Q = \frac{\phi A D_a^2}{32 \mu L} \Delta P . \qquad (3.1.15)$$

It will be shown in Chapter 5 that D_a can be measured by mercury intrusion porosimetry.

Equation 3.1.15 is an analytical equation which can be used to calculate the flow-pressure relationship through a woven wire cloth in terms of the properties of the medium and the fluid. The validity of this equation will be proven experimentally for several wire cloth media as well as for one sintered metal depth medium.

3.2 Cascaded Media. The flow properties of multi-layered media are also of interest, since multiple layers of material are often used. In some applications a backup wire mesh is required to give the primary filter medium structural support. In other cases multiple layers are used to improve the filtration performance by means of the depth filtration characteristics of the resultant medium.

Consider a cascaded medium consisting of n individual layers, iden-

tified by the subscripts, 1, 2, ..., n-1, n. Applying Equation 3.1.15 the flow through the i-th layer is given by

$$Q_i = \left(\frac{\phi A D_a^2}{32 \mu L}\right)_i \Delta P_i = C_{fi} \Delta P_i \,. \qquad (3.2.1)$$

where:

C_{fi} is the flow constant for the i-th layer.

The total pressure loss through the cascaded medium is equal to

$$\Delta P = \sum_1^n \Delta P_i = \sum_1^n \left(\frac{32 \mu L Q}{\phi A D_a^2}\right)_i = \sum_1^n \frac{Q_i}{C_{fi}} \,. \qquad (3.2.2)$$

If it is assumed that the areas of each of the layers are equal and that the temperature of the fluid is constant, Equation 3.2.2 can be simplified to read

$$\Delta P = \frac{32 \mu Q}{A} \sum_1^n \left(\frac{L}{\phi D_a^2}\right)_i \,. \qquad (3.2.3)$$

Expressed in terms of the flow rate the equation becomes

$$Q = \frac{A/32\mu}{\sum_1^n \left(\frac{L}{\phi D_a^2}\right)_i} \Delta P \,, \qquad (3.2.4a)$$

or

$$Q = \frac{\Delta P}{\sum_1^n \frac{1}{C_{fi}}} \,. \qquad (3.2.4b)$$

Equations 3.2.4a and 3.2.4b are general forms of the flow equation for cascaded media. However, practical limits such as allowable pressure loss requirements probably preclude the use of more than three layers of media in series. For two layers of material the equations are

$$Q = \frac{A/32\mu}{\frac{L_1}{\phi_1 D_1^2} + \frac{L_2}{\phi_2 D_2^2}} \Delta P \,, \qquad (3.2.5a)$$

and

$$Q = \frac{\Delta P}{\frac{1}{C_{f1}} + \frac{1}{C_{f2}}} \quad . \tag{3.2.5b}$$

For three layers in cascade the equation is

$$Q = \frac{\Delta P}{\frac{1}{C_{f1}} + \frac{1}{C_{f2}} + \frac{1}{C_{f3}}} \quad . \tag{3.2.6}$$

3.3 Parallel Media. Filters using media in parallel configurations are not common, although in some instances low flow rate elements are used in parallel with high flow rate elements having poorer filtration characteristics. It will be shown in Chapter 6 that media having different filtration characteristics can be effectively used in parallel to obtain a desired filtration characteristic. Consequently, it is of interest to derive the appropriate flow equation for parallel media.

Consider n filter media in parallel. The total flow rate is given by the summation of the flows through the individual media.

$$Q = \sum_{1}^{n} Q_i \quad . \tag{3.3.1}$$

Substituting the expression from Equation 3.2.1 and recognizing that the pressure loss through each medium is the same, the equation becomes

$$Q = \Delta P \sum_{1}^{n} C_{fi} = \frac{\Delta P}{32\mu} \sum_{1}^{n} \left(\frac{\phi A D_a^2}{L} \right)_i \quad . \tag{3.3.2}$$

For two media in parallel the flow equation reduces to

$$Q = \left(\frac{\phi_1 A_1 D_1^2}{L_1} + \frac{\phi_2 A_2 D_2^2}{L_2} \right) \frac{\Delta P}{32\mu} \quad . \tag{3.3.3}$$

CHAPTER IV

DEVELOPMENT OF FILTRATION PERFORMANCE MODELS

The various methods used to evaluate and rate the filtration performance of filter media tell very little about the medium. Generally, all that is established is how much of the specified contaminant the filter removed under the imposed operating conditions. To accurately describe filtration performance, the capillary size distribution curve for a medium should be known. As discussed in Section 2.2, Cranston (17) showed how the capillary size distribution curve can be obtained from the filtration efficiency curve. Other authors have applied Cranston's theories to obtain the capillary distribution curves for various media, but none has attempted to describe the resultant distributions other than graphically.

It is desirable to express the capillary size distribution in a more general manner than by simply having it displayed as a curve. For design applications it is advantageous to describe the distribution curve by a mathematical or statistical model. In this chapter, the hypothesis will be made that the capillary size distribution curve for wire cloth filter media can be described by a Gaussian or normal distribution function. The filtration models for media in cascade and in parallel will be determined on this basis. For all of the derivations, the assumption is made that the medium is essentially clean.

4.1 Single-Layered Medium. The assumption of a normal distribution

for the capillary sizes of woven wire cloth media appears reasonable when the structure of the cloth and the manufacturing processes are considered. The cloth is usually woven from stainless steel wires whose diameters must meet tolerance requirements on the order of plus or minus one micron. The mesh counts, i.e., the number of wires per linear inch, are also controlled within specified limits. The allowable tolerances for three Dutch twill media are given in Table IV.

TABLE IV

ALLOWABLE TOLERANCES ON WIRE SIZE AND MESH COUNT OF DUTCH TWILL MEDIA

Nominal Mesh Count	Mesh Count Range (no. wires/in.)		Wire Size Range(micron)	
	Warp*	Shoot**	Warp	Shoot
325x2300	325± 2	2100± 50	38 ± 1	25± 0.5
200x1400	200 ± 2	1350 ± 30	70 ± 1	40 ± 1
165x1400	165 ± 2	1350 ± 30	70 ± 1	40 ± 1

*Warp wires are the wires running the long way of the cloth as woven.

**Shoot wires are the wires running across the short way of the cloth as woven.

The capillary size distribution of a medium is directly dependent upon the uniformity of the weaving process. Since the products of most manufacturing processes exhibit a normal distribution about the nominal product, it can be expected that the variations in wire cloth will also exhibit a normal distribution. A variable x is said to be normally distributed if its density function is given by

$$n(x) = \frac{1}{\sqrt{2\pi}\,\sigma} e^{-\frac{(x-\bar{x})^2}{2\sigma^2}} . \qquad (4.1.1)$$

where:

$\bar{X}$ is the mean of the distribution.

σ is the variance of the distribution.

X may vary between $\pm\infty$.

The function in Equation 4.1.1 actually represents a two parameter family of distributions. Variations in $\bar{x}$ change the position of the distribution curve along the x axis; variations in σ change the shape of the distribution curve. As the value of σ increases, the broadness of the distribution curve also increases. Figure 4.1.1 shows two normal distribution functions with different means and variances. Since n(x) is given to be a density function, it is implied that

$$N(x) = \int_{-\infty}^{x} n(x)\, dx \,, \qquad (4.1.2)$$

and

$$N(\infty) = 1 \,.$$

where:

N(x) is the cumulative distribution function.

Figure 4.1.2 shows the cumulative distributions of the two normal distribution functions in Figure 4.1.1.

In applying the concept of a normal distribution to the variation of capillary sizes within a wire cloth medium, it is apparent that the particle removal efficiency curve for the medium is actually a cumulative distribution curve. However the limits on the variable are no longer minus and plus infinity, but are zero to infinity. Letting the cumulative capillary size distribution for the medium be represented by E(D), Equation 4.1.2 becomes

$$E(D) = \int_{0}^{D} e(D)\, dD, \qquad (4.1.3)$$

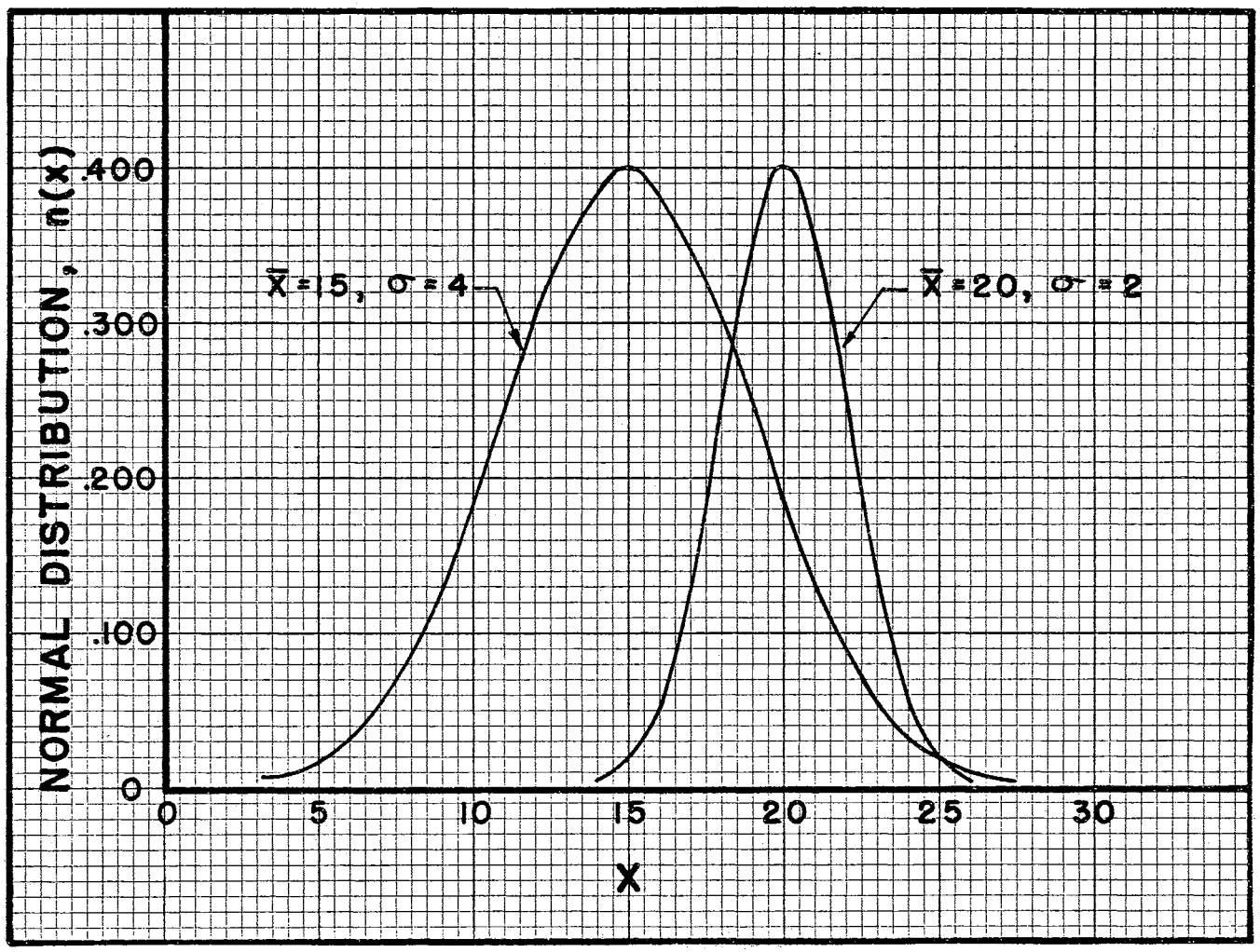

Figure 4.1.1. Normal Distribution Curves

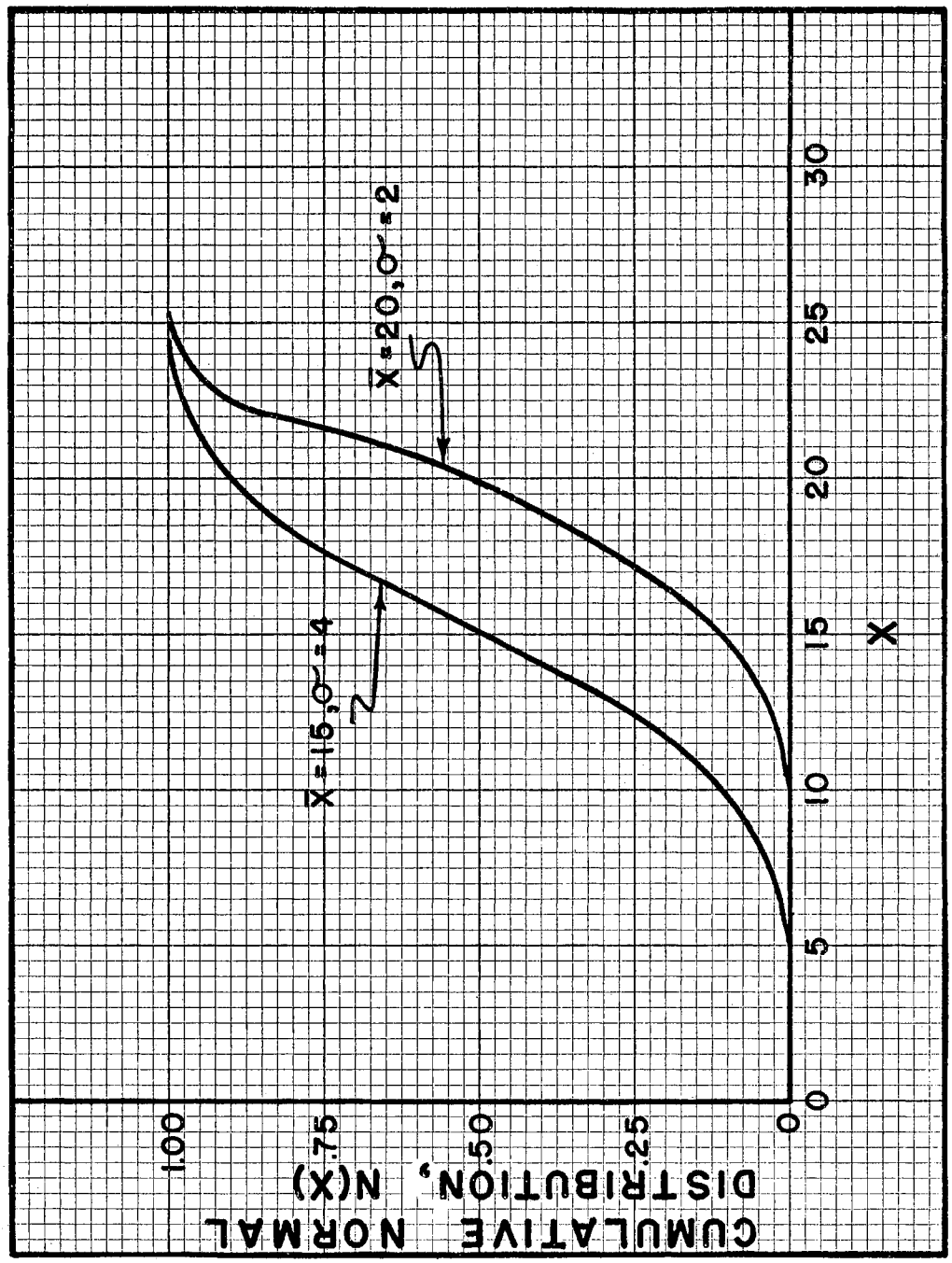

Figure 4.1.2. Cumulative Normal Distribution Curves

and

$$E(\infty) = 1 .$$

where:

e(D) is the capillary size distribution function.

Differentiating, the capillary size distribution function is obtained as

$$e(D) = \frac{dE(D)}{dD} . \qquad (4.1.4)$$

For e(D) to be distributed normally then it must satisfy Equation 4.1.1 as shown below.

$$e(D) = \frac{1}{\sqrt{2\pi}\sigma} e^{-\frac{(D-\bar{D})^2}{2\sigma^2}} . \qquad (4.1.5)$$

where:

$\bar{D}$ is the average capillary diameter.

If a medium has a normal distribution of capillary sizes then the average diameter of the distribution coincides with the diameter for which the efficiency is fifty percent. The complete definition of the capillary size distribution function requires the entire efficiency curve.

From a manufacturing standpoint the efficiency curve for an ideal wire cloth medium would be the step curve shown in Figure 4.1.3. Such a medium would have a spike for the distribution curve, Figure 4.1.4, which indicates that there is only one pore size within the medium. An evaluation of the manufacturing techniques of various suppliers of wire cloth can be made by comparing the relative sharpness of the capillary size distribution curves of the media. Media manufactured under superior quality controls will have distributions with smaller values for the variance.

Figure 4.1.3. Efficiency Curve for an Ideal Wire Cloth

Figure 4.1.4. Capillary Size Distribution Curve for an Ideal Wire Cloth

Describing the filtration performance of a wire cloth medium by determining its capillary size distribution function is a more meaningul approach than measuring a nominal rating for the medium. The distribution function is a property of the medium while the nominal rating merely measures the performance of the medium under certain test conditions. Because of rigid manufacturing controls, the distribution functions for wire cloth media should follow the normal curve of Equation 4.1.5. For other media, such as sintered metals or paper, the capillary distribution might be described by a skewed model such as the gamma distribution.

4.2 Cascaded Media. A study of the filtration performance characteristics of cascaded filter media is important in two respects. First, the efficiencies of cascaded media are improved over that of any of the individual layers. Economically two layers of a coarse, less expensive wire cloth might replace a single layer of expensive cloth. Another important reason for knowing the filtration performance of cascaded media is associated with recirculating systems. In effect, each time the fluid makes a complete cycle, the filter appears as another layer of medium in cascade. Therefore, for a system with a given initial contaminant level, the level after two or more complete circulations through the filter can be calculated from the performance characteristics of cascaded media.

The effects of cascading media can be calculated from the cumulative capillary size distribution curves for the individual layers. For example, consider a medium whose cumulative capillary distribution, i.e. its efficiency, is given by E(D). At any diameter D_1 the medium has an efficiency given by the equation

$$E(D_1) = \int_0^{D_1} e(D)\,dD . \qquad (4.2.1)$$

Associated with this point the medium also has a transmission factor, $T(D_1)$, such that

$$E(D_1) + T(D_1) = 1 . \qquad (4.2.2)$$

In terms of the filtration process, Equation 4.2.2 states that the fraction of particles of size D_1 retained by the filter plus the fraction which pass through equals the total number of particles presented to the filter. Applying the results of Equation 4.2.1, the transmission factor at D_1 is given by

$$T(D_1) = 1 - \int_0^{D_1} e(D)\,dD . \qquad (4.2.3)$$

$T(D_1)$ represents the probability that a particle of size D_1 will pass through the medium.

It follows that if n media of various types are placed in series the overall probability of passing a particle of size D would be the product of the probabilities of the particle passing through each individual layer. This assumes that the performance of each layer is independent of the others. In equation form, the overall transmission factor at D is given by the product

$$T_c(D) = \prod_1^n T_i(D) . \qquad (4.2.4)$$

where:

$T_c(D)$ is the overall transmission factor for the cascaded media.

$T_i(D)$ is the transmission factor for the i-th individual layer of medium.

The resultant efficiency at D for n cascaded media may be calculated from Equations 4.2.2 and 4.2.4 as

$$E_c(D) = 1 - T_c(D) = 1 - \prod_1^n T_i(D) . \qquad (4.2.5)$$

where:

$E_c(D)$ is the overall efficiency of the cascaded media to particles of size D.

Using Equation 4.2.3, the overall efficiency for the cascaded media may also be expressed by

$$E_c(D) = 1 - \prod_1^n \left[1 - \int_0^D e_i(D)\, dD\right] . \qquad (4.2.6)$$

where:

$e_i(D)$ is the capillary size distribution function for the i-th medium.

Equation 4.2.6 can be used to calculate the efficiency characteristics of cascaded media. However, it is usually more straight forward to construct the efficiency curve from Equation 4.2.5.

A special case of the theory discussed above deserves mention because of its applicability. This is the case in which the individual layers consist of the same material. The performance of a filter in a recirculating system is also included in this category. For both of these cases the overall transmission factor at a diameter D_1 is equal to

$$T_c(D_1) = \left[T(D_1)\right]^n . \qquad (4.2.7)$$

where:

$T(D_1)$ is the transmission factor for one layer of the medium.

n is the number of layers of cascaded media or the number of cycles of the fluid through the filter.

The overall efficiency for this special case is

$$E_c(D_1) = 1 - [T(D_1)]^n . \qquad (4.2.8)$$

Figure 4.2.1 shows the efficiency curves for one, two, and five layers of the same medium. These curves coincide with the effective efficiency of a single filter when the fluid makes one, two, and five passes through it. The broken curve is the limiting case for an infinite number of layers or an infinite number of passes through a single filter.

4.3 Parallel Media. The analytical description of the filtration performance of media in parallel requires both a description of the capillary size distributions of the individual media and the equations of flow for parallel media. To illustrate, consider n media with different properties in a parallel configuration. The removal efficiency of each medium is applied to the fraction of the total number of particles in the feed which are presented to it. This fraction is equal to the fraction of the total flow which passes through the individual medium. Recalling Equation 3.2.1 and 3.3.2, the fraction for the i-th layer is

$$\frac{Q_i}{Q} = \frac{C_{fi}}{\sum_1^n C_{fi}} . \qquad (4.3.1)$$

If the total number of particles of size D in the feed is $N_u(D)$, the number presented to the i-th layer is

$$N_{ui}(D) = \frac{C_{fi}\, N_u(D)}{\sum_1^n C_{fi}} . \qquad (4.3.2)$$

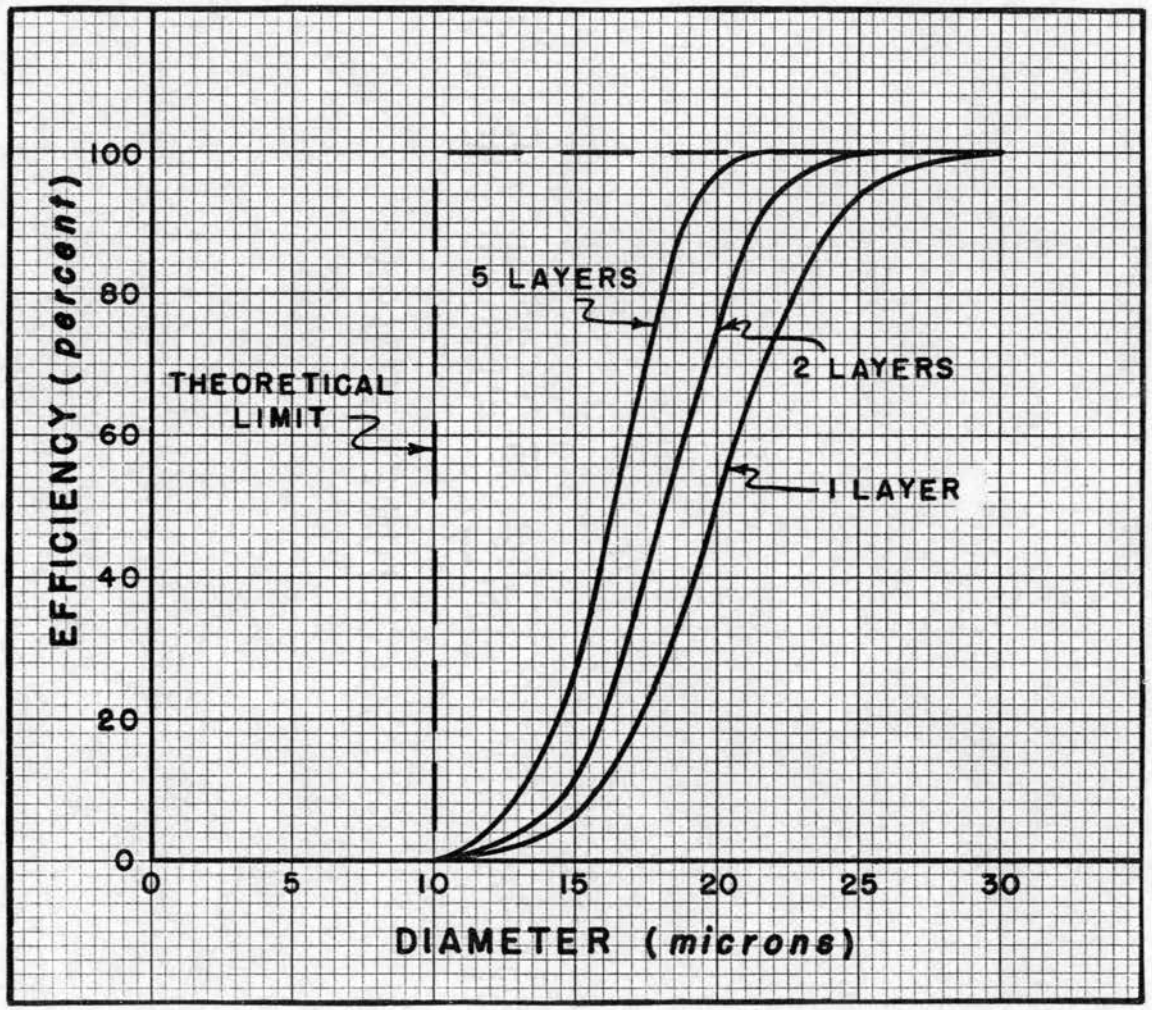

Figure 4.2.1. Typical Efficiency Curves for Cascaded Media

The number of particles of size D passing through the i-th medium, $N_{di}(D)$, may be found from the equation

$$N_{di}(D) = T_i(D)\, N_{ui}(D) = \frac{C_{fi}\, T_i(D) N_u(D)}{\sum_1^n C_{fi}} \,. \qquad (4.3.3)$$

The total number of particles of size D which pass through the parallel media is

$$N_d(D) = \sum_1^n N_{di}(D) = \frac{\sum_1^n C_{fi}\, T_i(D)}{\sum_1^n C_{fi}}\; N_u(D) \,. \qquad (4.3.4)$$

The equation for the transmission factor for parallel operation is then

$$T_p(D) = \frac{N_d(D)}{N_u(D)} = \frac{\sum_1^n C_{fi}\, T_i(D)}{\sum_1^n C_{fi}} \,. \qquad (4.3.5)$$

From Equation 4.3.5 the efficiency in parallel can be calculated as

$$E_p(D) = 1 - \frac{\sum_1^n C_{fi}\, T_i(D)}{\sum_1^n C_{fi}} \,. \qquad (4.3.6)$$

The complete efficiency curve for parallel media can be determined by evaluating Equation 4.3.6 for various values of D.

CHAPTER V

EXPERIMENTAL VERIFICATION OF FLOW MODELS

The utilization of the flow equations developed in Chapter 3 depends upon the accuracy with which the various properties of the filter media can be measured. Consequently, a brief discussion of the various experimental methods used to measure the media parameters will precede the experimental verification of the flow equations for single-layered media and multiple media in cascade and parallel.

5.1 Experimental Methods. Recalling the basic equation for flow through a single layer of filter material, Equation 3.1.15, there are five properties of either the medium or the fluid which must be measured before the flow-pressure relationship can be defined. Several of these properties are readily obtainable while the others require some effort. The thickness of the medium, L, and the area exposed to flow are easily measured. For the flow tests reported in this chapter the media were sealed into the sample holder of Figure 5.1.1, which exposed π square inches to flow.

Several methods exist to measure the fraction of void space or porosity of a porous medium. For the present case, the solid matrix of the medium consists of a homogeneous material of known properties, and the density method emerges as the most straight forward approach. The total volume of a filter medium is given by the sum of the pore volume and the volume of the solid material;

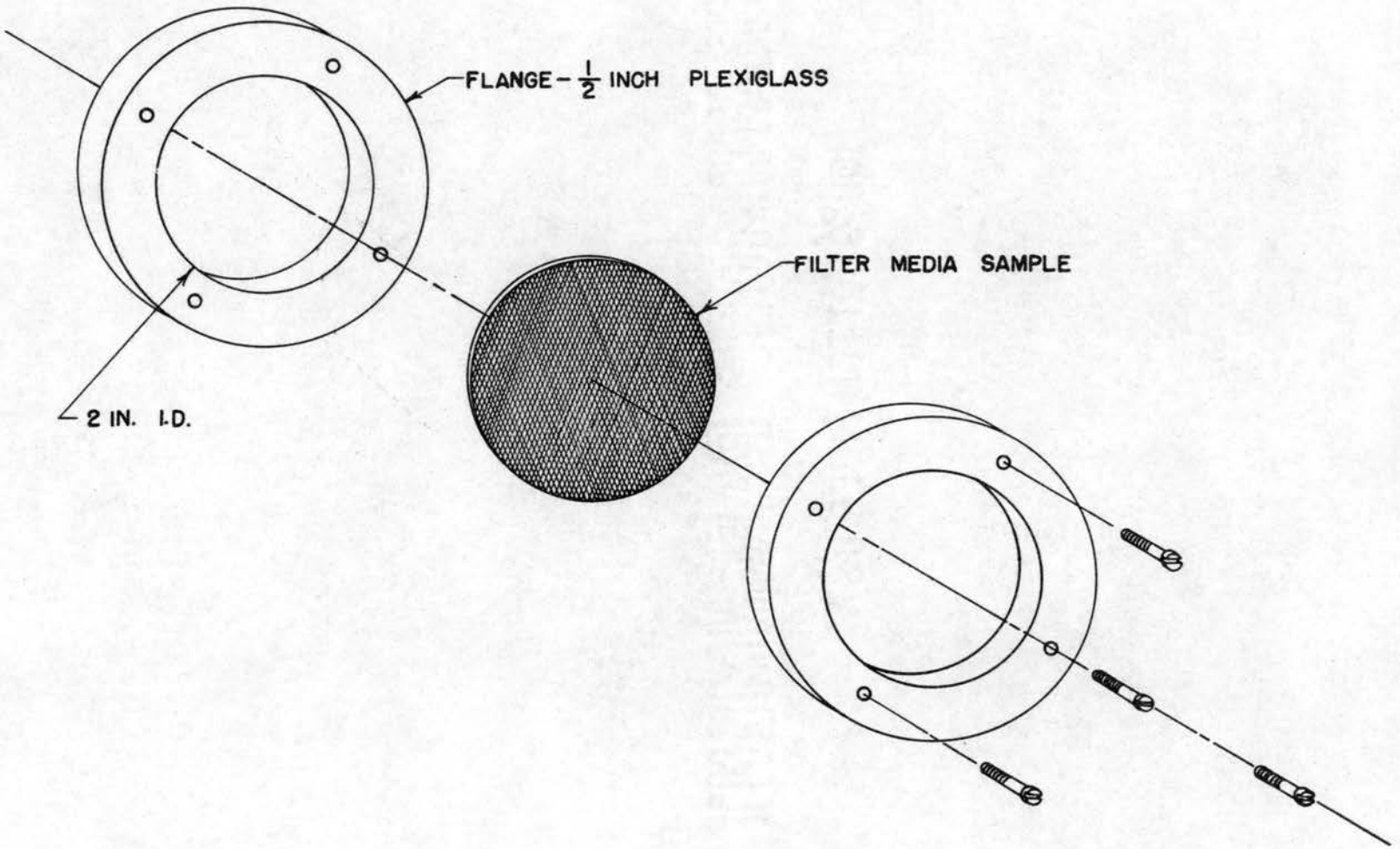

Figure 5.1.1. Filter Media Sample Holder

$$V_T = V_P + V_S \quad . \tag{5.1.1}$$

Recalling the definition of porosity, the pore volume can be given by the product,

$$V_P = \phi V_T \quad . \tag{5.1.2}$$

If the porous material is dry and weighed in air, its solid volume is

$$V_S = \frac{W}{\rho_S} \quad . \tag{5.1.3}$$

where:

W is the weight of the medium.

ρ_s is the density of the solid material.

Substituting the results of Equations 5.1.2 and 5.1.3 into Equation 5.1.1 and solving for ϕ yields

$$\phi = 1 - \frac{W}{\rho_s V_T} \quad . \tag{5.1.4}$$

The dependence of this method upon an accurate knowledge of the density of the solid medium is the primary source of error in the results. However, all of the media tested in the present study are stainless steel, and the density is essentially constant. A value of 8.1 gm./cc. was used for the density of stainless steel. The weights of the samples of media were measured with a Satorious Semi-Micro Balance with a readibility of 10^{-5} gram.

The property of the medium most difficult to measure is its capillary size. This is true because there may be several pores within a medium whose diameters could be chosen as characteristic of the medium. For example, the Dutch twill of Figure 2.2.1 has rectangular pores at

the surface and triangular pores within the material. Either of these pores could be used to characterize the medium. For describing the filtration performance of a Dutch twill cloth the size of the triangular pore is important since it offers the primary restriction to the passage of contaminants. However, to describe the flow performance of a Dutch twill medium, neither of these pore sizes can be used. As discussed in Section 3.1, an average diameter based on the capillary volume is the appropriate diameter for studying the flow performance of a filter medium.

A diameter based on the capillary volume of a porous medium can be measured using the mercury intrusion porosimetry techniques described in Appendix A. Briefly stated, the process is one of forcing mercury into the interstices of a porous medium. As the pressure on the mercury is increased, smaller pores in the medium become saturated with mercury. By measuring the volume of mercury which passes into the medium for each increase in pressure, a curve of volume injected versus pressure can be obtained. This curve is a cumulative distribution curve from which a distribution curve of frequency of pore volume versus pressure can be calculated by evaluating the slope of the cumulative curve at various pressures. Applying a static balance of forces within the medium, the applied pressure can be related to the size of the capillary being saturated. Ultimately, a curve of frequency of pore volume versus capillary size can be prepared. The diameter at which the peak of this distribution curve occurs gives the average capillary diameter on a volumetric basis.

The viscosity of the fluid medium is the only property of the fluid that enters into the flow-pressure relationship. The fluid used was

Mil-H-5606 hydraulic fluid whose temperature was maintained at 100°F. for testing all of the flow performance models. The viscosity of this fluid was measured by a Brookfield Synchrolectric viscometer and found to be 12 centipoise at 100°F.

The actual measurement of the flow performance characteristics of single layer, cascaded, and parallel media was carried out using the Filter Media Performance Test Stand described in Appendix B. A test sample was sealed in the sample holder of Figure 5.1.1, using a gasket sealing compound. The holder was installed in the housing shown in Figure 5.1.2 and the assembled unit placed in the test section of the stand. Pressure differential versus flow rate data were obtained on each filter sample for a number of flow rates up to 16 gpm. The pressure differentials were taken in accordance with SAE ARP-24A. A curve giving the line losses between the pressure pick-up points as a function of flow-rate was also measured and used to calculate the true pressure-flow curve for the filter medium.

5.2 Single-Layered Medium. As shown in Section 3.1, the flow-pressure relationship through a single layer of filter material is given by

$$Q = \frac{\phi A D_a^2}{32 \mu L} \Delta P = C_f \Delta P. \qquad (3.1.15)$$

Measuring the various constituents of this equation in common units, the equation becomes

$$Q(\text{gpm}) = 0.87 \times 10^{-4} \frac{\phi A(\text{Sq. In.}) D_a^2(\text{microns}^2) \Delta P(\text{psi})}{\mu(\text{centipoise}) L(\text{In.})} . \qquad (5.2.1)$$

The validity of the flow performance model described by this equa-

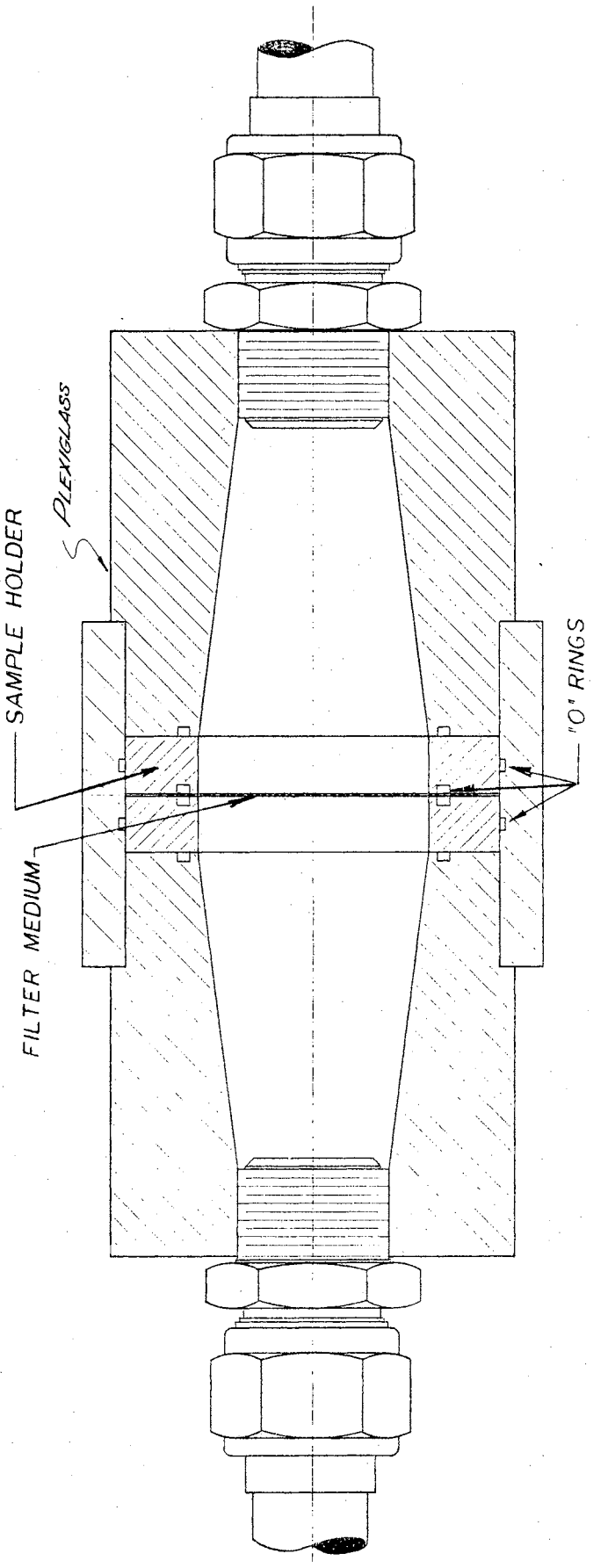

Figure 5.1.2. Filter Media Test Housing

tion was tested using four different media. Three of the media were woven wire cloths and the fourth was a depth medium manufactured by sintering stainless steel fibers together. The latter material was included in the experimental program to evaluate the applicability of the model to depth media. The measured properties of the test media are given in Table V.

TABLE V

MEDIA PROPERTIES

Nominal Mesh	Weaving Pattern	Thickness L (in.)	Porosity ϕ	Effective Diameter D_a (microns)
200x600	Dutch Twill (single)	0.0055	0.60	35
165x1400	Dutch Twill (double)	0.0058	0.40	24
200x1400	Dutch Twill (double)	0.0055	0.38	20
Depth Medium	--------	0.0290	0.67	19

Using the properties from Table V and recalling that the flow area of the medium is π square inches and the viscosity of the fluid at 100°F. is 12 centipoise, the slope of the ΔP versus Q curve was calculated using a rearranged form of Equation 5.2.1;

$$\frac{\Delta P}{Q} = \frac{1.14 \times 10^4 \mu L}{\phi A D_a^2} = \frac{1}{C_f} . \qquad (5.2.2)$$

The calculated values for the slopes of the flow curves for each of the four media are given in Table VI.

TABLE VI

CALCULATED VALUES OF $\Delta P/Q$ FOR SINGLE MEDIA

Nominal Mesh	C_f (gpm/psi)	$\Delta P/Q$ (psi/gpm)
200x600	3.03	0.33
165x1400	0.90	1.11
200x1400	0.63	1.59
Depth Medium	0.19	5.26

Experimental pressure-flow tests were performed on each of the four media. Both the calculated curves and the experimental data are shown in Figure 5.2.1. Table VII compares the theoretical and experimental values of the slopes of the pressure-flow curves.

TABLE VII

FLOW PERFORMANCE RESULTS FOR SINGLE MEDIA

Nominal Mesh	Theoretical $\Delta P/Q$ (psi/gpm)	Experimental $\Delta P/Q$ (psi/gpm)	Deviation (Percent)
200x600	0.33	0.30	9
165x1400	1.11	1.10	1
200x1400	1.59	1.72	8
Depth Medium	5.26	6.67	21

Examination of Figure 5.2.1 and Table VII reveals that the theoretical model was adequate for describing the flow performance of the three wire cloth media. These materials are typical of the spectrum of wire cloth media used in the manufacture of hydraulic filter elements.

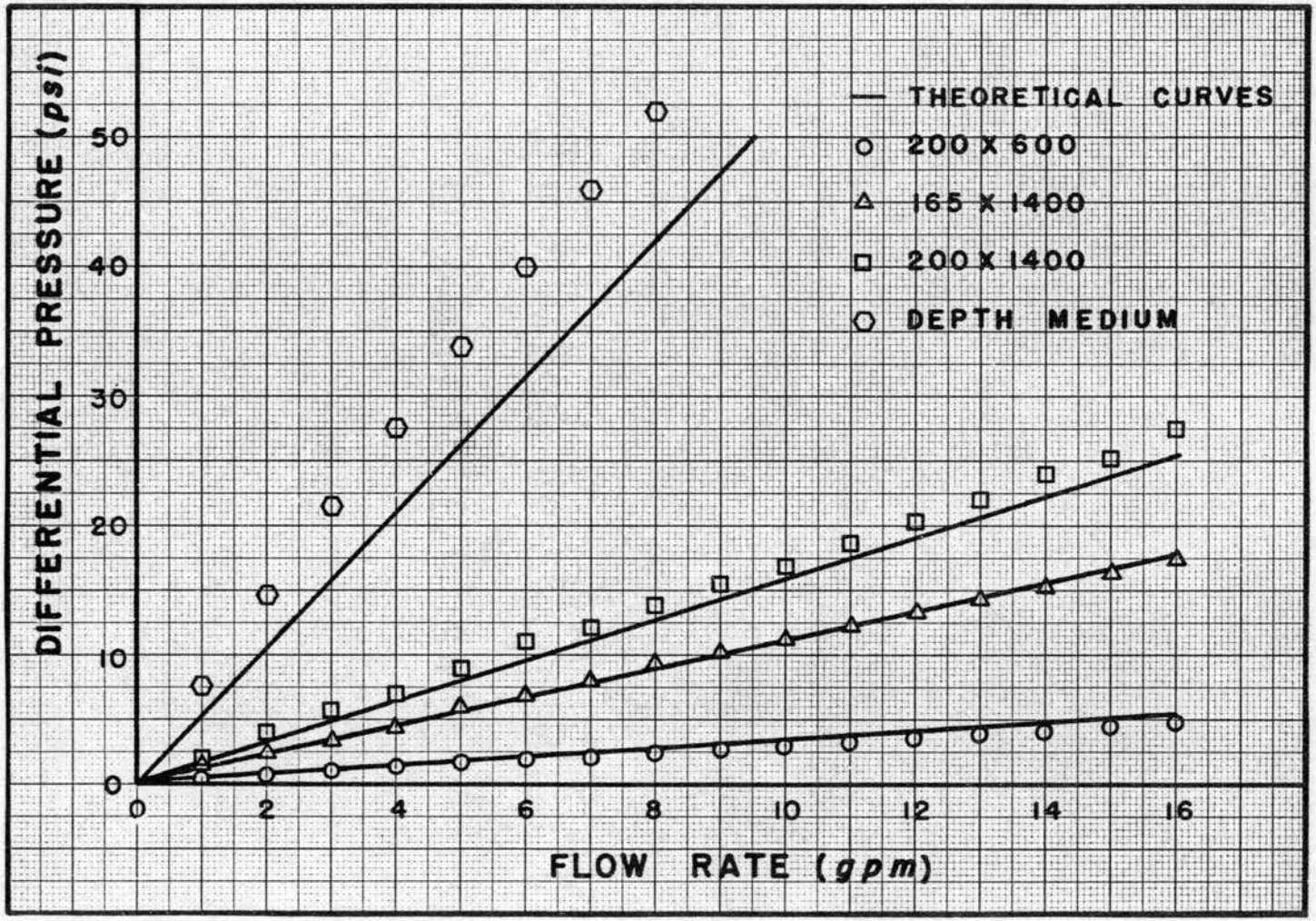

Figure 5.2.1. Flow Performance Curves for Single-Layered Media

Therefore it can be concluded that the theoretical model can be applied with equal success to other wire cloth media. Although the success of the theoretical model was not as great when applied to the depth medium, additional testing with depth media may prove this deviation to be a characteristic of the material tested.

5.3 Cascaded Media. In Chapter 3 an equation was developed for predicting the flow-pressure relationship for wire cloth filter media in series;

$$Q = \frac{\Delta P}{\sum_{1}^{n} \frac{1}{C_{fi}}} \cdot \qquad (3.2.4)$$

To test the validity of the equation, flow-pressure tests were performed on both two and three layers of the 165x1400 Dutch twill medium. For layers of the same medium the equation above simplifies to

$$Q = \frac{C_f}{2} \Delta P \qquad (5.3.1)$$

for two layers, and

$$Q = \frac{C_f}{3} \Delta P \qquad (5.3.2)$$

for three layers. Using the value for C_f from Table VI, the slopes of the pressure-flow curves can be calculated. The results are given in Table VIII.

TABLE VIII

CALCULATED VALUES OF $\Delta P/Q$ FOR CASCADED MEDIA

Number of Layers	$\Delta P/Q$ (psi/gpm)
1	1.11
2	2.22
3	3.33

For the experimental tests the media were cascaded by clamping them together in the sample holder. Figure 5.3.1 shows the experimental results along with plots of the theoretical curves. Comparison of the curves reveals that the theoretical model of Equation 3.2.4 is adequate to describe the flow performance of wire cloth media in series.

In applications where a layered material is used, the layers are commonly joined together by a sintering process. In this process the layers are clamped together and heated in a hydrogen furnace to temperatures in excess of 1700°F. At these temperatures the individual layers are bonded together at points of contact. To test for possible deviations from the theoretical model as a result of this process, double layers of the 165x1400 mesh were sintered together. The effects caused from the relative orientation of the sintered media were also investigated. To accomplish this four pairs of cloth were sintered together in such a manner that the warp wires of the individual layers were oriented at angles of 0, 30, 60 and 90 degrees.

Pressure-flow tests were then performed on the sintered media in each of the four angular orientations. The curves obtained generally exhibited higher differential pressures than had been obtained for the test on the unsintered media. No noticible trend was observed from the various orientations of the media. Figure 5.3.2 displays the theoretical curve and the experimental data points which gave the maximum deviation from the theoretical curve. Each of the four curves fell within 4 percent of the predicted curve. The compression of the layers during the sintering process probably altered the structure of the media enough to account for this slight change.

5.4 Parallel Media. Equation 3.3.2 states that the flow-pressure

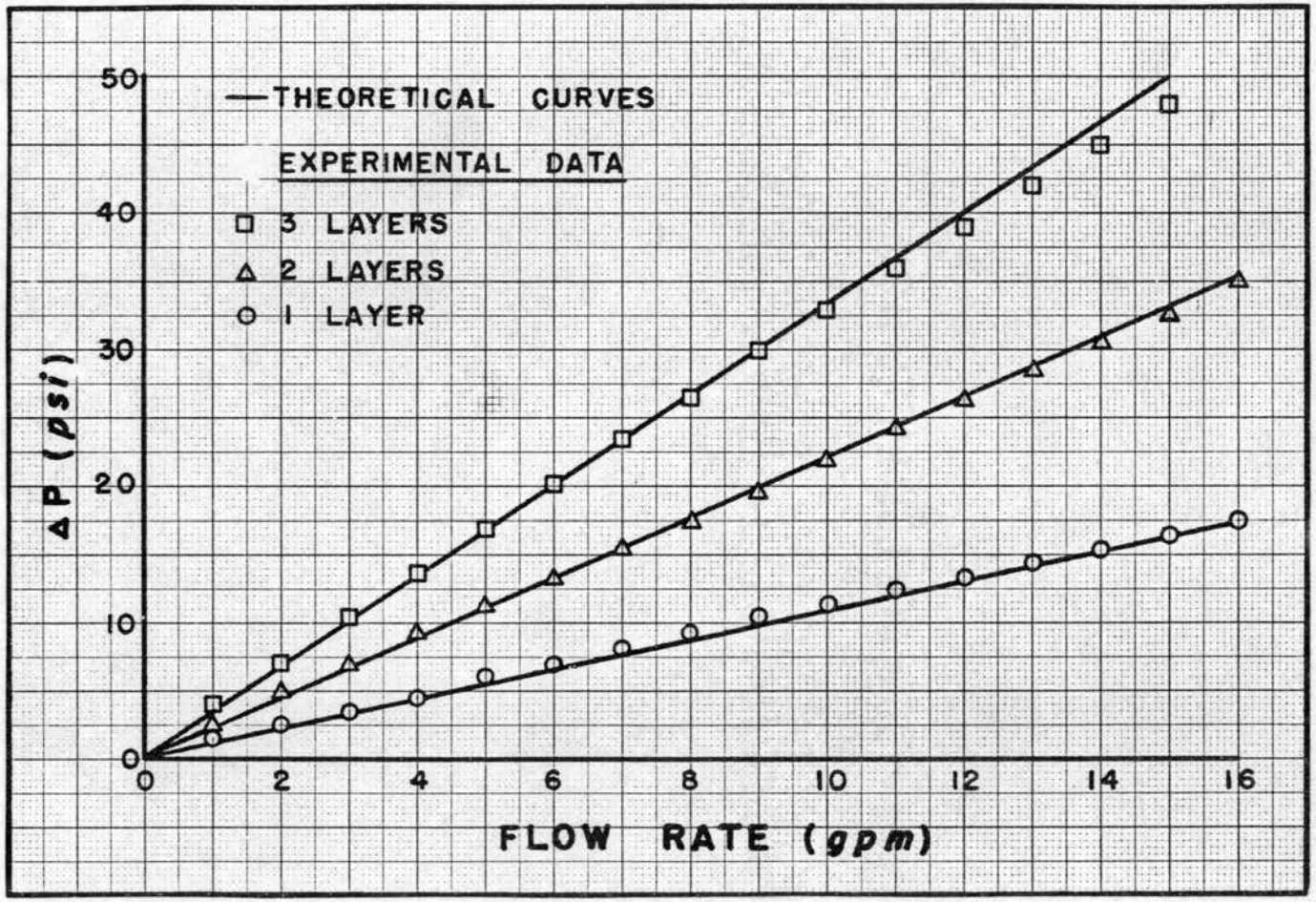

Figure 5.3.1. Flow Performance Curves for Cascaded Media

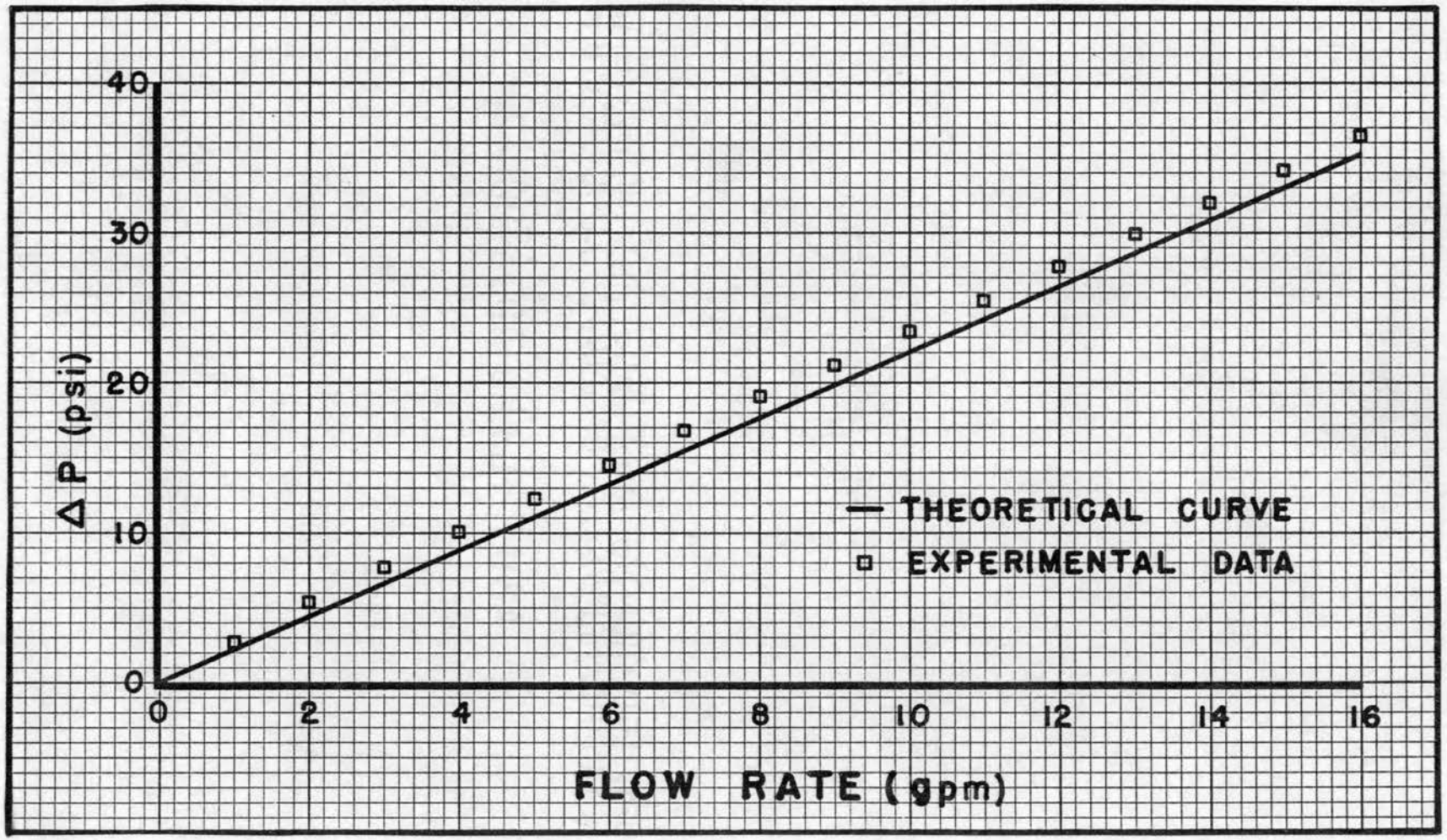

Figure 5.3.2. Flow Performance Curve for Two Layers Sintered Together

relationship for filter media in parallel is

$$Q = \Delta P \sum_{1}^{n} C_{fl} \ . \qquad (3.3.2)$$

To test this model the 165x1400 mesh was placed in parallel with the 200x1400 mesh. Taking the appropriate values of C_f from Table VI the theoretical relationship for this configuration is

$$Q = (0.90 + 0.63)\Delta P = 1.53\,\Delta P, \qquad (5.4.1)$$

or

$$\Delta P = 0.65\,Q \ . \qquad (5.4.2)$$

Figure 5.4.1 shows the comparison between the experimental results and the theoretical curve. The curve through the experimental data can be approximated by the straight line,

$$\Delta P_{exp.} = 0.70\,Q_{exp.} \ . \qquad (5.4.3)$$

Hence the theoretical curve deviates from this result by 7 percent. Recalling that the 200x1400 mesh exhibited a 8 percent variation between the theoretical and experimental flow performance curves, a deviation of this magnitude is understandable. It can be concluded from the results that the parallel flow model of Equation 3.3.2 is applicable within the accuracy of the model for single-layered media.

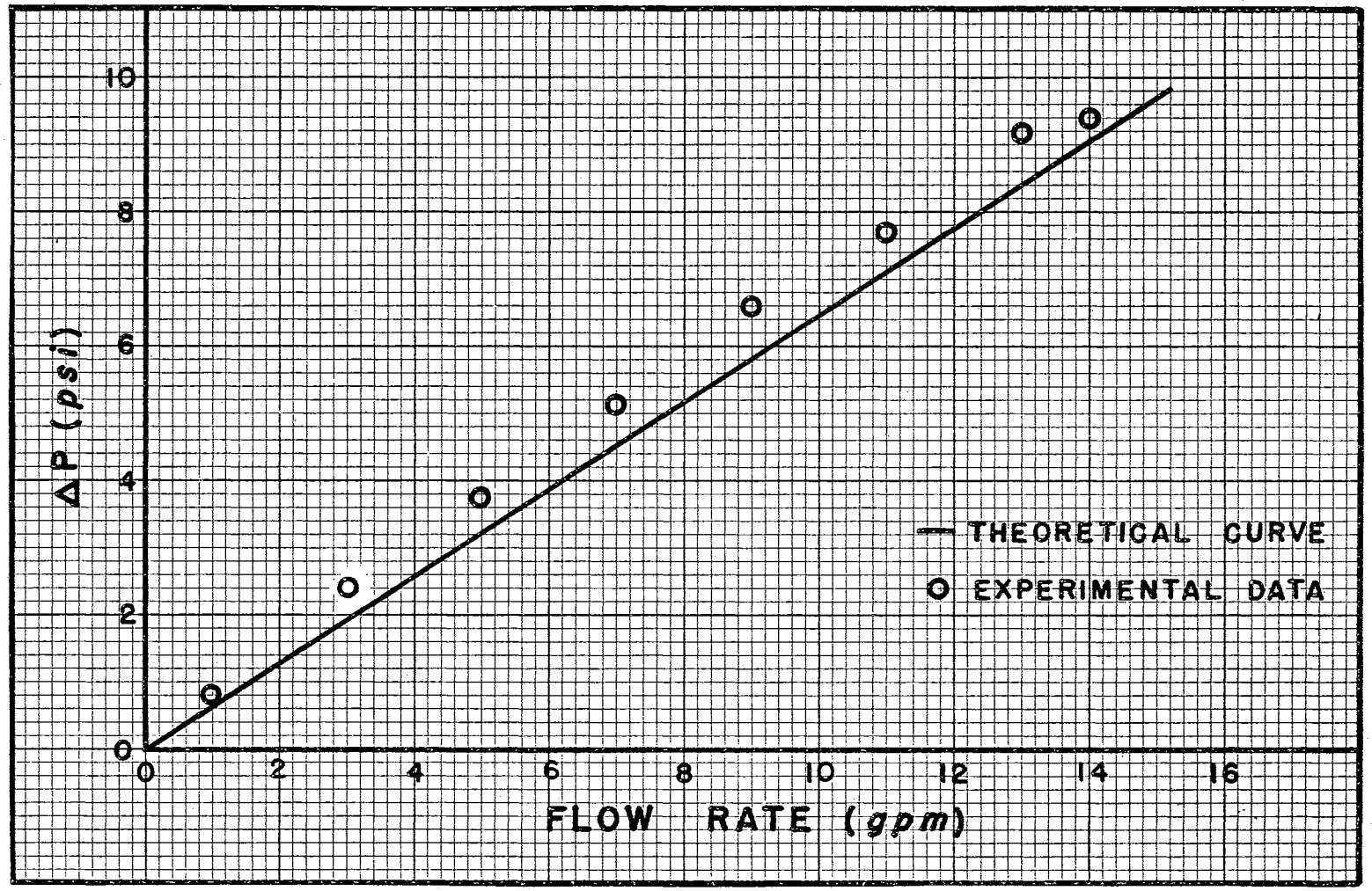

Figure 5.4.1. Flow Performance Curve for Parallel Media

CHAPTER VI

EXPERIMENTAL VERIFICATION OF FILTRATION MODELS

This chapter details the experimental verification of the filtration models proposed in Chapter 4 for single media and for media in series and parallel. This verification entailed the measurement of the efficiency curves for media in each of these configurations. Since measurements of this sort are highly dependent upon the prodecure used, a considerable portion of the chapter will be devoted to describing the experimental techniques employed.

6.1 Experimental Methods. The measurement of the efficiency characteristics of filter media requires rigid control on all of the experimental techniques. Seemingly routine tasks such as the injection of contaminants and the sampling from the feed and filtrate can yield erroneous results if caution is not exercised. The measurement of the particle distributions in the feed and filtrate can also be a source of error in the analysis. Because of the importance of these experimental techniques to the ultimate goal, the procedures used will be discussed in some detail.

The primary contaminants for the filtration performance testing were glass beads which had been classified into narrow size distributions. The reasons for the selection of glass beads were twofold. First, glass beads are readily distinguishable from naturally occurring

contaminants because of their uniform shape and therefore can be easily sized and counted using a microscopic technique. Also the circular cross section of the sphere presents a standard particle shape to the capillaries and gives a true meaning to the term capillary diameter. Classified AC Fine Test Dust was used as a secondary contaminant to determine the efficiency of a medium to irregularly shaped particles.

The efficiency tests were performed with the media mounted in the same housing that was used for the flow performance tests. The contaminant injection system shown in Figure 6.1.1 was placed in the test section of the Filter Media Performance Test Stand immediately upstream of the housing containing the filter medium. A 297 millimeter diameter membrane filter with a 0.45 micron rating preceeded the injection system. For each test a flow rate of 0.5 gpm was established through the medium.

The contaminant for each test was weighed on an analytical balance and placed in a clean dry bottle. For most of the tests 15 milligrams of 10 to 20 micron and 10 milligrams of 20 to 30 micron glass beads were used. The bottles were filled with hydraulic fluid and mixed in an ultrasonic cleaner just prior to being added to the system. This slurry was then poured into the contaminant injection chamber. After closing the chamber, a portion of the system flow was bypassed through the chamber to carry the contaminant to the filter.

Fluid samples from the feed and filtrate were withdrawn so that the contaminant injection period was bracketed. That is, sampling was begun before initiating the injection and was continued until after the conclusion of the injection period. The samples were withdrawn immediately upstream and downstream from the test housing through bleeder type sampling valves. Attached to each valve was a 2 inch length of 0.024 inch

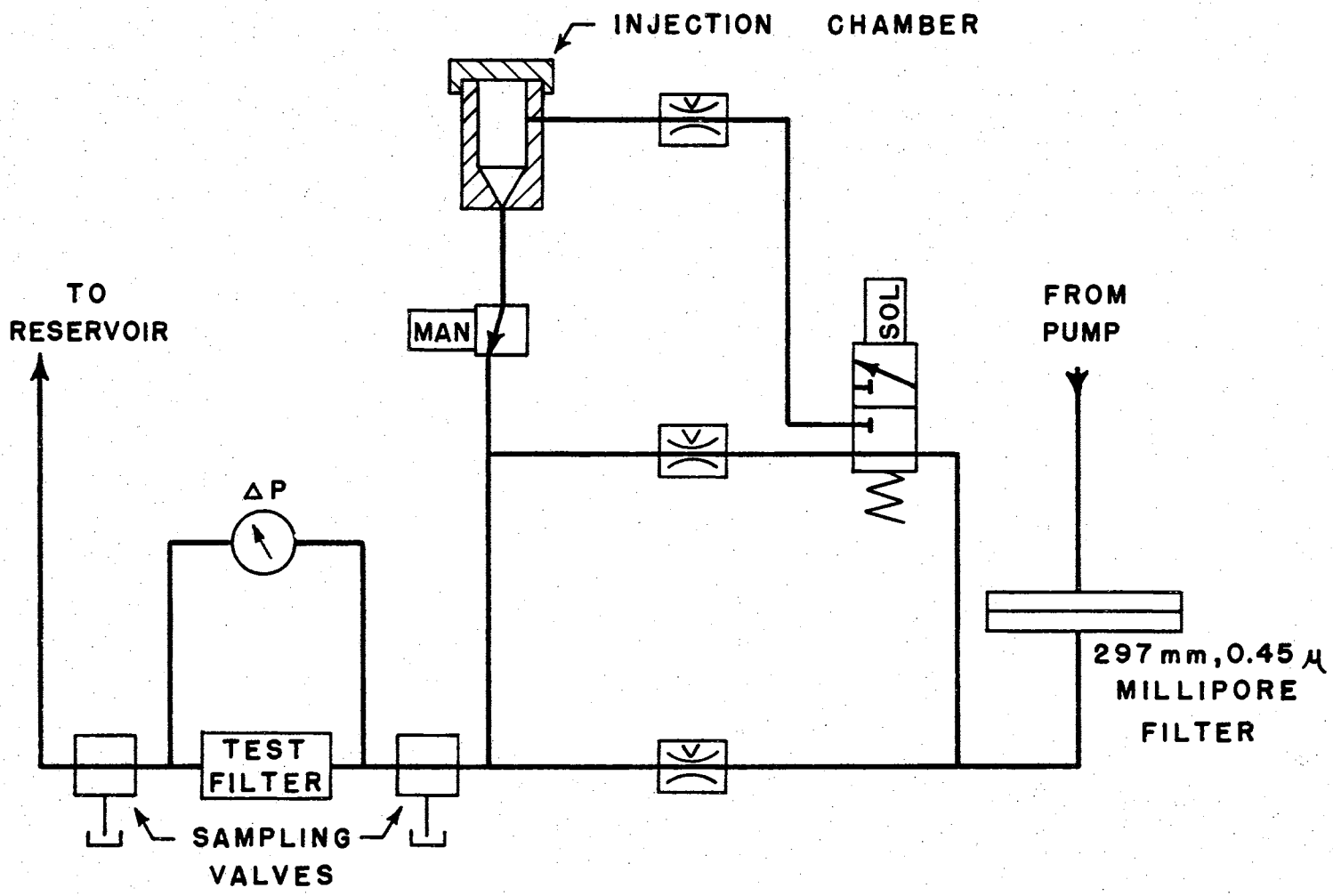

Figure 6.1.1. Contaminant Injection System

I.D. capillary tubing. The purpose of the tubing was to reduce the flow rate from the system by causing a large pressure loss without restricting the flow of the contaminants. With this arrangement the sample valve could be fully opened so that no filtration across the valve could result. Prior to each test the valves were flushed with system fluid to remove any residual contamination.

The fluid samples from the feed and filtrate were microscopicly analyzed using a modified form of the SAE ARP-598 (37) particle counting technique. An image splitting eyepiece was substituted for the filar micrometer eyepiece called for in the ARP. A description of the image splitting eyepiece as well as a complete discussion of the particle counting technique is included in Appendix C.

6.2 Single-Layered Medium. Two different media were tested to determine the validity of assuming a normal distribution for the capillary size distribution of wire cloth filter media. The two media were the 165x1400 and 200x1400 Dutch twill cloths used in the flow performance testing. Two efficiency tests were conducted on each medium using the procedures outlined in the previous section and in Appendix C. The results from these two tests were averaged to give a consensus.

To test the assumption, the points on the efficiency curves were plotted on probability graph paper. On this special paper cumulative normal distributions graph as a straight line. Since the efficiency curve represents a cumulative distribution, the assumption is verified if the points lie on a straight line. Figure 6.2.1 shows the efficiency data points for each of the two media tested. Also shown are straight lines which pass through the data points for the respective media.

The means of the distribution functions represented by the curves

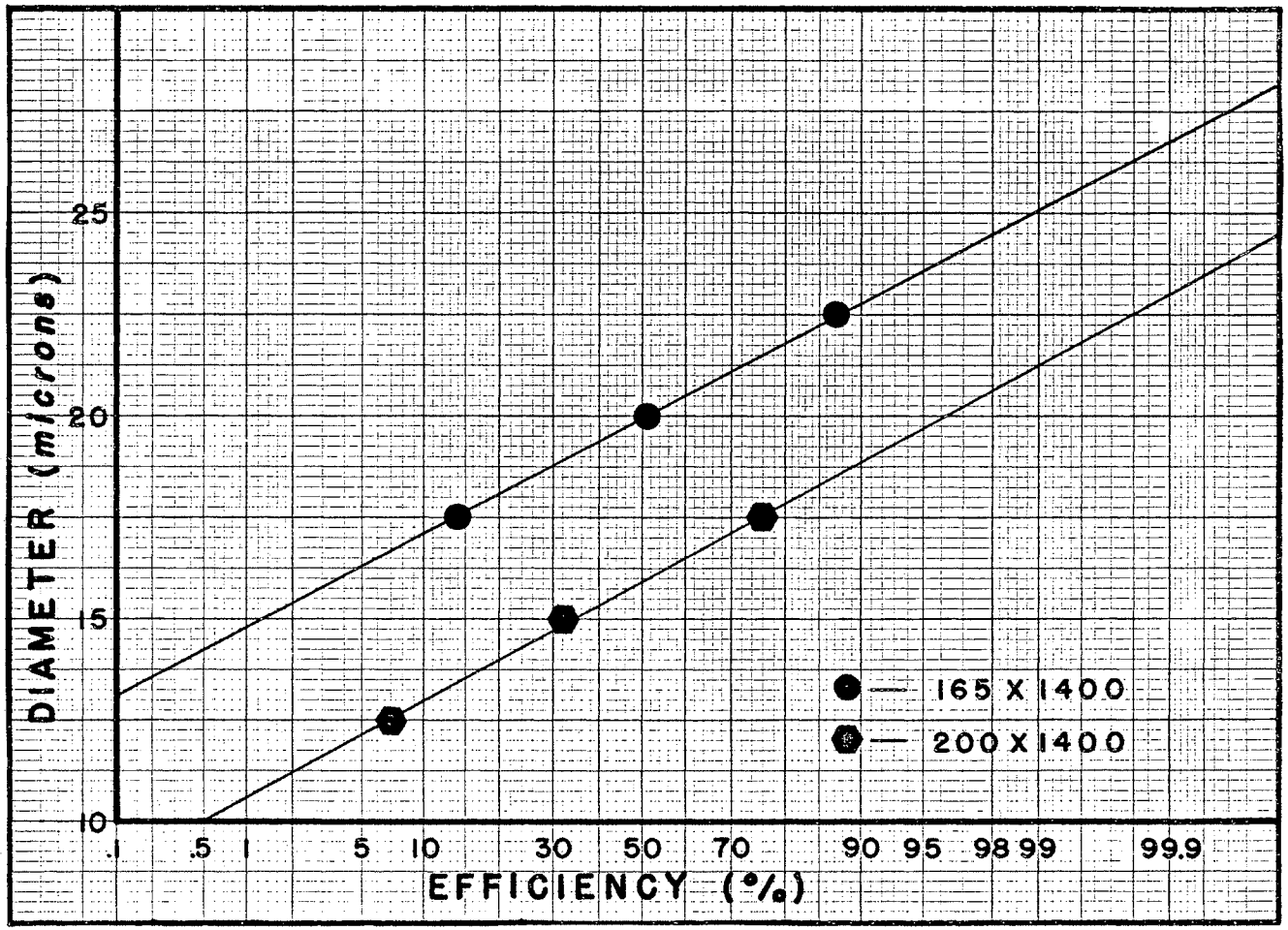

Figure 6.2.1. Efficiency Curves for Test Media

of Figure 6.2.1 are readily obtained since they occur at the 50 percent efficiency points. The variance of the distribution can also be obtained from the graph. For a normal distribution, 68 percent of the events occur within the interval bounded by $\bar{x} \pm \sigma$. Therefore, considering the cumulative distribution curves of Figure 6.2.1, the variance of the distributions can be calculated from

$$\sigma = D_{84} - D_{50} = D_{50} - D_{16} . \qquad (6.2.1)$$

where:

σ is the variance of the normal distribution.

D_N is the diameter for which the efficiency is N percent.

In Table IX the defining parameters are given for the capillary size distributions of the two media tested. It is interesting to note that the variances of the two distributions are equal. This result is to be expected since the two media had the same weaving pattern and were woven by the same manufacturer. The distributions for other weaving patterns or for the same type of media from other manufacturers can be expected to have different values for the variance.

TABLE IX

CAPILLARY SIZE DISTRIBUTION PARAMETERS

Nominal Mesh	Mean (microns)	Variance (microns)
165x1400	20	2.25
200x1400	16	2.25

Tha capillary size distributions for these two media were compared

with the respective distribution curves obtained from the porosimeter test. The curves for the 165x1400 mesh are shown in Figure 6.2.2 and those for the 200x1400 mesh are in Figure 6.2.3. The comparison of the results, Table X, shows that the average diameter on a volumetric basis is four microns larger than the filtration diameter. This variation can also be expected to be a characteristic of the weaving pattern.

TABLE X

COMPARISON OF DIAMETERS FROM POROSIMETER AND EFFICIENCY TESTS

Nominal Mesh	Average Diameter (microns)	
	Porosimeter Test	Efficiency Test
165x1400	24	20
200x1400	20	16

The efficiency characteristics of the 165x1400 mesh were also measured using AC Fine Test Dust to simulate an actual contaminant. The results, Figure 6.2.4, show that a different distribution curve is obtained. Since the particle counts are based upon the longest dimension of the particle, the increased variance of the distribution curve is due to the irregular shape of the AC Dust. Table XI lists the parameters of the distribution curves for the two contaminants.

TABLE XI

CAPILLARY SIZE DISTRIBUTION PARAMETERS OF 165x1400 MESH FOR DIFFERENT CONTAMINANTS

Glass Beads		AC Test Dust	
Mean (microns)	Variance (microns)	Mean (microns)	Variance (microns)
20	2.25	20	5.25

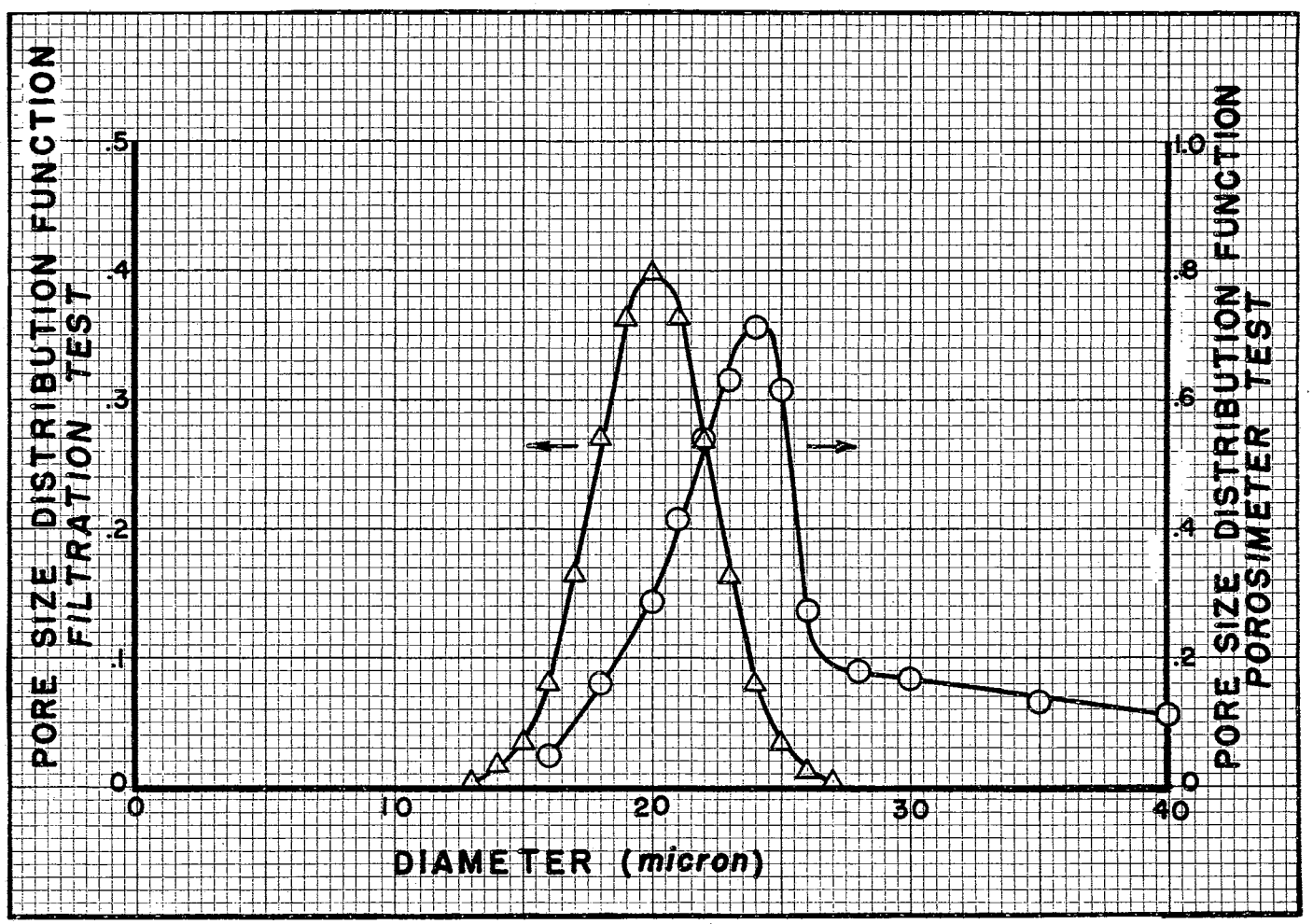

Figure 6.2.2. Distribution Curves for 165x1400 Cloth from Efficiency and Porosimeter Tests

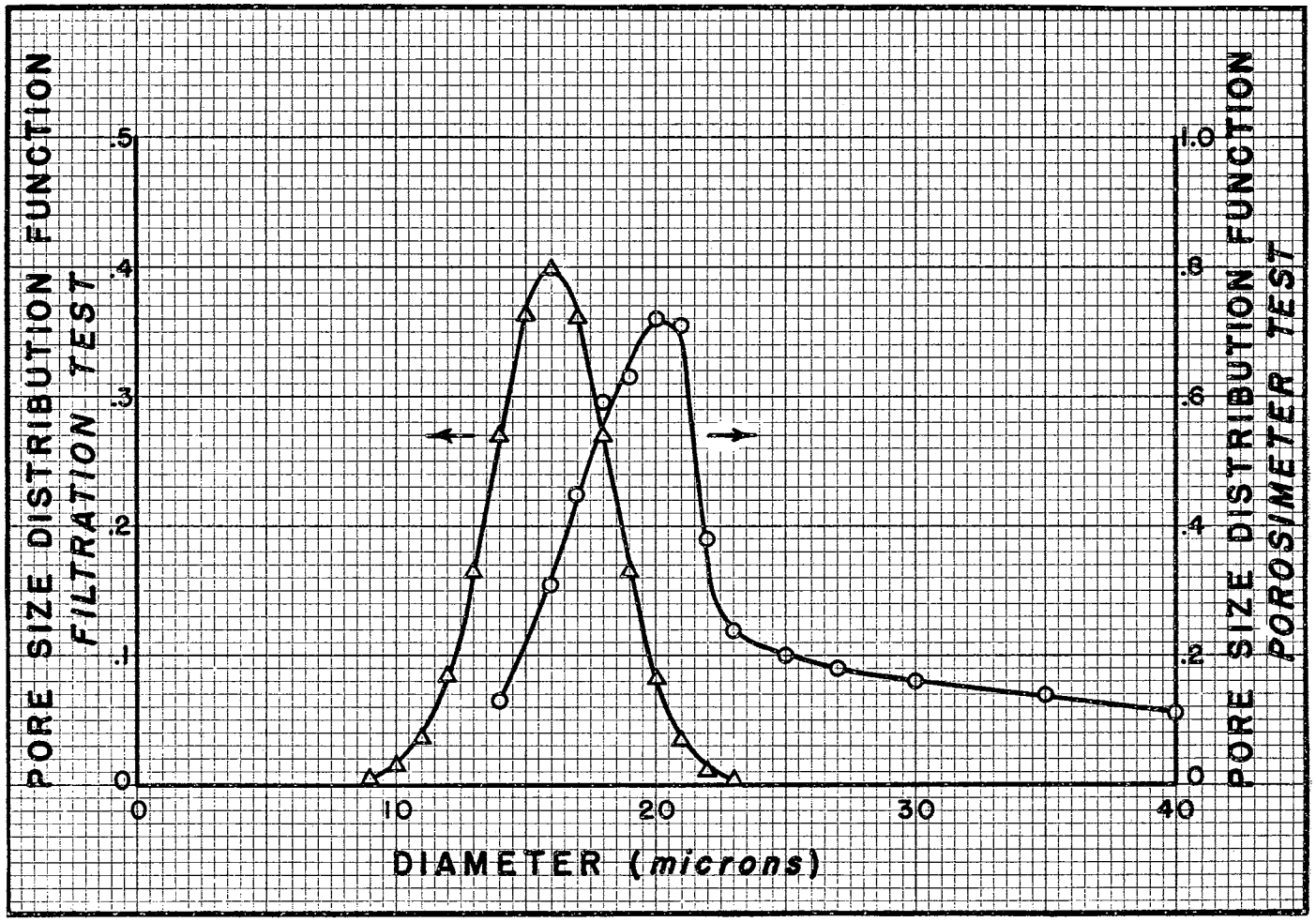

Figure 6.2.3. Distribution Curves for 200x1400 Cloth from Efficiency and Porosimeter Tests

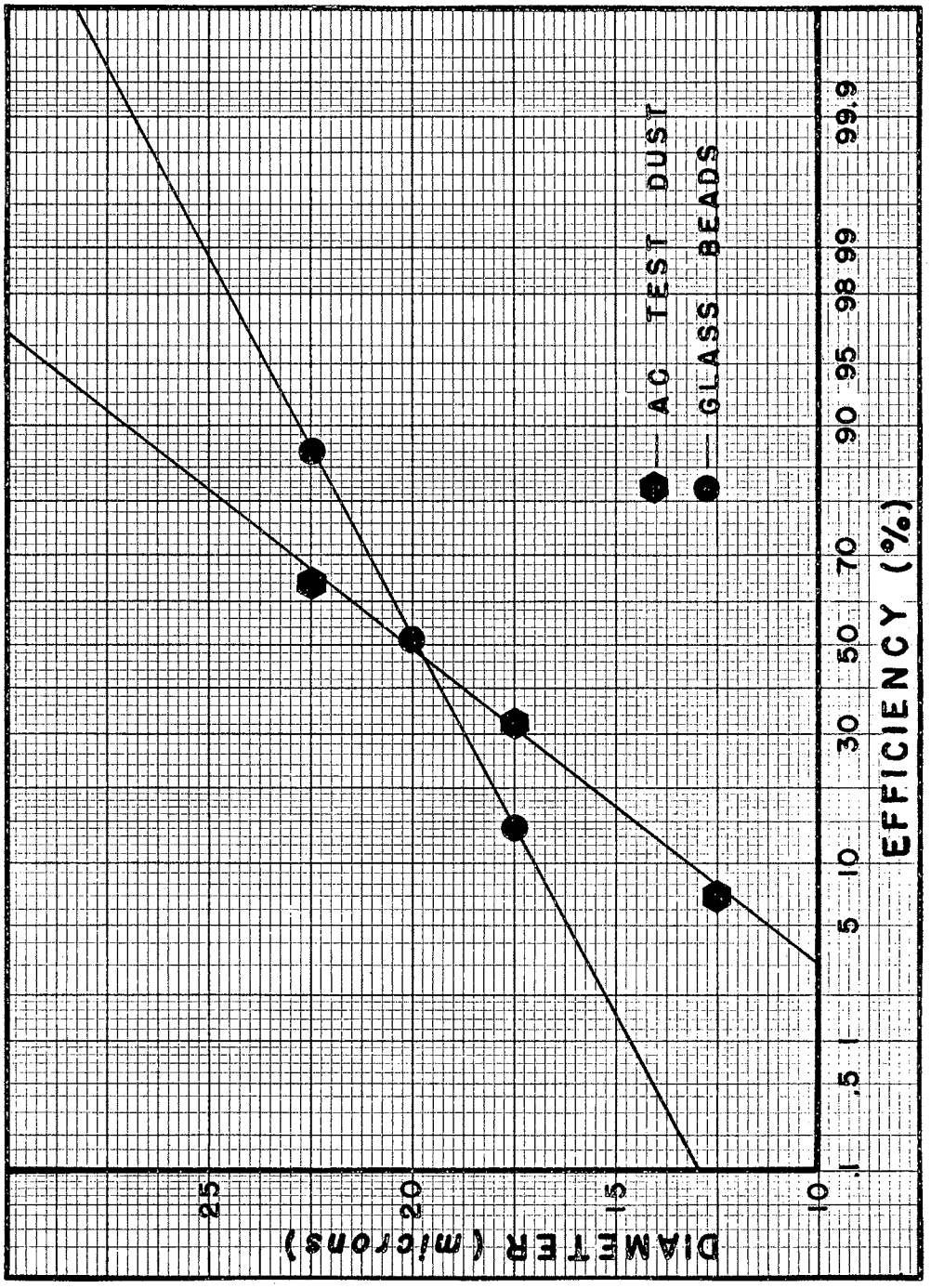

Figure 6.2.4. Efficiency Curves for 165x1400 Cloth for Different Contaminants

The experimental tests show that the capillary size distributions of single-layered Dutch twill wire cloth media follow a normal distribution model. These distributions are characterized by a mean diameter and a variance which is a function of the type of weave and the manufacturing process. Since these two parameters completely describe the capillary size distribution, they could be used to rate filter media. This would eliminate the use of such vague terms as nominal rating and absolute rating.

6.3 Cascaded Media. The theoretical model for the filtration performance of cascaded media that was developed in Section 4.2 was experimentally tested using multiple layers of the 165x1400 mesh. Recalling the discussion in this section, the efficiency for multiple layers of the same medium is given by

$$E_c(D) = 1 - [T(D)]^n . \qquad (4.2.8)$$

where:

T(D) is the transmission factor at diameter D for the individual medium.

n is the number of layers of media.

This relationship was tested for two and three layers in series. An overall efficiency curve for each case was constructed using the distribution curve for the mesh, Figure 6.2.1, and the equation above. Two efficiency tests were then performed for each configuration and the averaged results of these tests were compared with the expected curve.

Figure 6.3.1 shows the theoretical curve and the data points from the efficiency test for two layers in cascade. The curve and data points for three layers in series are given in Figure 6.3.2. Comparison

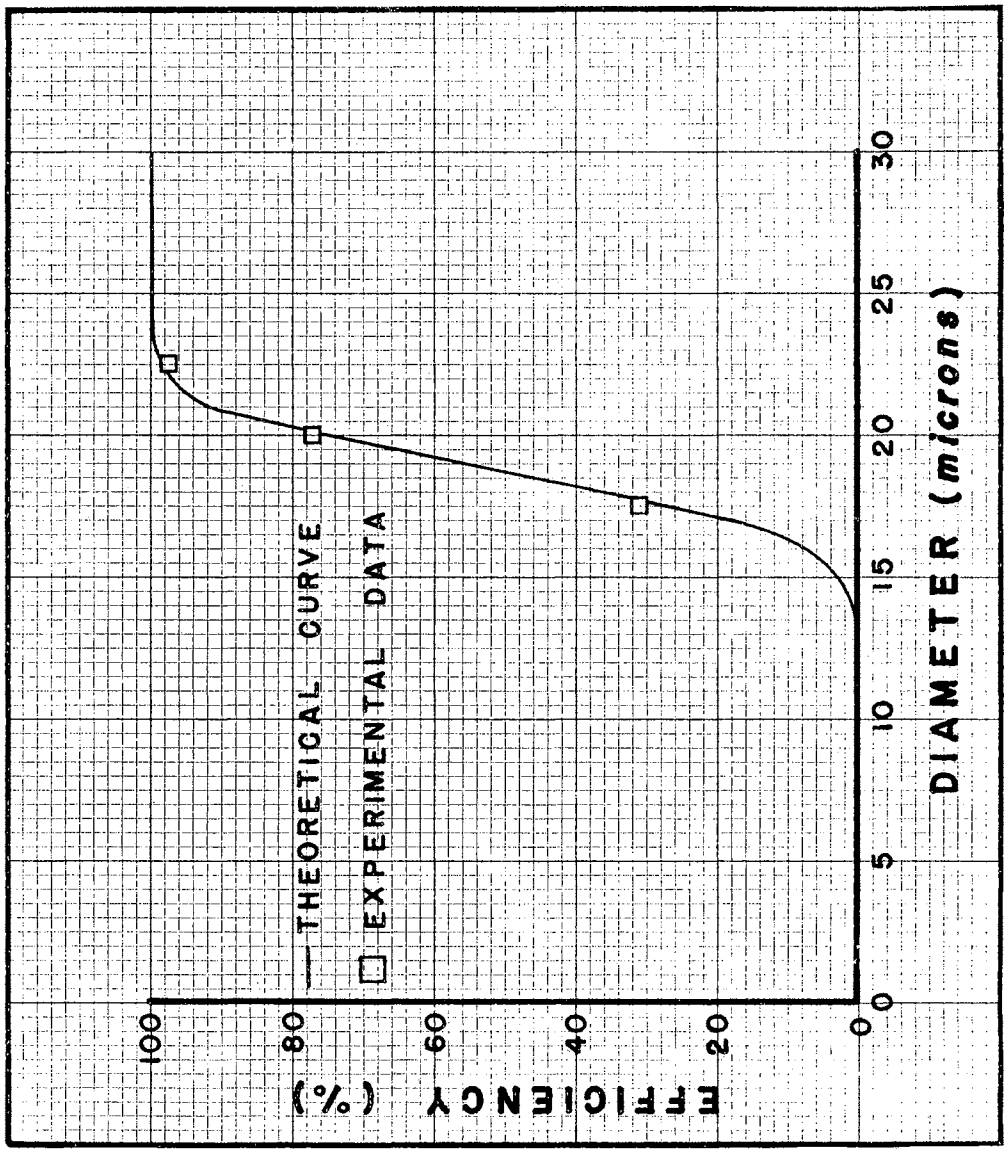

Figure 6.3.1. Efficiency Curve for Two Layers in Series

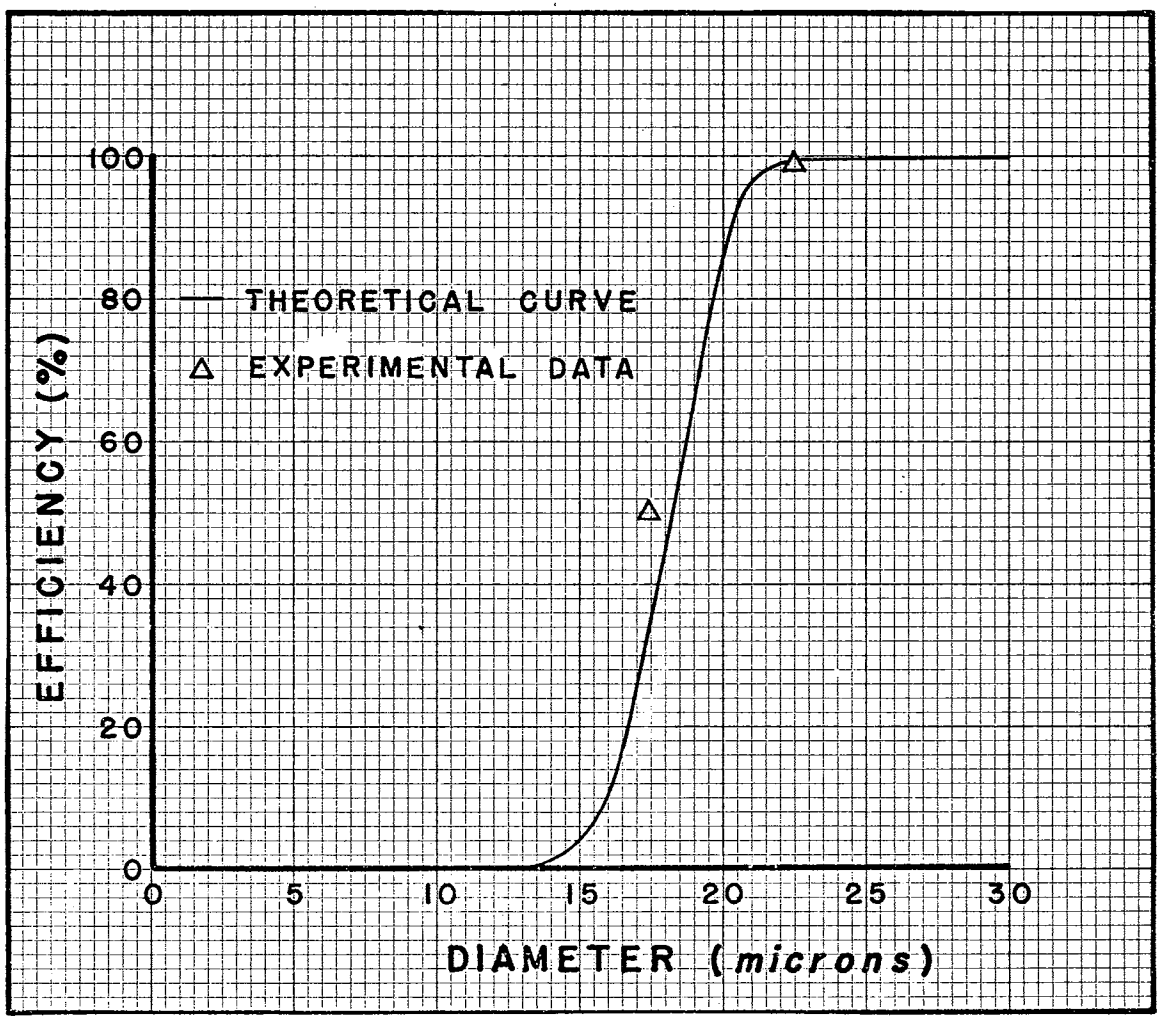

Figure 6.3.2. Efficiency Curve for Three Layers in Series

of the experimental data with the predicted curve shows that the filtration performance of cascaded media can be determined using the individual capillary distributions of the media.

The filtration performance of the cascaded media which had been sintered together was also measured. Efficiency tests were conducted on the two samples which had the greatest variation in the orientation of the warp wires, namely, 0 and 90 degree orientation. Figure 6.3.3 shows the theoretical curve and the efficiency test data for the two orientation patterns. As discovered in the results of the flow tests, no appreciable deviations from the expected were caused by variations in the arrangement of the layered media.

6.4 Parallel Media. In Section 4.3 a relationship was derived for the efficiency characteristics of filter media in parallel. This relationship required not only the filtration properties of the individual media but also the flow performance properties of the media. Restated, the equation is

$$E_p(D) = 1 - \frac{\sum_1^n C_{fi}\, T_i(D)}{\sum_1^n C_{fi}} \,. \qquad (4.3.6)$$

This filtration model was tested by performing efficiency tests on the 165x1400 and 200x1400 mesh media in parallel.

The theoretical efficiency curve for the two media can be calculated using the calculated flow constant data in Table VI and the distribution curves of Figure 6.2.1. Substitution of the respective flow constant values simplifies the equation to

$$E_p(D) = 1 - \frac{0.90\, T_1(D) + 0.63\, T_2(D)}{1.53} \,. \qquad (6.4.1)$$

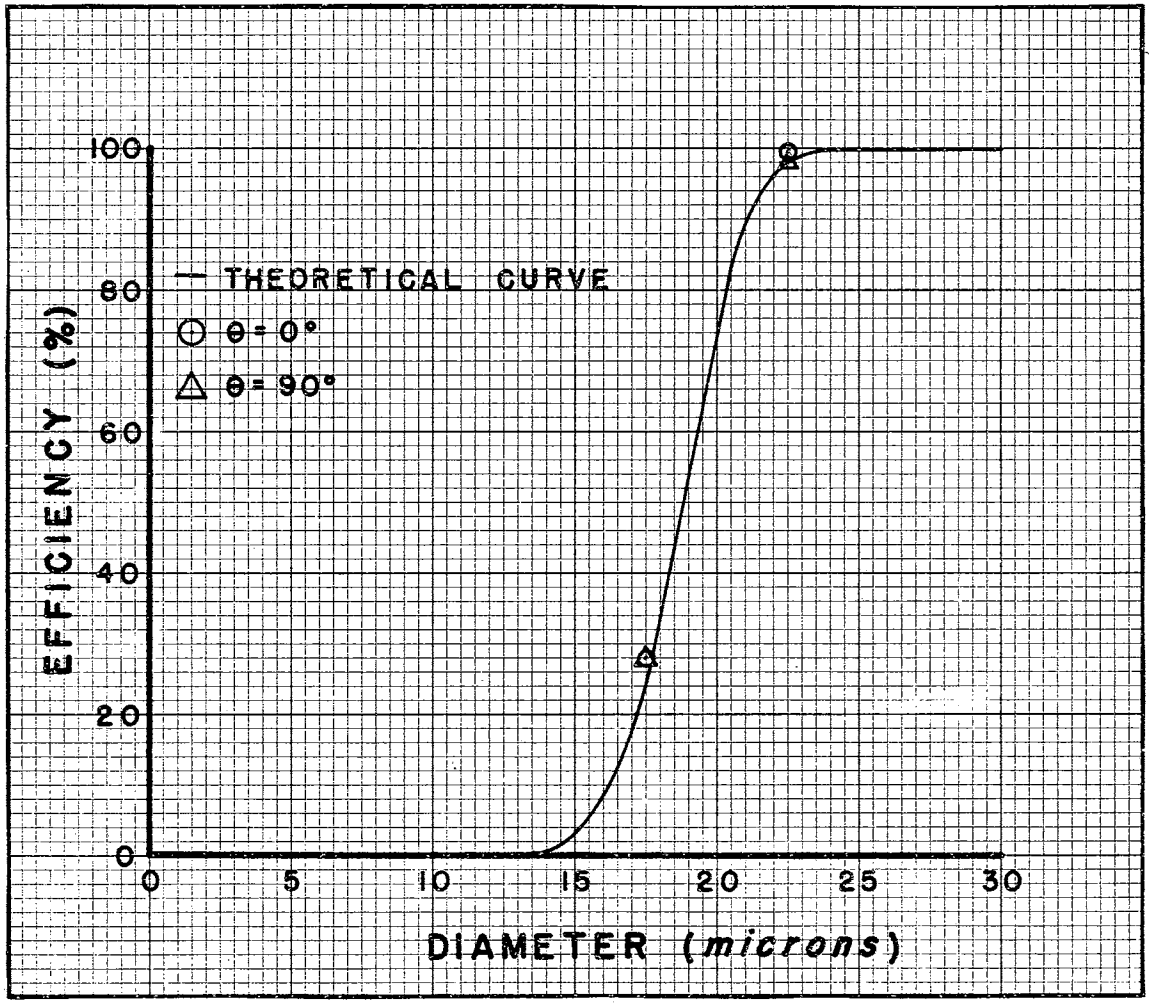

Figure 6.3.3. Efficiency Curves for Two Layers Sintered in Different Orientations

where:

$T_1(D)$ is the transmission factor at D for the 165x1400 mesh.

$T_2(D)$ is the transmission factor at D for the 200x1400 mesh.

Referring to the curves of Figure 6.2.1, the efficiency at any diameter can be calculated from the equation above. For example, the efficiency at 20 microns is equal to

$$E_p(20) = \frac{(0.90)(0.50)+(0.63)(0.04)}{1.53} = 0.69 \qquad (6.4.2)$$

The complete efficiency curve was calculated in this manner and compared with the points on the efficiency curve which were measured experimentally. The results in Figure 6.4.1 show that the experimental points closely follow the theoretical curve. Therefore it can be concluded that the proposed model does describe the filtration performance of wire cloth media in parallel.

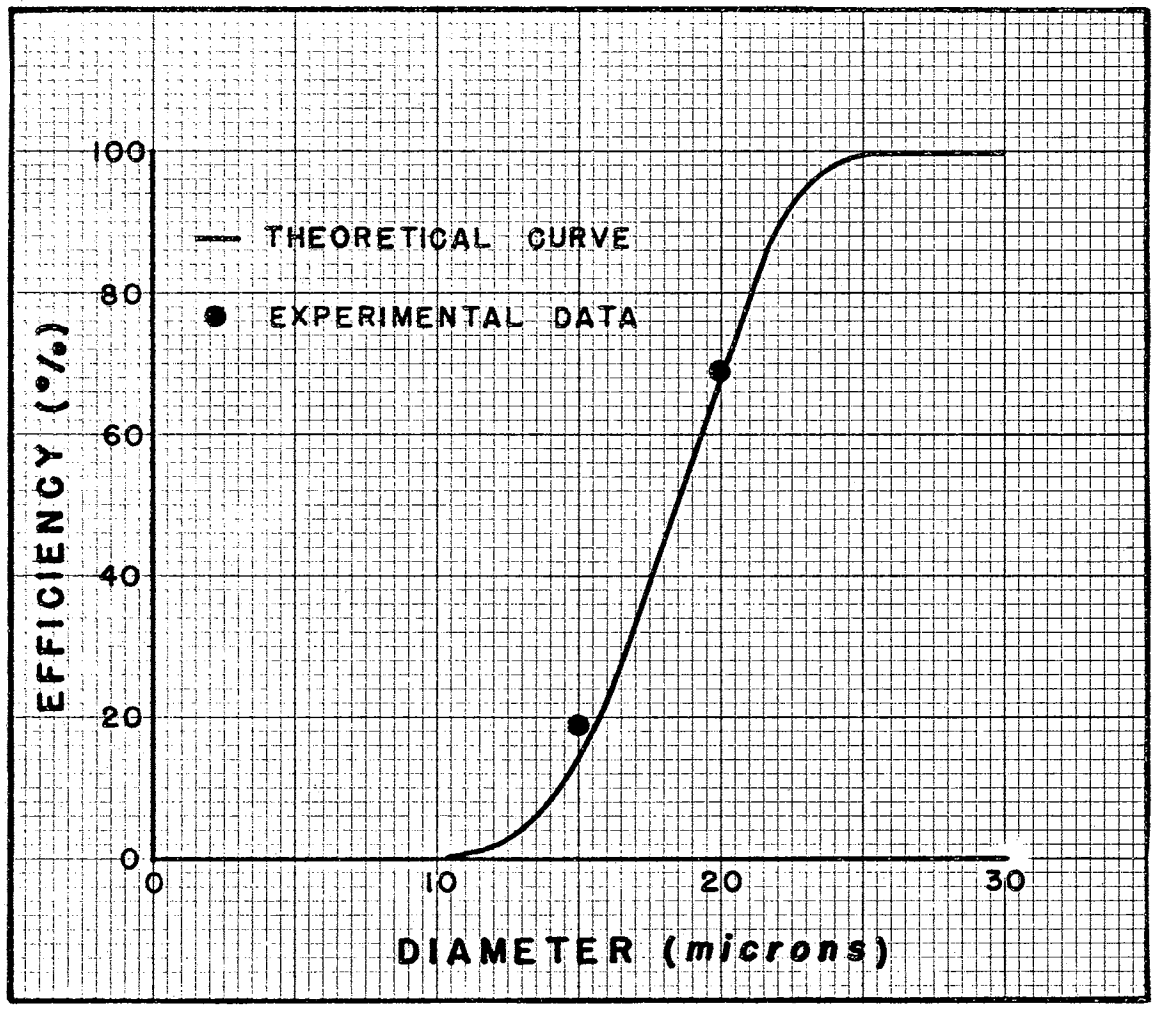

Figure 6.4.1. Efficiency Curve for Two Media in Parallel

CHAPTER VII

APPLICATIONS OF THE RESEARCH TO CURRENT PROBLEMS

The design of a filter for a hydraulic system application is based on three characteristics of the medium. These distinguishing properties are:

(1) Flow resistance,

(2) Capillary size distribution,

(3) Contaminant holding characteristics.

The present research is directly applicable to the first two of these properties and partially applicable to the third.

7.1 Flow Performance. The nature of a filter in a hydraulic system is such that it acts as a passive element in the circuit. Although it serves a vital function in assuring the proper operation of the system components, the filter represents an inefficiency in the distribution of hydraulic power to the working components. Therefore, the pressure loss through a filter must be known to ascertain whether the filter is compatible with the available hydraulic power of the system.

In many applications the maximum allowable pressure loss across the element is a known quantity, fixed either by a specification or by system requirements. For example, each of the filter specifications referenced in Section 2.3 places a limit upon the maximum allowable pressure drop for a given operating condition. The design of a filter for the suction side of a pump is another example where the pressure drop across

the element must be maintained at a low value. If the pressure drop becomes too great, cavitation will be induced in the pump and a complete pump failure can result.

The flow performance theories resulting from this research are important to any application where the flow resistance of the filter medium must be known. Using the equations of Chapter 3, the area of a filter element can be calculated prior to its manufacture so that the completed element will meet imposed pressure drop requirements. The theories for cascaded media should become increasingly important for filter applications. There is a growing trend among filter manufacturers to use multiple layers of media to achieve a desired filtration performance. For the effective design of filters of this type, the flow-pressure characteristics of cascaded media must be known.

The flow performance model for a single-layered medium can be used effectively to design new and perhaps superior filter media. Since the relationships between the properties of a medium are defined by an equation, the effects of changes in a particular parameter can be predicted. This can be especially important in designing metal fiber media. The manufacturing process for this material is such that its properties can be readily altered. For example, a medium can be constructed to a given porosity or thickness by a slight alteration in the process. By using the theoretical relationship and varying the properties where possible, a medium with a given filtration performance could be optimized to have a minimum flow resistance.

7.2 Filtration Performance. An important application for the filtration performance models of Chapter 4 is for the rating of filter media. The mechanisms of filtration are governed by the theory of proba-

bilities. A medium with an average capillary diameter of 25 microns has a greater probability of removing a 25 micron particle than a medium with a diameter of 30 microns. However, because of manufacturing flaws, both media might pass the same number of 50 micron particles. Since the filtration process is influenced by probability theory, it is reasonable to apply a statistical definition to the filtration rating of a medium.

It was hypothesized in Chapter 4 and verified in Chapter 6 that the capillary size distribution of a Dutch twill medium follows a Gaussian distribution model. Therefore, this distribution can be described by two parameters, the mean capillary diameter and the variance of the distribution. The mean diameter is a function of the type of weave, the nominal wire count, and the wire sizes. The variance is a function of the quality control on the materials and the weaving process. Media woven under superior process controls will display a smaller variance about the mean diameter.

The specification of degree of filtration requirements for Dutch twill media could easily be accomplished by stating the maximum allowable values for the two statistical parameters. For example, a filter specification could require a mean capillary diameter no greater than 25 microns and a variance no greater than 3 microns. This specification could be satisfied by either of the two media tested in Chapter 6 along with several other types of cloth. However from a practical standpoint the medium with the lowest flow resistance would be selected. Rating filter media in this manner would eliminate the need for ambiguous terms such as nominal rating and absolute rating.

The performance of a filter medium in a given application can also be predicted using the theories of Chapter 4. As an example, consider a

fluid system with the initial contaminant level shown in Figure 7.2.1. If a filter manufactured from a 165x1400 mesh is placed into the system, the contaminant level at any time can be calculated using the capillary size distribution curve of Figure 6.2.1. Figure 7.2.1 also shows the expected contaminant level after one and five complete cycles of the system fluid.

The filtration performance theories proposed in this research provide the filter designer with the information that is necessary to design an element to satisfy contaminant tolerance requirements. This area of filter design will become increasingly important as hydraulic component manufacturers begin to specify the contaminant environments in which their components must be operated. The contaminant tolerance of a component is synonymous with the allowable particle size distribution which may pass through the protecting filter. The distribution upstream of the filter is set by the internal and external sources of contamination for the system.

With the description of the contaminant levels upstream and downstream of the filter, the necessary filtration efficiency characteristics are defined. This process can be demonstrated for a general case. Consider a hydraulic component whose contaminant tolerance level is specified by the particle size distribution, $n_t(D)$. The contaminant producing characteristics of the hydraulic system are such that the contaminant level of the system has the distribution $n_s(D)$. The allowable transmission factor for the protecting filter at any diameter D_1, is given by the ratio of these distributions evaluated at D_1;

$$T(D_1) = \frac{n_t(D_1)}{n_s(D_1)} \quad . \tag{7.2.1}$$

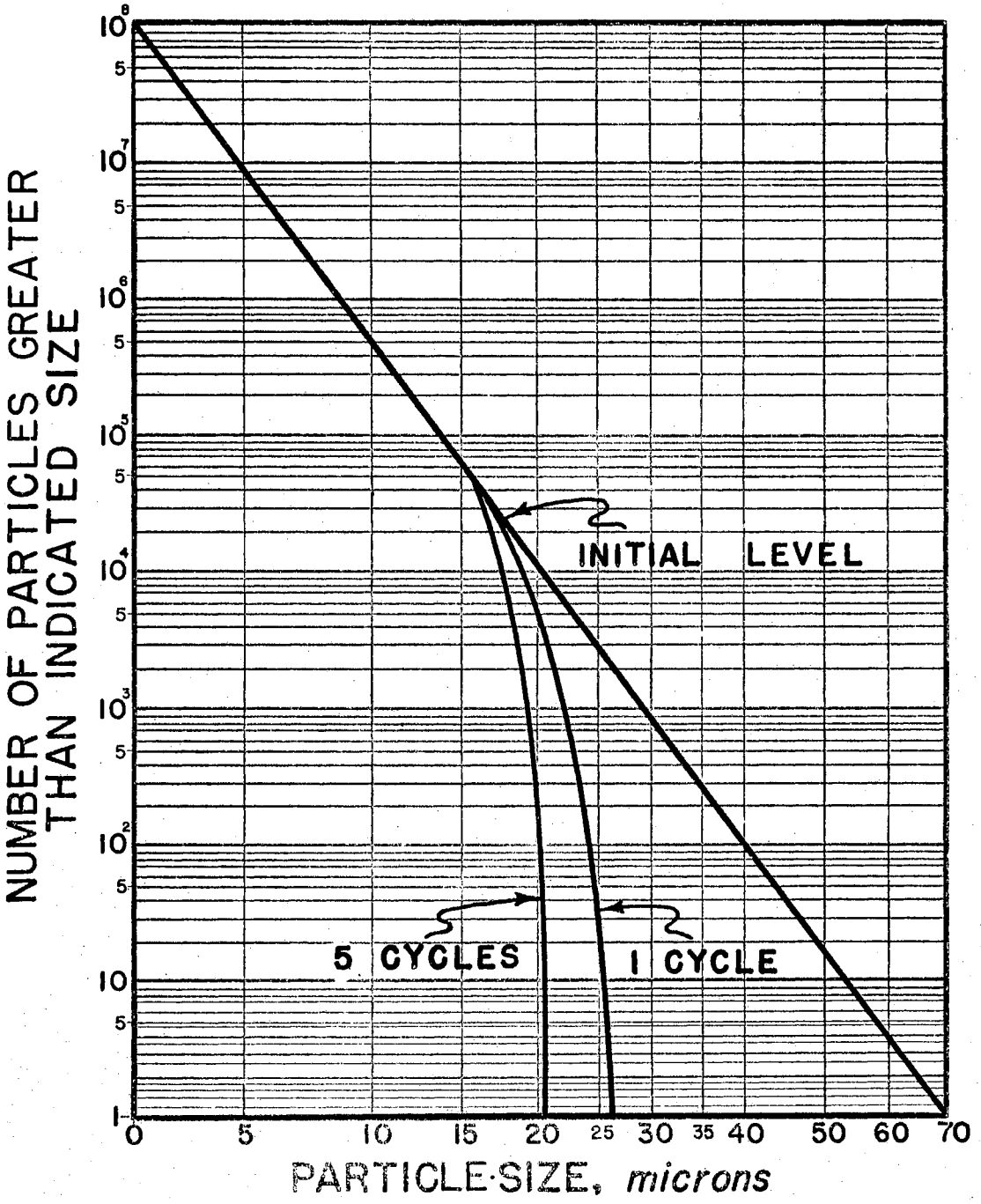

Figure 7.2.1. Influence of Filtration on System Contamination Level

The efficiency at D_1 is equal to

$$E(D_1) = 1 - \frac{n_t(D_1)}{n_s(D_1)} \cdot \qquad (7.2.2)$$

By evaluating Equation 7.2.2 at a number of diameters, the efficiency characteristics for the required filter are known.

From this point the filter design problem evolves into one of selecting a medium which satisfies the filtration requirements of the particular application. If there is no medium which effectively satisfies the requirements, then the designer is equipped with equations which may enable him to design a suitable filter using multiple media. In effect, the design process becomes one of taking the available media and combining them to meet the filtration requirements.

A typical filter design problem might be the protection of the pump whose contaminant tolerance curve was shown in Figure 2.4.2. The results of the tests showed that particles in the 25 to 30 micron size range caused a decrease in the output flow from the pump. Contaminant below this size had no apparent effect on pump performance. Since the contaminant level below 25 microns is not limited, the only requirement on the filter is that it remove essentially all of the contamination greater than 25 microns in size. Referring to Figure 6.2.1, the efficiency of the 165x1400 mesh is 99 percent at 25 microns while that of the 200x1400 mesh is 99.99 percent. Either of these media would adequately protect the pump, however the 165x1400 medium would be the practical choice due to its lower flow resistance.

The importance of the filtration performance theories developed in this thesis can be summarized as falling into one of two areas. First, the characterization of the filtration properties of a medium by a sta-

tistical model provides a workable and meaningful method to describe and rate filter media. Second, the theories for describing the filtration performance of media in multiple configuration give the designer the tools to design a filter to specific requirements.

CHAPTER VIII

SUMMARY AND CONCLUSIONS

8.1 Summary. This thesis considers two problems. The first problem is the development of mathematical models which describe the flow-pressure relationships for liquids flowing through wire cloth filter media. The model that is proposed is a modified form of the Hagen-Poiseuille equation for laminar flow through straight cylindrical capillaries. A flow equation is derived from the model in terms of the following properties of a filter medium: porosity, thickness, total area, and average flow diameter. The viscosity of the fluid also enters the equation as a parameter. Using the basic model for flow through a single medium, mathematical models are derived for the flow relationships for multiple media in series and parallel configurations.

The validity of the flow model for a single medium is tested by comparing the experimental flow-pressure relationships of four media with the theoretical model. The test media include three wire cloths and a metal fiber depth medium. The theoretical models for flow through wire cloth media used in series and parallel are also tested for validity.

The second problem considered is the mathematical description of the filtration performance of wire cloth media. A Gaussian or normal distribution is assumed for the distribution of capillary sizes within a wire cloth. Based on this assumed model, equations are derived which describe the filtration performance of wire cloth media used in multiple

arrangements.

The assumption of a normal distribution model was tested by measuring the efficiency characteristics of two wire cloth media. Since the efficiency curve is a cumulative capillary size distribution curve, the assumption is verified if the curve has the properties of a cumulative normal distribution. Using the distribution functions that characterize the media tested, an evaluation is made of the applicability of the filtration equations for media in multiple configurations. This is done by calculating the expected efficiency curves for media in series and parallel and comparing experimental points with the curves.

8.2 Conclusions. The experimental tests of the flow performance models verify that the mathematical equations accurately describe the flow relationships for wire cloth media. For the woven materials all of the theoretical models agreed with the experimental data within ten percent. The model deviated by twenty-one percent for the metal fiber medium. The flow performance models for wire cloth media have two important applications:

(1) Filter elements can be designed so that their flow properties satisfy imposed restrictions.

(2) New filter media can be designed with properties that minimize the flow resistance.

The capillary size distributions of wire cloth media follow a Gaussian distribution model. Therefore, the filtration performance of a medium is described by the mean and variance of its capillary distribution. Using the distribution parameters for individual materials, the filtration performance can be calculated for media in series and parallel configurations. The filtration models offer the following advantages:

(1) The filtration performance of media can be designated in meaningful terms.

(2) Media can be combined to produce a desired filtration characteristic for a particular application.

The theoretical models developed in this thesis, to the author's knowledge, represent the first successful description of the performance of wire cloth filter media from an analytical approach. In most disciplines, the development of acceptible mathematical models usually marks the transition of the discipline from an empirical art to an engineering science. Therefore, the greatest benefit from this research may be to provide the necessary impetus to effect the transition of filtration mechanics from an art to a science.

8.3 Recommendations for Further Study. As a result of the work initiated in this research, several areas of investigation appear to warrant additional efforts. In this regard, the following recommendations are made:

(1) The flow models should be tested for their application to filter media other than wire cloth.

(2) The capillary size distributions of typical depth media should be characterized by statistical models.

(3) The relationship between the capillary size distribution of a medium and its contaminant holding capabilities should be determined.

(4) Simplified test methods should be developed to allow the measurement of filtration efficiency characteristics on a routine basis.

BIBLIOGRAPHY

(1) Scheidigger, A. E. The Physics of Flow Through Porous Media. New York: Macmillan Co., 1960.

(2) Kozeny, J. S. - Ber. Wiener Akad. Volume 136. (1927) 271; quoted in (1).

(3) Carman, P. C. Trans. Inst. Chem. Eng. Lond. Volume 15. (1938) 150; quoted in (1).

(4) Sullivan, R. R. Journal of Applied Physics. Volume 12. (1941) 503; quoted in (1).

(5) Green, L. and P. Duwez. "Fluid Flow Through Porous Metals." Journal of Applied Mechanics. Volume 73. (March, 1951) 39-45.

(6) Rainard, L. W. "Air Permeability of Fabrics." Textile Research Journal. Volume 17. (March, 1947) 167-170.

(7) Baines, W. D. and E. G. Peterson. "An Investigation of Flow Through Screens." A.S.M.E. Transactions. Volume 73. (July, 1951) 467-480.

(8) MacDougall, D. A. "Pressure Drop Through Screens." M.S. thesis, Ohio State University, 1953.

(9) Weighardt, K. E. G. "On The Resistance of Screens." The Aeronautical Quarterly. Volume 6. (February, 1953) 186-192.

(10) Cornell, W. G. "Losses in Flow Normal to Plane Screens." A.S.M.E. Transactions. Volume 80. (May, 1958) 791-799.

(11) Wuest, W. "Wire Mesh In Flow Research." Wire. Volume 57. (February, 1962) 1-7.

(12) Lovett, R. E. "How to Design Parts From Wire Mesh." Product Engineering. Volume 33. (July 9, 1962) 67-73.

(13) Seed, R. G. and A. A. Fowle. A General Study of Diverse Filtration Phenomena With Possible Applications to Aircraft Fuel Filtration. Wright Air Development Center Report No. 54-181. (November, 1952).

(14) Lewis, F. D. "Liquid Flow Through Wire Screens." M.S. thesis, Georgia Institute of Technology, 1959.

(15) Grace, H. P. "Structure and Performance of Filter Media." A.I.Ch.E. Journal. Volume 2. (September, 1956) 307-336.

(16) Fitch, E. C. A Basic Science Program In Filtration Mechanics. Oklahoma State University Engineering Bulletin No. 126. (1963).

(17) Cranston, R. W. "Filtration of Fine Particles." Aircraft Engineering. Volume 24. (June, 1952) 154-159.

(18) Hermans, P. H. and H. L. Bredee. Rec. Trav. Chim. Volume 54. (1935) 680; quoted in (15).

(19) Gonsalves, V. E. Rec. Trav. Chim. Volume 69. (1950) 873; quoted in (15).

(20) Stone, K. L. "A Study of the Effects of Filter Housing Design and Contaminant Size on the Contaminant Capacity of a Wire Cloth Filter Element." M.S. report, Oklahoma State University, 1965.

(21) Ludvig, E. Evaluation of Filter Media. Purolator Products Report No. 2633. (March 23, 1960).

(22) Casaleggi, C., E. Ludvig and H. L. Forman. Evaluation of Low Pressure Aircraft Fuel Filters. Wright Air Development Center Report No. 55-317. (September, 1953).

(23) Wheeler, H. L. "Filter Design For Aerospace Systems." Hydraulics and Pneumatics. Volume 14. (December, 1961) 88-90.

(24) _____. Military Specification: Filters and Filter Elements, Fluid Pressure, Hydraulic Micronic Type. Mil-F-5504B. (October 17, 1958).

(25) _____. Military Specification: Filter and Filter Elements, Fluid Pressure, Hydraulic, Line, 15 Micron Absolute, Type II Systems. Mil-F-8815A. (August 14, 1963.)

(26) _____. Military Specification: Filter, Fluid, Pressure, Absolute 5 Micron, Hydraulic. Mil-F-27656A. (November 7, 1962).

(27) LeGrand, R. "What Filtration Can Do For You." American Machinist. Volume 93. (June 30, 1949) 84-90.

(28) Nutt, H. V. "Filtration of Diesel Fuel and Lubricating Oils." S.A.E. Journal. Volume 52. (December, 1944) 573-585.

(29) Fitch, E. C. Perspective of Fluid Contamination Control. Oklahoma State University Engineering Bulletin No. 148. (1966).

(30) Bose, R. E. "The Effect of Cavitation on Particulate Contamination Generation." (unpub. Ph.D. dissertation, Oklahoma State University, 1966).

(31) Cole, F. W. Particle Count Rationalization. Bendix Corporation, Filter Division Technical Report. (February, 1966).

(32) Thayer, W. W. "Modern Hydraulic Reservoir: How It Provides Micron-Range Filtration and Pump Supercharging." A.S.M.E. Transactions. Volume 66. (October, 1944) 589-594.

(33) Stokes, E. A. and G. H. Vokes. "Methods of Testing Filter Performance and Characteristics of Some Types of Filters." Scientific Lubrication. Volume 10. (January, 1958) 12-19.

(34) Osgood, R. E. "How Contamination Affects Servo Valve Design." Applied Hydraulics. Volume 12. (February, 1959) 79.

(35) Klevin, P. S. "Contamination and Its Control." Hydraulics and Pneumatics. Volume 14. (December, 1961) 83-85.

(36) Fitch, E. C., C. R. Gerlach and D. L. Fincher. Valve Contamination Sensitivity. Oklahoma State University Engineering Research, OCAMA Report 65-1. (January, 1966).

(37) _____. Procedure For the Determination of Particulate Contamination of Hydraulic Fluids by the Particle Count Method. S.A.E. Aerospace Recommended Practice No. 598. (March, 1960).

(38) Washburn, E. W. "Note On a Method of Determining the Distribution of Pore Sizes in a Porous Material." Proceedings of the National Academy of Sciences. Volume 7. (April 15, 1921) 115-116).

(39) Drake, L. C. and H. L. Ritter. "Pore-Size Distribution in Porous Materials." Industrial and Engineering Chemistry. Volume 17. (December, 1945) 787-791.

APPENDIX A

MERCURY INTRUSION POROSIMETER

The most important property of a filter medium is its capillary size, since this governs its effectiveness as a filter material. In addition, there are two distinct capillary sizes that are important for describing a medium. One of these is the capillary size which represents the filtration properties of the medium. The other is the average or effective capillary size which is characteristic of the flow properties of a medium. This latter measurement can be made using mercury intrusion porosimetry.

The development of the mercury intrusion method of measuring capillary size distributions is attributed to Washburn (38). The technique was further refined by Ritter and Drake (39). The principle relationship is developed from a static balance of forces within a capillary. Consider the case where a liquid is being forced into a capillary. At an equilibrium condition, the external force is balanced by an internal force resulting from the surface tension of the liquid at the perimeter of the opening, as shown in Figure A.1. This equilibrium condition can be stated mathematically as

$$F = PA_p = \sigma L_p \cos\theta . \qquad (A.1)$$

where:

F is the force required.

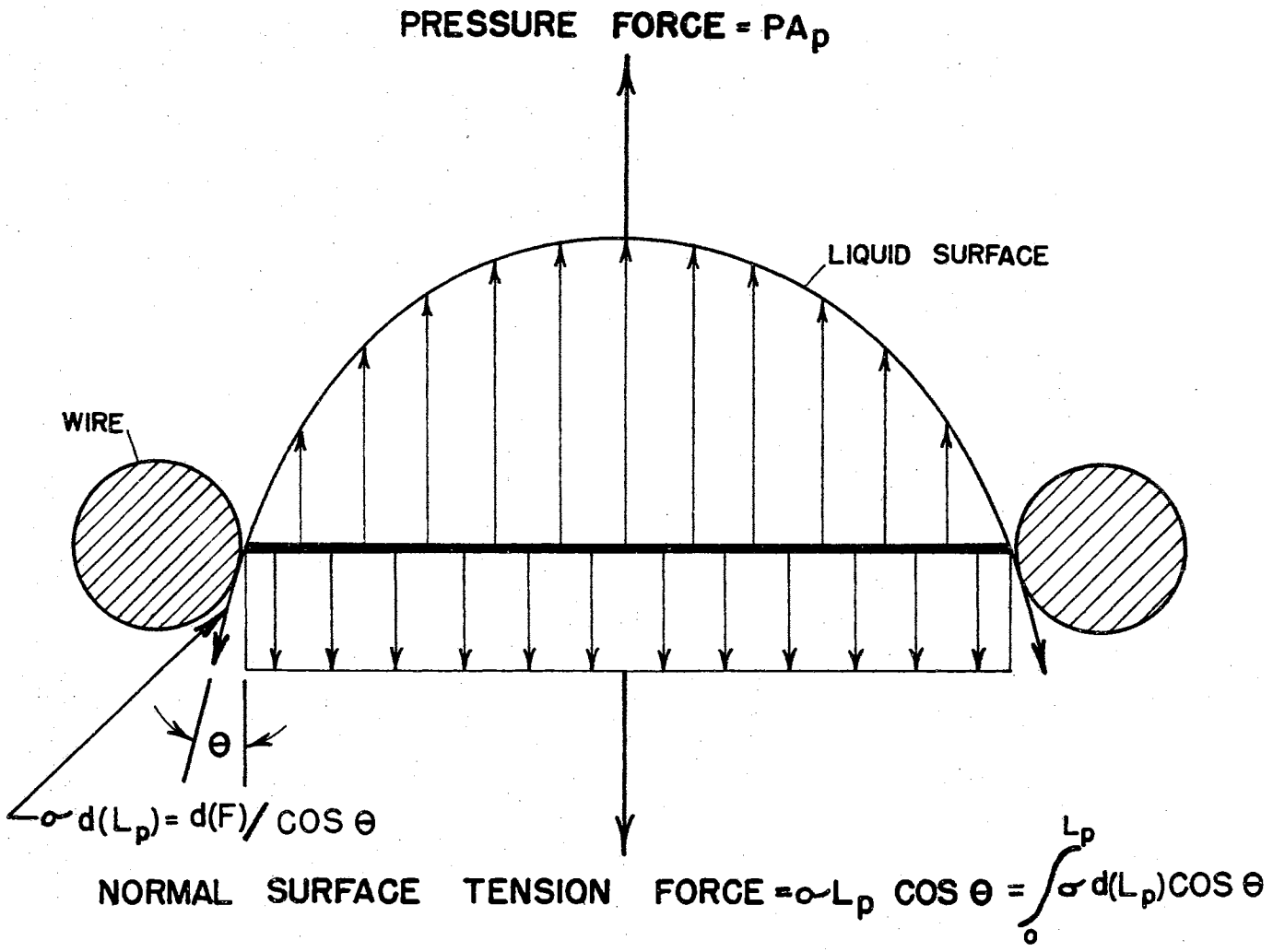

Figure A.1. Static Force Balance within a Capillary

P is the absolute pressure,

A_p is the cross sectional capillary area.

L_p is the length of wetted perimeter of capillary.

σ is the surface tension of liquid.

θ is the wetting angle of liquid on solid.

If Equation A.1 is applied to a capillary of circular cross section, the values for A_p and L_p become

$$A_p = \frac{\pi D^2}{4}, \tag{A.2}$$

and

$$L_p = \pi D . \tag{A.3}$$

Thus, the force equation readily reduces to

$$D = \frac{4\sigma \cos\theta}{P} . \tag{A.4}$$

The equation above has been thought to be restricted to circular capillaries; however, re-examination of the theory shows that it is a much more powerful tool in the determination of media capillary sizes. Consider the force balance within a triangular capillary of sides a, b, and c. The cross sectional area is given by the expression,

$$A_p = \left[S(S-a)(S-b)(S-c)\right]^{1/2} . \tag{A.5}$$

where:

$$S = \tfrac{1}{2}\,(a + b + c)$$

Since the wetted perimeter for this case is

$$L_p = a + b + c = 2S,$$

substitution into Equation A.1 yields

$$D = \frac{2[S(S-a)(S-b)(S-c)]^{1/2}}{S} = \frac{4\sigma \cos\theta}{P} . \qquad (A.6)$$

The diameter D, given in A.6, is the diameter of the circle which can be inscribed in the triangle. It should be noted that this is also equal to the hydraulic diameter, D_h, defined for a non-circular flow passage as

$$D_h = \frac{4A_p}{L_p} . \qquad (A.7)$$

The validity of the theory for triangular pore openings is noteworthy because many common wire cloth configurations have triangular pores as their primary barrier.

An analysis of the forces within a rectangular capillary also has important applications since media with a plain weave have pores of this type. Considering a rectangle with a width W and a length L, the cross sectional area and wetted perimeter are given by

$$A_p = WL \qquad (A.8)$$

and,

$$L_p = 2\ (W + L). \qquad (A.9)$$

Substitution into equation A.1 yields

$$D_h = \frac{2WL}{W+L} = \frac{4\sigma \cos\theta}{P} . \qquad (A.10)$$

Representing L by some multiple of W, KW, and recognizing that W is the diameter of the largest sphere which will pass through the pore, Equation A.10 may be written as

$$D = \frac{(1+K)}{2K} \frac{4\sigma \cos\theta}{P}. \qquad (A.11)$$

It can be observed from Equation A.11 that for a square pore, where K equals 1, the equation reduces to the same form as Equations A.4 and A.6.

The principles above are utilized in determining capillary sizes by means of the intrusion of mercury into the pores of a medium. The instrument used in this test, a mercury intrusion porosimeter manufactured by the American Instrument Company, is designed to give capillary size distribution information on porous media whose diameters may range from 0.035 to 100 microns (Figures A.2 and A.3). In performing the test, a filter sample is placed in a small chamber to which a graduated stem is attached. After evacuating the sample, mercury is added to the chamber. The pressure on the mercury is increased incrementally, and the volume change is noted in the graduated stem. As the pressure is increased, the mercury passes into pores of decreasing diameter until the void volume is completely filled with mercury. In this manner a plot of pressure versus volume injected can be prepared (Figure A.4).

Considering the porous medium being analyzed, let the incremental pore volume between diameters D + dD and D be represented by

$$dV_p = -F(D)\, dD. \qquad (A.12)$$

where:

V_p is the capillary volume

F(D) is the Pore Size Distribution Function

For mercury on stainless steel Equation A.4 reduces to

$$D(\text{Microns}) = \frac{175}{P(\text{psia})}. \qquad (A.13)$$

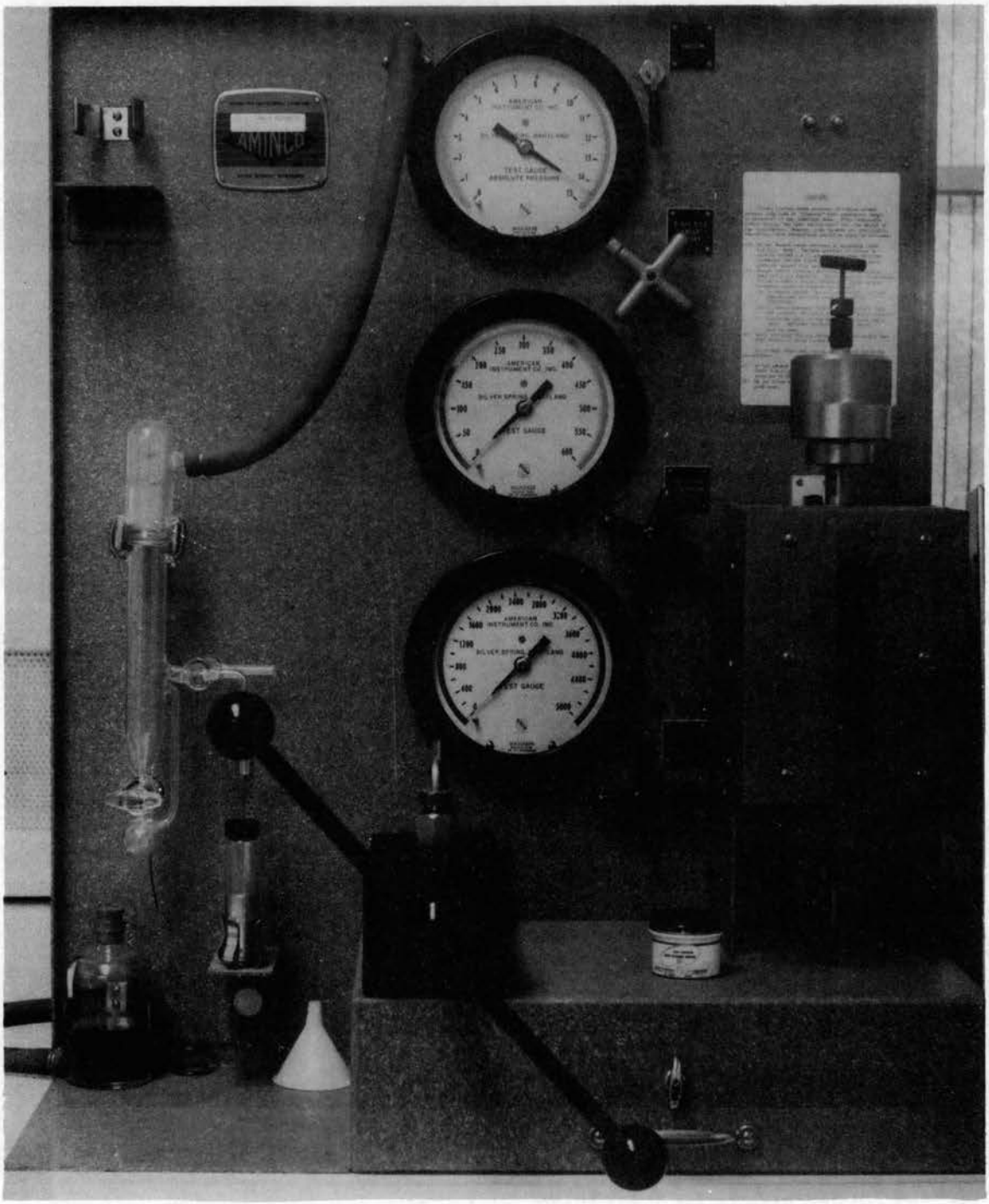

Figure A.2. Mercury Intrusion Porosimeter

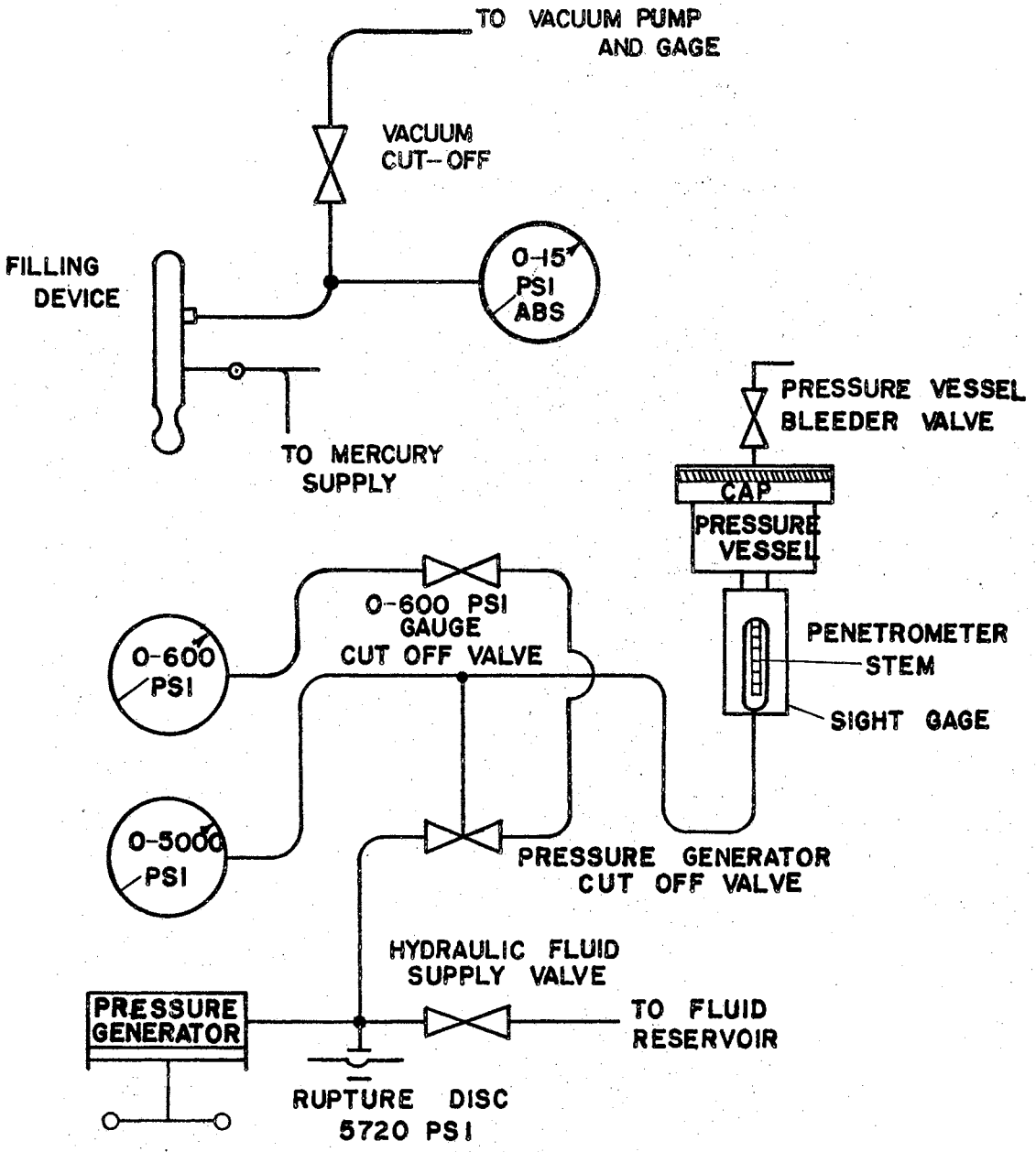

Figure A.3. Circuit Diagram of Porosimeter

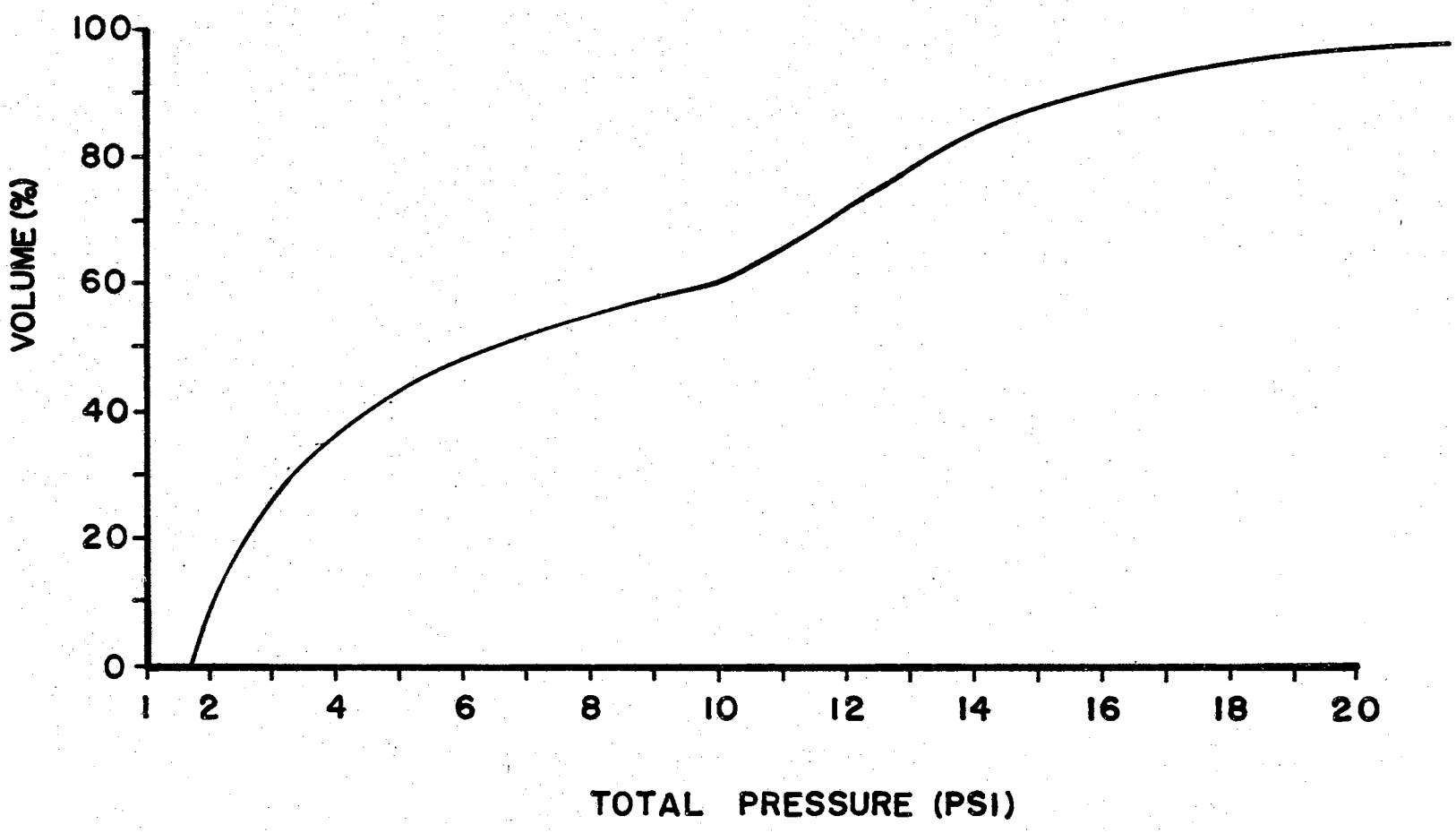

Figure A.4. Mercury Intrusion Curve

Differentiation of Equation A.13 yields

$$PdD + DdP = 0 \qquad (A.14)$$

Solving for dD and substituting into Equation A.12 gives an expression for the distribution function;

$$F(D) = \frac{P}{D} \frac{dV_p}{dP} \cdot \qquad (A.15)$$

The capillary size distribution function may be determined for various pore diameters using Equation A.13 and the slope of the V_p versus P curve. Figure A.5 shows a plot of F(D) versus D for a medium with a Dutch twill weave. The highest point which F(D) obtains occurs at the average capillary size of a medium on a volume basis.

The value of this method lies in the fact that it is applicable to both surface and depth type filter media. The test can be performed on a two square inch sample of material in less than one hour.

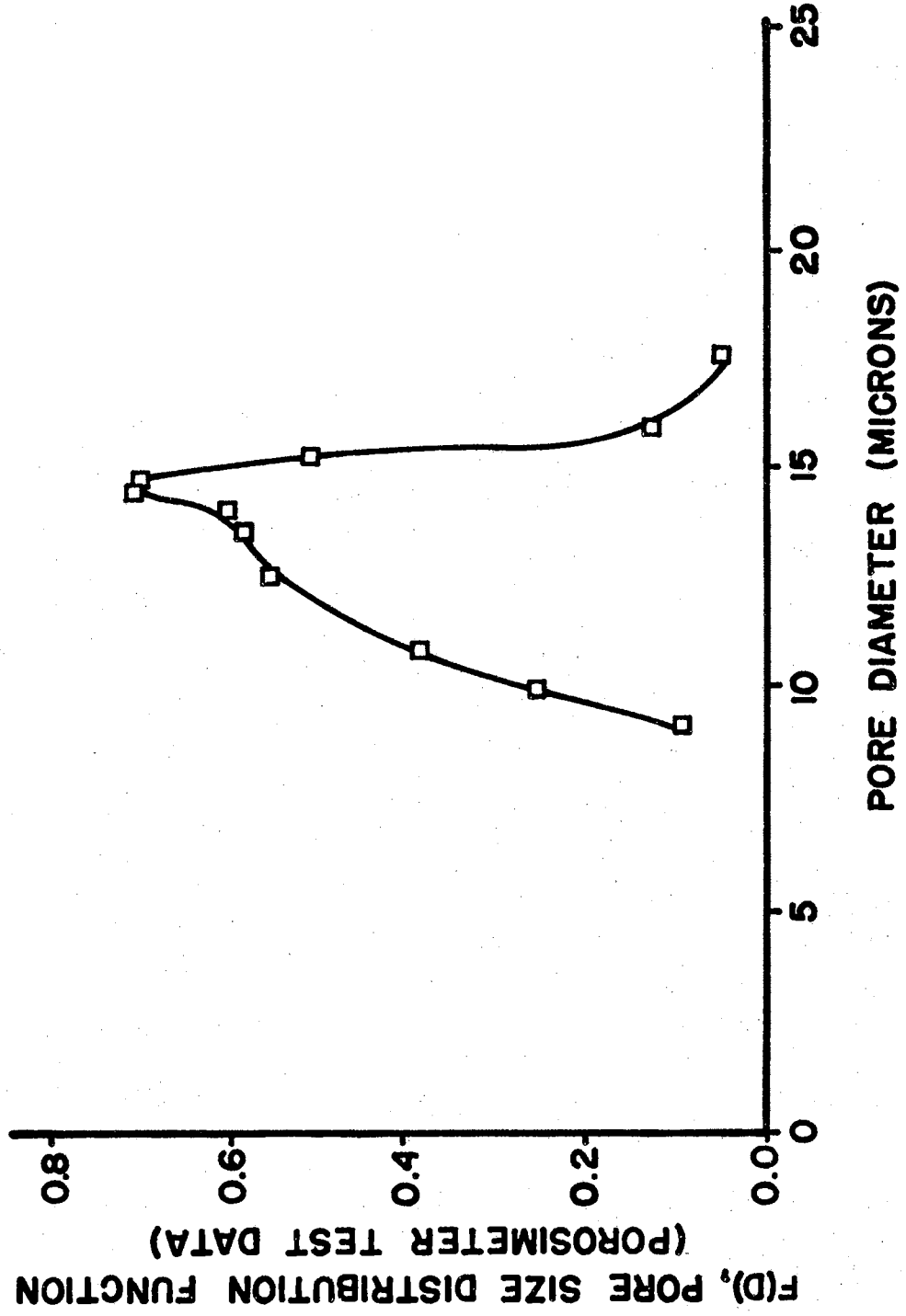

Figure A.5. Pore Size Distribution Curve

APPENDIX B

FILTER MEDIA PERFORMANCE TEST STAND

The inter-relationships between the flow rates through and the differential pressures across filter media were measured experimentally using the Filter Media Performance Test Stand. A photograph and the circuit diagram of the stand are shown in Figures B.1 and B.2, respectively. The test stand is designed so that flow rates from 0 to 25 gpm can be established through an experimental sample. It is equipped with a 0.5 micron system filter to protect the test sample from contamination during a test.

Extremely accurate instrumentation is incorporated into the stand to insure the reliability of the flow resistance test results. The flow rate is measured with a Fischer and Porter turbine flowmeter which is accurate to 0.1 percent. The pressure differential measurements are taken with a Fischer and Porter "Press-I-Cell", a differential pressure instrument with a readability of 0.05 psid and a repeatability of 0.066 psid. In order to maintain a constant viscosity, the fluid temperature is maintained to within 0.5° F of the desired temperature using a Minneapolis-Honeywell temperature controller. Because of the precise nature of the instruments, the test results obtained from the Filter Media Performance Test Stand are virtually free from experimental error.

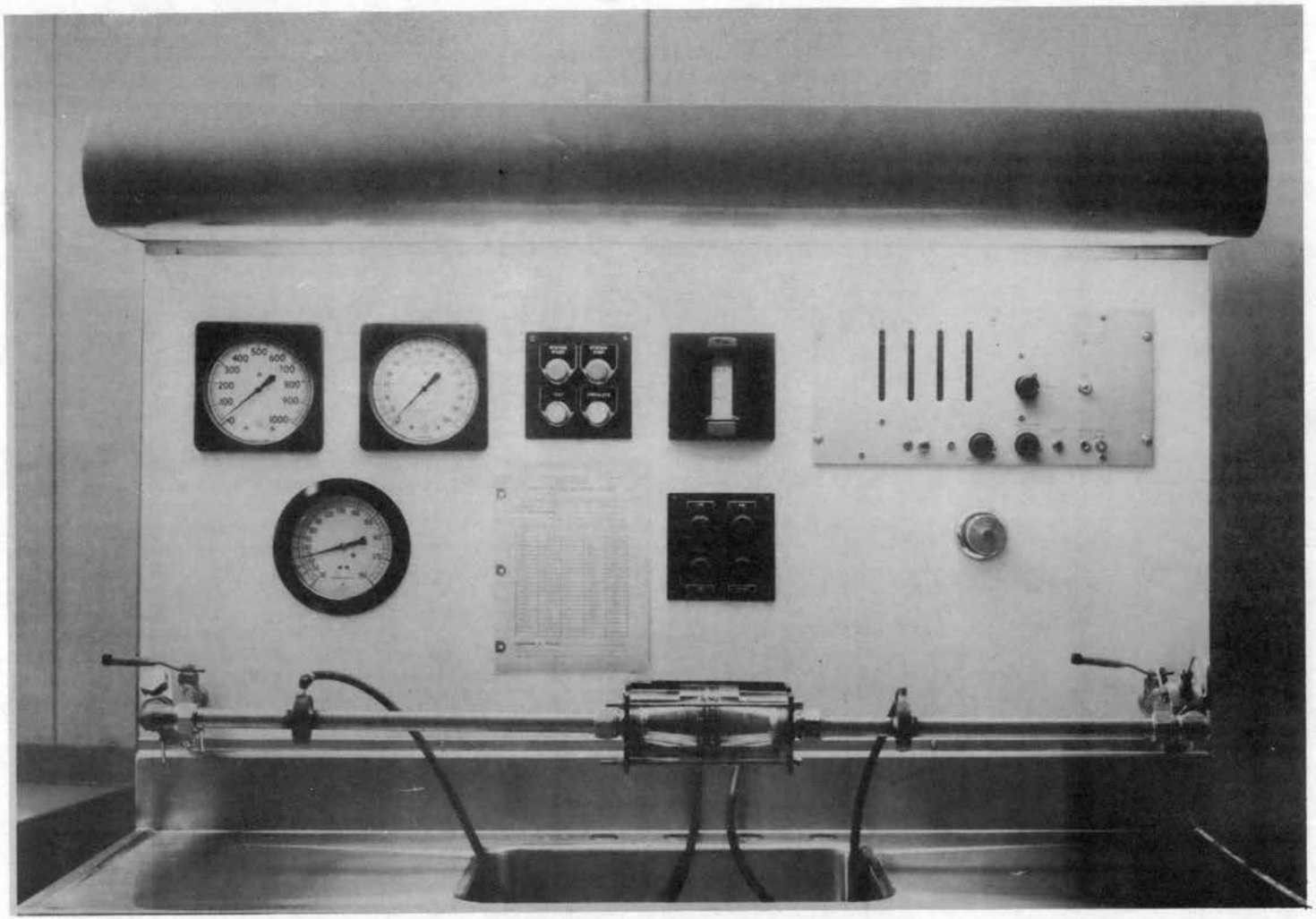

Figure B.1. Filter Media Performance Test Stand

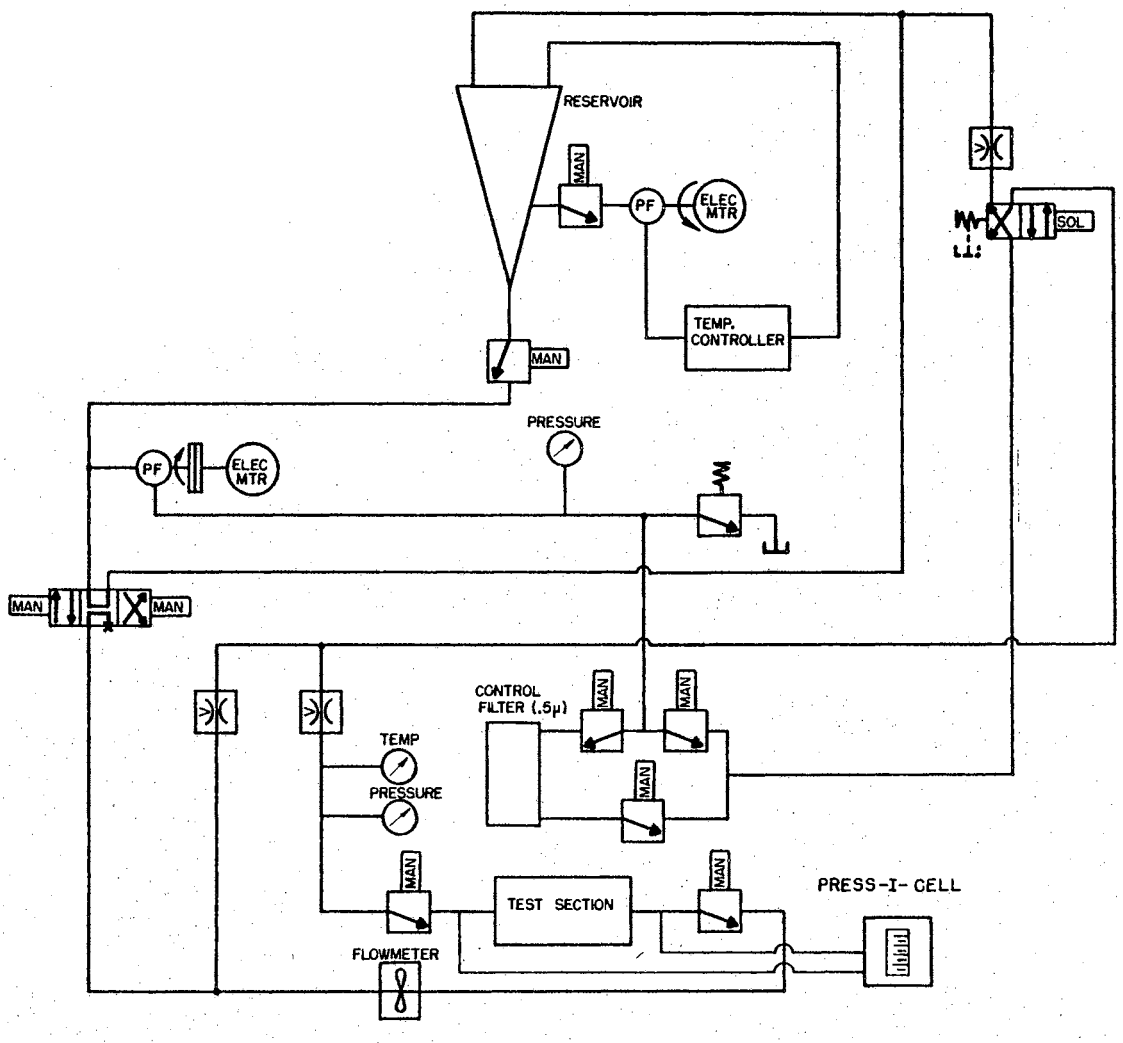

Figure B.2. Circuit Diagram of Test Stand

APPENDIX C

PARTICLE COUNTING TECHNIQUES

The particle counting techniques used to support the experimental work of Chapter 6 basically follow the SAE ARP-598 procedure. The sample is prepared by vacuum filtering the fluid through a 0.45 micron, black, gridded membrane filter pad as recommended in the ARP. The deviation from the ARP is in the optical equipment used on the microscope. An image splitting eyepiece was substituted for the recommended ocular micrometer eyepiece.

Figure C.1 shows a drawing of the image splitting eyepiece. The optical system in the eyepiece includes two prisms whose relative angular orientation can be set by the micrometer adjustment knob. Relative rotation of the knob creates the effect of dual or split images of objects in the field of view of the eyepiece. Depending upon the setting of the knob, i.e. the magnitude of the rotation of the prisms, the two images will overlap, touch, or be separated. These three possibilities are illustrated graphically in Figure C.1 by three particles of differing size, labled (a), (b), and (c). The setting of the adjustment knob for the illustrated case is such that the two images of particle (b) are just touching. The images of particles larger than (b) will overlap as demonstrated by (c). Images of particles that are smaller than the set size are separated as illustrated by (a). The settings on the micrometer adjustment knob are calibrated for a given microscope system by using a

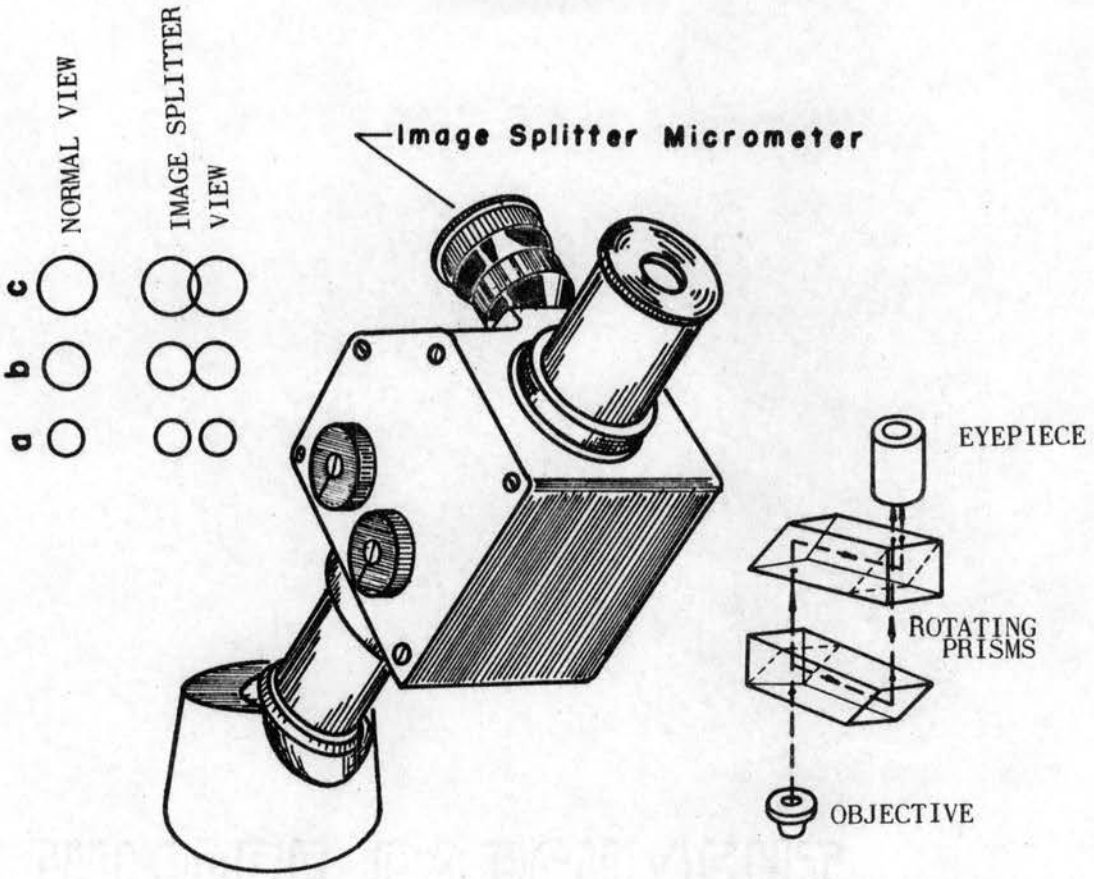

Figure C.1. Image Splitting Eyepiece

calibration slide. In practice, if particles 10 microns in diameter and larger are to be counted, the adjustment knob is placed at the setting corresponding to 10 microns. All particles whose images touch or overlap are then counted. To count in another range the knob is changed to the new setting and the procedure is repeated.

In order to better facilitate the counting of the particles, an eyepiece with a calibrated scale was used in conjunction with the image splitting eyepiece (Figure C.2). This scale was not used to size the individual particles, but instead it was used as a reference line or "gate" under which the particles were passed for counting. By moving the micrometer stage on the microscope, the particles on the filter pad pass under the scale. As they do so, their size is noted and those equal to or greater than the size set on the adjustment knob are tabulated. In this manner a unit area of length equal to one grid square length on the filter pad and width equal to the length of the eyepiece scale is surveyed and the particles thereon are counted. The unit areas corresponding to the objective magnifications used are shown in Figure C.3.

The total number of particles on the filter in each size range is found by scaling the area of the filter actually counted to the total effective filter area.

$$T_p = N_t \times \frac{960}{N \times A}. \qquad (C.1)$$

where:

T_p is the total number of particles of a given size range on the filter.

N_t is the total number of particles counted in N unit areas.

N is the number of unit areas counted.

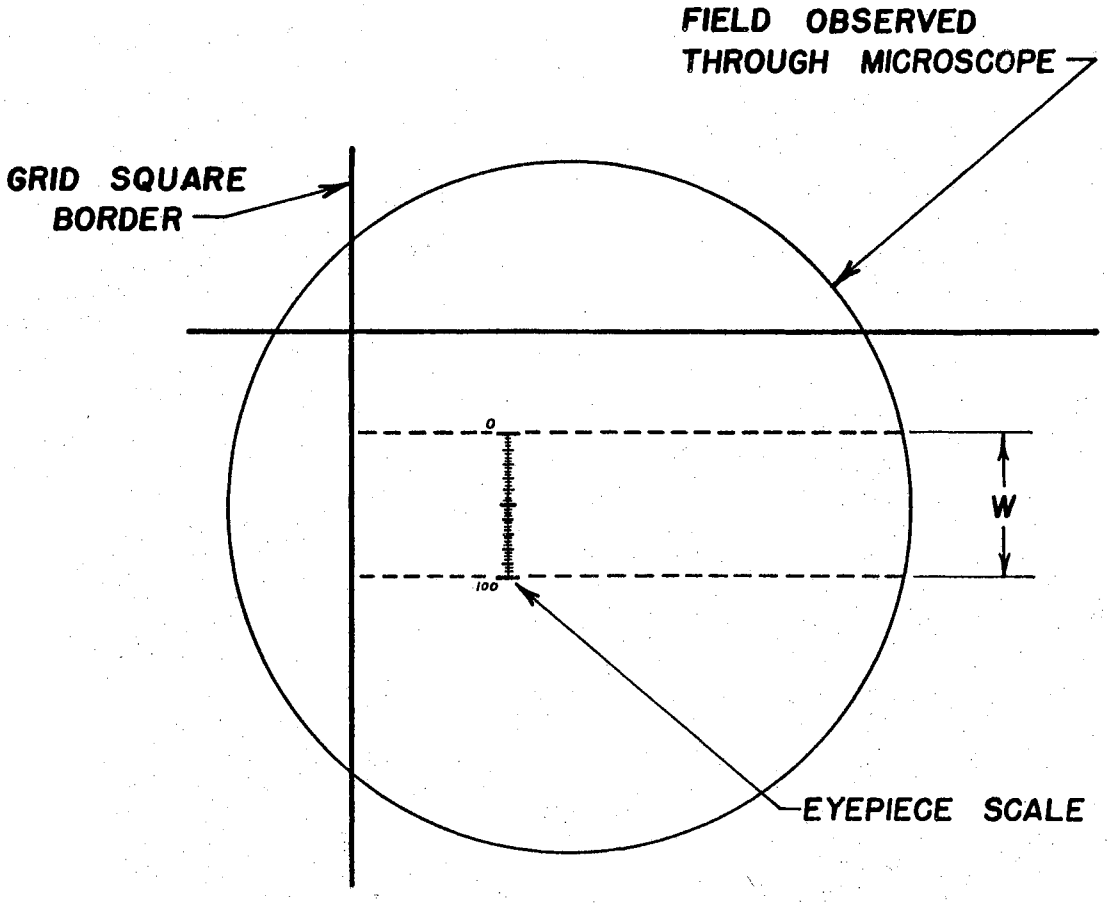

Figure C.2. Field of View Showing Area Counted

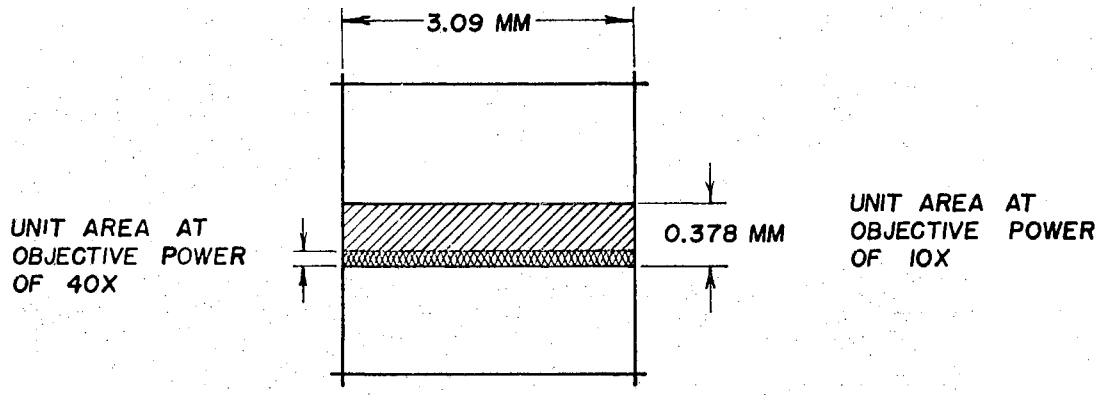

Figure C.3. Unit Areas at Objective Powers Used

A is the unit area $(mm)^2$

960 is the total effective filter area $(mm)^2$

The unit area is given by,

$$A = (3.09)\ W. \qquad (C.2)$$

where:

W is the width of unit area $= \frac{3.78}{M_o}$.

M_o is the objective power of microscope.

3.78 is the length of eyepiece scale at $M_o = 1$.

Substituting these values into Equation C.1 reduces it to

$$T_p = 82.2 \frac{N_t}{N} M_o \ . \qquad (C.3)$$

Two magnifications were used to count the particles in the feed and filtrate. A magnification of 520x was used to count particles smaller than 15 microns when AC Fine Dust was used as the contaminant. This magnification was obtained using an objective power of 40x in conjunction with the 13x magnification of the image splitting eyepiece. This higher magnification is required to distinguish the images of small, irregularly-shaped particles. A magnification of 130x was used for all of the size ranges when glass beads were used and for AC Dust larger than 15 microns in size.

Counts were made on twenty unit areas selected at random from the filter pad. This was equivalent to counting 2.4 percent of the total pad area for the 130x magnification, and 0.6 percent for the 520x magnification. The particles were sized in 5 micron intervals; the mean of the interval was selected as the characteristic dimension of the size range.

The use of the image splitting eyepiece in conjunction with the ARP-598 technique has demonstrated an accuracy of within plus or minus 10 percent limits, as compared to the plus or minus 33 percent limits associated with the standard ARP method. This represents a marked improvement in the expected accuracy associated with optical counting procedures.

VITA

Roger Harrell Tucker

Candidate for the Degree of

Doctor of Philosophy

Thesis: THE DEVELOPMENT AND VERIFICATION OF THEORETICAL MODELS FOR THE PERFORMANCE OF WIRE CLOTH FILTER MEDIA

Major Field: Mechanical Engineering

Biographical:

Personal Data: Born in Wichita, Kansas, July 30, 1939, the son of Clyde J. and Winston H. Tucker.

Education: Graduated from Putnam City High School, Oklahoma City, Oklahoma in 1957; received the Bachelor of Science degree in Mechanical Engineering from Oklahoma State University in May, 1961; received the Master of Science degree in Mechanical Engineering from Oklahoma State University in May, 1963; completed the requirements for the Doctor of Philosophy degree in July, 1966.

Professional Experience: Employed by Continental Oil Company, Ponca City, Oklahoma, during the summer of 1960. Employed by the School of Mechanical Engineering of Oklahoma State University from February, 1961 to August, 1963 as a Graduate Research Assistant; employed by the School of Mechanical Engineering since September, 1963 as an Instructor.

Honorary Organizations and Awards: Member of Pi Tau Sigma, Omicron Delta Kappa, Phi Eta Sigma, and "Who's Who Among Students in American Universities and Colleges", 1960-1961.